Characterization of motor functions of the human Superior Colliculus using fMRI

Dissertation

zur Erlangung des Grades eines

Doktors der Naturwissenschaften

der Mathematisch-Naturwissenschaftlichen Fakultät

und

der Medizinischen Fakultät

der Eberhard-Karls-Universität Tübingen

vorgelegt von

Nikhil Gokuldas Prabhu

aus Hubli, Indien

2021

Tag der mündlichen Prüfung: 16.12.2021

Dekan der Math.-Nat. Fakultät: Prof. Dr. Thilo Stehle

Dekan der Medizinischen Fakultät: Prof. Dr. Bernd Pichler

1. Berichterstatter: PD Dr. Marc Himmelbach

2. Berichterstatter: Prof. Dr. Ziad Hafed

Prüfungskommission:

Prof. Dr. Ziad Hafed

PD Dr. Marc Himmelbach

Prof. Dr. Dr. Hans-Otto Karnath

Apl. Prof. Dr. Thomas Ethofer

Erklärung/Declaration

Ich erkläre, dass ich die zur Promotion eingereichte Arbeit mit dem Titel: **"Characterization of motor functions of the human Superior Colliculus using fMRI"**, selbständig verfasst, nur die angegebenen Quellen und Hilfsmittel benutzt und wörtlich oder inhaltlich übernommene Stellen als solche gekennzeichnet habe. Ich versichere an Eides statt, dass diese Angaben wahr sind und dass ich nichts verschwiegen habe. Mir ist bekannt, dass die falsche Abgabe einer Versicherung an Eides statt mit Freiheitsstrafe bis zu drei Jahren oder mit Geldstrafe bestraft wird.

I hereby declare that I have produced the work entitled ***"Characterization of motor functions of the human Superior Colliculus using fMRI"****, submitted for the award of a doctorate, on my own (without external help), have used only the sources and aids indicated and have marked passages included from other works, whether verbatim or in content, as such. I swear upon oath that these statements are true and that I have not concealed anything. I am aware that making a false declaration under oath is punishable by a term of imprisonment of up to three years or by a fine*

Tübingen, den ....

Datum/Date Unterschrift/Signature

Abstract

The Superior Colliculus (SC) is well established to be a structure that plays a major role in orienting the eyes and head towards objects of interest in the surroundings. Most of the studies in the SC thus far have been conducted on non-human primates. Although the neural architecture is presumed to be similar, existence of differences in anatomy, afferents and efferents between the SC of different mammals questions functional extrapolation of such studies to humans. Also, there have been very few electrophysiological studies that have investigated the role of the SC in reaching and finger tapping movements. An fMRI study in humans conducted earlier in the lab was the first to show that the SC is involved in reaching movements in humans. In order to further elucidate the motor functions of the SC in humans, we conducted three experiments and analysed one pre-acquired dataset. These studies used two simple and classical paradigms – reaching, and finger tapping movements.

The SC is widely believed to be a visually driven structure, supported by numerous studies in macaques. With our first study, we sought to decipher if the SC is also active in response to reaching, guided by tactile stimulation. We designed a task where subjects had to maintain fixation while performing reaching movements to peripheral targets that were either visual or tactile in nature, separated by their respective blocks. We found that the SC indeed shows activity in response to somatically or visually guided reaching, but not to visual stimulation or somatic stimulation on their own. In addition, we also observed a strong signal contribution from button presses in tasks with control conditions, which were required to be performed by subjects in response to oddball stimuli, to make sure that they were engaged in the tasks.

Our second study was divided into two parts. The first part consisted of an analysis of the finger tapping task (motor task section) from the Human Connectome Project

(HCP) database. The second part of the study investigated whether complex finger tapping and simple finger tapping movements, paced by visual or auditory stimuli, caused an activation in the SC. We found no activation in response to the finger tapping task from the HCP data. We also found that the SC did not take part in either the complex or simple finger tapping tasks that we conducted. This, together with the results corresponding to finger tapping from the HCP data, and the finger tapping (recorded as button presses) results from the first experiment, led us to postulate that the SC might be involved only when finger tapping movements occur in response to novel stimuli.

With our third and final study, we investigated the response of the SC to novel stimuli. In the experiment, subjects responded with button presses or counting to oddballs involving the same modalities as the first experiment: visual and somatic stimulation. We found some activity in response to all oddball conditions combined together. This activity was further weakened when oddballs were bifurcated into four conditions by the sensory modalities involved - visual and somatic stimulation and the corresponding responses - button presses and counting. Although these results hint that the SC might respond to oddball stimulation, these effects were not consistent across subjects warranting further investigation for more concrete conclusions.

Taken together, our results conclusively show that apart from visual information the SC integrates sensory information such as touch towards the execution of reaching movements. In addition, the SC does not play a role in the execution of movement sequences that are repetitive, irrespective of whether they are complex or simple movements. For a concrete conclusion regarding responses to novel stimuli, more sensitive experiments are necessary.

Table of Contents

Abbreviations

AC	Auditory complex
BOLD fMRI	Blood oxygen level dependent functional magnetic resonance imaging
CSF	Cerebo spinal fluid
CI	Confidence interval
EPI	Echo planar imaging
FEF	Frontal eye field
FOV	Field-of-view
FWE	Family-wise error
FWHM	Full-width half-maximum
GLM	General linear model
HCP	Human Connectome Project
HRF	Haemodynamic response function
ITI	Inter-trial interval
LED	Light emitting diode
LGN	Lateral geniculate nucleus
MNI	Montreal Neurological Institute
MT	Medial temporal (cortical area)

PBMT-S	Permutation based maximum t-statistic test
PMd	Dorsal pre-motor (cortical area)
ROI	Region-of-interest
SBP	Somatic button press (experimental condition)
SC	Superior colliculus
SCO	Somatic counting (experimental condition)
SD	Standard deviation
SE	Standard error
SM	Somatic motor (experimental condition)
SNR	Signal-to-noise ratio
SPM	Statistical Parametric Mapping (software)
SS	Somatic sensory (experimental condition)
SST	Somatic stimulus (experimental condition)
TE	Echo time
TR	Repetition time
TTL	Transistor-transistor logic
VBP	Visual button press (experimental condition)
VC	Visual complex (experimental condition)
VCO	Visual counting (experimental condition)
VM	Visual motor (experimental condition)

VOI	Voxel-of-interest
VS	Visual sensory (experimental condition)
VST	Visual stimulus (experimental condition)

Chapter 1

Introduction

1.1 Preamble

The Superior Colliculus (SC) is a tiny mid-brain structure whose proposed role in behaviour seems to increase in complexity with every study aimed at it. The endeavour to study the SC first began in the 1970's when the SC was seen to respond to saccadic eye movements in addition to responses towards visual stimulation. In over four decades of research, the most established role of the SC has been in initiating and orienting movements towards objects of interest in the surroundings. Along with this, it has also been seen to be implicated in myriad other behaviours such as attention, target selection, visually-guided movements, decision making etc.(see Basso and May, 2017 for a review). Although a lot is known about the SC, unanswered questions remain. One of the less studied areas pertains to control of motor functions by the SC, particularly, mechanisms of sensory integration that lead to motor behaviours. This is exactly what I address in this thesis. With the three studies and analysis of one pre-acquired dataset detailed in this thesis, we used various sensory modalities and motor responses to map the human SC using fMRI.

1.2 Location and anatomy of the human SC

The SC forms the roof of the tectum in the mid-brain. It is located just below the Thalamus surrounding the Pineal glands, it is posterior to the periaqueductal gray, and immediately superior to the inferior colliculus. The SC is known to be

comprised of three functional layers: the superficial, intermediate and deep layers. The superficial layer is sensory in nature. It has afferents and efferents to and from the retina, the frontal eye fields (FEF), and the visual cortex. The intermediate layer is known to take part in both visual and motor transformations and hence responsible for oculomotor control. The deep layer is known to be multisensory and also contains visuomotor neurons (May, 2006).Anatomically, each of these layers are further divisible into more fine layers but this is beyond the scope of the studies in this thesis. The functional division of the SC into layers is based on studies in mammals and non-human primates like the macaques. Recent advances in analytical methods are being used to elaborate these divisions in the human SC through other studies in our lab, and elsewhere.

The primary sources of visual inputs to the SC are: projections from the retina and the visual cortex, especially from the primary visual area (V1), V2, V3, V4 and the middle temporal area (MT). The primary outputs of the SC are to the LGN, the pulvinar complex, and inward to the intermediate layer of the SC (SCi). The connections to the LGN and pulvinar and hence the extrastriate visual cortex are presumed to play a role in influencing visual signals that reach the cortex. The connections to the pre-motor parts of the SCi are presumed to play a role in modulating visually-guided orienting and in interactions between bottom-up (sensory) and top-down (goal-related) processes (see book chapter on the SC by White and Munoz, 2012). The SC is known to be organised into topographical maps which is the central organising principle of the brain and plays a crucial role in spatially-guided behaviour. These topographical maps are said to be multisensory in nature.

1.3 Known functions of the SC

The purpose of this section is not to review all the functions of the SC but to focus on those aspects that are relevant to this thesis. In general, the SC is known to be part

Figure 1.1: Location of the SC in relation to the structures surrounding it.

of a fast detecting, first responding system, that reacts to elements of surprise in the surroundings (see Soares et al., 2017 for a review). One of the everyday examples that could help understand this is to imagine yourself walking on a street and an object comes flying in your direction. The eyes see the object in the periphery and the body reacts at once to this incoming object, for example, by a rapid ducking response. It is only after the object has gone by that one realises what the object was. The initial rapid reaction to the unusual stimulus is the process in which the SC is known to participate. This includes integration of sensory information necessary to quickly identify size, trajectory, velocity etc. of the incoming object along-with the motor output necessary to quickly evade the object. The recognition of the object which is a comparatively slower process is supposed to be brought about later by cortical areas. Although, the evidence for this sort of reflexive behavior by the SC is very strong, recent studies have shown that the SC is also involved in functions that have originally been attributed to the cortex. These functions include but are not limited to behaviours such as target selection, attention, decision-making etc. (see Basso and

May, 2017 for a review). Since this thesis focuses on the motor functions of the SC, and to an extent, the interaction between attention, decision-making, and movements these are the only aspects that I have focused on in the upcoming sections.

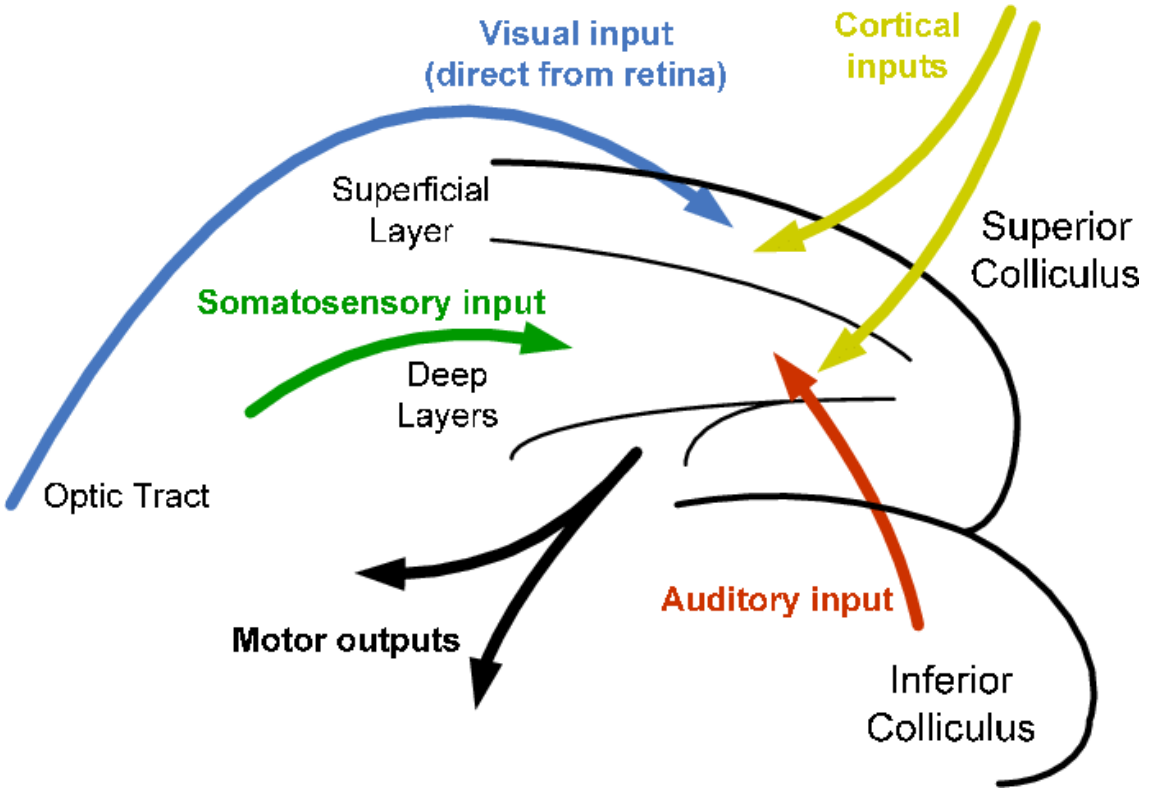

Figure 1.2: A schematic diagram of the primary inputs and outputs from the two main layers of the SC. Reproduced from (Pavlou and Casey, 2010) ©2010 IEEE.

1.3.1 Role of the SC in eye and head movements

Some of the major functional roles of the neurons in the SC have been in generation of saccades, and changing and holding gaze. Mostly, movement control in the SC has been intensively studied through saccades (May, 2006). Saccade related neurons in the SCi discharge action potentials for a range of saccade amplitudes and directions that define a movement field; the region of space to which a directed saccade affects the firing of that neuron (Goldberg and Wurtz, 1972a; Munoz and Wurtz, 1995a; Sparks,

1978; Sparks and Mays, 1980). Execution of large-amplitude saccades when the head is free to move is not possible by movements of the eyes alone. These movements are typically executed with the head following the eyes, with the SC playing a role in their execution (see Freedman, 2008 for a review). Apart from eye and eye-head movements, the SC also participates in generation of eye-head-body movements in order to evade harmful stimuli (see Gandhi and Katnani, 2011 for a review).

1.3.2 Role of the SC in reaching movements

The SC is supposed to be playing a major role in sensorimotor transformations (Sparks and Mays, 1990). The 'reach' neurons in the SC are intermingled but distinct from visuomotor and motor neurons that are responsible for saccadic eye movements (Stuphorn et al., 2000; Werner et al., 1997a). According to the former study, unlike saccade-related responses associated with head movements in the SC, neurons responsible for reaching movements do not exhibit topographical organization. Arm movement control in the SC has also found support in micro-stimulation studies. Stimulation of the deep-layers of the SC was seen to have elicited proximal shoulder movement (Cowie and Robinson, 1994). But, spreading of the current to the reticular formation, and these movements being twitches instead of 'reaching' movements, are arguments offered against it (Gandhi and Katnani, 2011). Microstimulation of the SC has also been seen to give rise to arm movements (Philipp and Hoffmann, 2014). Also, stimulation of the SC in cats is known to have perturbed movement trajectories (Courjon et al., 2004). The human SC is known to have taken part in visually-guided movements (Linzenbold and Himmelbach, 2012). Other aspects of visually-guided movements like gaze anchoring (Reyes-Puerta et al., 2010) and activity on contact of an object which increases with the intensity of the push (Nagy et al., 2006) have also been observed in the SC.

1.3.3 Role of the SC in spatial attention

The first evidence that the SC plays a role in spatial attention was offered by the 'Sprague effect' (Sprague, 1966). Discovered by Sprague in 1966, it refers to ablation of the contralateral SC after a lesion in the parietal or occipital cortex of one side of the brain leading to recovery of the symptoms of neglect caused by the cortical lesion. Since then, numerous studies have tried to decipher the exact role of the SC in spatial attention. Most of these studies have implicated the SC either in shifts of attention that occur during saccades - overt attention (Bell et al., 2004; Fecteau et al., 2004; Fecteau and Munoz, 2006), or in those that occur without any specific orientation movement - covert attention (Bogadhi et al., 2018; Hafed and Clark, 2002; Hafed et al., 2013; Herman JP and Krauzlis RJ, 2017; Müller et al. 2005) and in both together (Ignashchenkova et al., 2004). Microstimulation and opto-genetic studies have been conducted in the SC to establish a causal role in spatial attention. Several studies showed that application of microstimulation to the SC during orientation detection tasks resulted in an increase in detection performance and decrease in reaction times (Cavanaugh et al., 2006; Cavanaugh and Wurtz 2004; Lovejoy and Krauzlis, 2010; Müller et al. 2005). The opposite effect was seen when the SC was inhibited through opto-genetics (Wang et al., 2020). These results suggest that the SC has a major role to play in the application of spatial attention.

1.3.4 Role of the SC in decision-making

The idea that the SC could be involved in perceptual decision making first evolved with the observations of a rise in neuronal activity in the intermediate layers of the SC, with the onset of visual stimuli, and later with the onset of saccades. A tonic discharge of neurons was seen in the interval between display of visual stimuli and actions made in response i.e. while the monkeys waited to perform saccadic eye movements (Glimcher and Sparks, 1992; Munoz and Wurtz, 1995). These studies were

followed by more concrete ones that tested target selection in monkeys with (McPeek and Keller, 2004) and without (Basso and Wurtz, 1997, 1998) reversible inactivation of the SC which showed that it played a role in target selection. Indication that the SC selects targets based on accumulation of evidence in the delay-period prior to saccades was brought about by a series of studies (Horwitz et al., 2004; Horwitz and Newsome, 1999, 2001; Ratcliff et al., 2003, 2007). Recent evidence has strengthened this view with studies using electrical interventions (Crapse et al., 2018), modeling (Herman et al., 2018), opto-genetics, (Wang et al., 2020) and electro-physiology with a multi-foraging value task (Zhang et al., 2021), implicating the SC strongly in decision-making.

1.4 Statistical Parametric Mapping (SPM) and fMRI analysis

SPM is a software package that is used in the construction and assessment of statistical processes for testing hypothesis with neuroimaging data. It is widely used for identifying region-specific effects and for characterisation of functional anatomy in fMRI research. SPM uses the General Linear Model (GLM) as its workhorse to integrate a variety of statistical tests. It also accommodates routines for pre-processing of fMRI data before the data can be used for analysis. In the following paragraphs, I will briefly touch upon parts of the SPM software that we used in our studies.

1.4.1 Pre-processing using SPM

We began pre-processing the data by first converting the raw images from the scanner (DICOM and IMA formats) to a standard neuroimaging format called Nifti (Neuroimaging Informatics Technology Initiative). These Nifti images were then used in the next step called realignment or motion correction. Since fMRI studies involve several scans acquired over several sessions, motions of the head between scans can

interfere with analysis. These discrepancies are corrected in the realignment procedure so that voxels in a part of the image correspond to the same site in the brain, across all scans. In the next step called co-registration, anatomical images which generally have a much higher spatial resolution than functional images are 'registered' together so that they point to the same anatomical region irrespective of their original orientations. The resulting images are then passed on to the next step of preprocessing called normalisation. fMRI studies typically involve several subjects, each with a slightly different shape along-with topographical differences in gyri and sulci in cortical regions and some morphological differences in deeper structures. A procedure that allows for comparison of images between subjects in the particular study, and to those that are acquired anywhere else in the world, becomes necessary. Normalisation achieves this using various transformations such as translation, rotation, scaling, and non-linear warping with the resulting images matching a standard template, which in our studies was the MNI (Monreal Neurological Institute) template. The normalised images are finally passed on to the last step called smoothing, where noise in the data is reduced typically by averaging voxels with their neighbours, which in our case was performed with a Gaussian filter with FWHM (full-width half-maximum) of 3mm.

1.4.2 GLM analysis

The pre-processed images are then used for analysis between voxels. First, a design matrix is constructed for GLM with experimental and confounding effects, also referred to as regressors of interest, and regressors of no-interest, respectively. Based on this matrix, images that map probability density functions which are usually either a Student's t-distrubution or F-distribution, are constructed. These maps can then be used for any univariate statistical analysis based on the GLM of the data. The resulting statistical maps called statistical parametric maps are assembled into an image which is then overlayed onto an anatomical image for visualisation. The color gradient represents statistical values such as t-values or z-scores. Correlations

between a task variable and activity in a certain brain area over time, are examined using a linear convolutional model, to understand how measured signals are caused by changes in underlying neural activity. Since many tests are conducted across several voxels, adjustments have to be made to control for type I errors (false positives). Adjustments are made using random field theory based on the number of voxels involved, to set new criterion for significance thresholds that are adjusted for multiple comparisons. Corrections for multiple comparisons are not used when a region of interest (ROI) is pre-defined. These results are typically reported at a very conservative threshold (for example, $p < 0.001$). Generally, contrast estimates or beta estimates are also plotted accompanying GLM results. Contrasts estimates indicate the effect size for the particular condition derived from an F-test of all conditions tested, and are plotted along-with 90% confidence intervals (CI) in SPM.

1.5 Challenges of functional measurements in the human SC

The human SC is not very straightforward to measure since it is a tiny structure embedded in the sub-cortex surrounded by CSF (Cerebro-spinal fluid) with a very low signal-to-noise ratio (SNR). These measurements require sequences that have been developed over a long time and hence attuned to measurements in the SC. Another consequence was that we had to measure the brain with a partial volume that covered the SC sometimes excluding important cortical structures.

In our experiments, subjects had to perform motor tasks, moreover, a reaching task in the first experiment where the probability of head movements is high. Untoward movements on their part would render the measurement unusable. With measurement times of more than an hour per session, finding suitable participants was difficult especially since we had completely darkened scanner rooms. Hence, we had to take

great care to recruit highly motivated and reliable participants who remained stable throughout the measurement. Even so, we had to work with weak signals typical of measurements in the SC. Our decision to measure a few reliable participants over several sessions for all our studies, instead of recruiting several subjects helped us greatly in this regard. This approach has been used not only to obtain more reliable measurements because of the large amount of data acquired from each subject but also to explore topographical features that are distinct from those seen in group measurements (Laumann et al., 2015; Xu et al., 2016; Gordon et al., 2017).

The Statistical Parametric Mapping (SPM) package which we used for analysis uses mostly cortical boundaries for co-registration of anatomical and functional scans, making it difficult to automatically co-register small structures in the brainstem like the SC. The employment of manual co-registration strategies like - registration of mean functional images (T2* weighted) with whole-brain T2* weighted images, normalisation of mean functional and structural images, co-registration of mean functional scans between sessions, and finally normalisation of functional images with structural images from each session of a subject's measurements, allowed us to obtain better alignment between the SC of different subjects. Although we tried to achieve the best co-registration possible, it is almost impossible to obtain exact co-registration at the SC. A slight change in the structure of the SC between subjects would mean that one part of the SC would not be aligned very well, when another is in good congruence. This issue was mostly circumvented by ensuring that the boundary of the SC with CSF was as best aligned as possible, between subjects.

We have made an earnest attempt to measure eye movements during all the studies that we conducted. Even so, to the best of our knowledge there are no eye trackers available as of date that would enable us to measure saccades lower than 0.1°in the MRI scanner. This effectively rules out measurement of microsaccades. Although this is not the ideal scenario, we relied on earlier studies that showed increased reach-related activity in the SC from trials where no microsaccades were seen (Reyes-Puerta

et al., 2010). In our third study, the activation in the SC could be attributed to microsaccades. But, if that were the case, we should have also seen similar activation in the SC corresponding to trials where oddball stimuli were counted, and in those where the oddball stimuli were responded to by a button press.

1.6 Goals of the current study

Since the SC displays rapid reactions to unusual stimuli of different modalities in the environment, we envisaged that it should also take part in integrating these modalities for its motor functions. As mentioned earlier, the SC has been known to play a role in visually-guided reaching movements. What about other sensory modalities? Could it also play a role in reaching movement of the arms to tactile targets? These are the questions that we sought to answer with our first study.

Characterisation of the motor functions of the SC would entail testing whether it demonstrates all the features that are exhibited by the motor centres in the rest of the brain. One of such investigations is to test whether the SC takes part in finger tapping movements. With our second study, we addressed questions such as - is the SC indeed a key motor structure that takes part in movements of varying complexity, more particularly, in simple and complex sequential finger movements?

The SC is known to participate in responding to stimuli in the environment that are of interest. Would the SC need to be informed by sensory stimuli in order to play a role in their execution? Would it take part in decisions of responding to some stimuli while not responding to some others? Since the SC is known to be a multi-sensory integration centre, it would be expected to participate equally in decisions of responding with movements to visual or somatic stimuli, would that be the case? The third study in the thesis helped us answer these questions.

In totality, these questions would help refine the placement of the SC in the sensory-

motor scheme of the brain. This in turn, would further the understanding of pathological conditions that involve interactions between the SC and other parts of the sensory-motor network. For example, deciphering interactions of the SC with the basal ganglia has implications in understanding the altered sensory-motor transformations that occur in Parkinson's disease, and could help plan interventions aimed at relieving its symptoms.

Chapter 2

Somatically guided reaching in the SC

2.1 Introduction

The Superior Colliculus (SC) is a mid-brain structure with a well-established role in orienting movements of the head, eyes, and arms (Gandhi and Katnani, 2011). Owing to decades of research on its contributions towards the generation of saccades in monkeys, so far, the SC has been largely considered to be a visually driven structure. The SC has been investigated for its role in visually guided arm movements in primates (Werner, 1993; Werner et al., 1997b) where it was shown that neurons in the SC were active either before, during, or after arm movements to visual stimuli. Studies by the Himmelbach group (Himmelbach et al., 2013; Linzenbold and Himmelbach, 2012) were the first to show the involvement of the 'human SC' in visually guided reaching movements using BOLD fMRI. Since the SC is a sub-cortical structure, it is likely that it would integrate multi-sensory information towards realisation of reaching movements. This could be tested with a reaching paradigm guided by sensory stimulation that is uninformed by visual information.

Somatic stimulation is easily localised, hence suitable as a target for reaching movements. Although it is known that the SC of cats and macaques possess a somatosensory map (Wallace et al., 1996) along with oculomotor ones (Ottes et al., 1986), a possible role of the SC in reaching movements guided by somatic stimulation has not yet been investigated. The only study that reported a finding concerning reaching movements and somatic stimulation is the one by Nagy et al., 2006. Even here, a higher firing rate in a few SC neurons was seen temporally aligned with contacting a

button, after completion of the reaching movement, as against during reaching movements to these buttons.

To decipher a possible role of the human SC in reaching movements guided by somatic stimulation, we designed an experiment that could validate earlier findings on visually guided reaching, while also looking for responses to somatically guided reaching movements, using BOLD fMRI. The experiment involved five subjects performing reaching movements towards visual and somatic targets compared with passive sensation of visual and somatic stimulation, while maintaining fixation throughout the experiment. Each subject repeated the experiment on four different days adding up to a dataset of four sessions per subject. We tested an a-priori hypothesis that activations could be expected in the SC at the peak location obtained from the earlier study in our lab involving reaching movements to visual targets (Linzenbold and Himmelbach, 2012). The respective MNI (Montreal Neurological Institute) peak voxel co-ordinate formed our VOI (voxel-of-interest) for a GLM (General Linear Model) analysis. The analysis revealed activation clusters in the SC at and around our VOI for visual as well as somatically guided reaching. A following time course analysis of the voxels immediately surrounding the peak voxel, allowed us to differentiate responses corresponding to various task conditions between voxels adjoining the VOI. We found strong responses in the SC for reaching movements towards visual and somatic targets whereas no response was seen corresponding to passive sensing of visual and somatic targets.

2.2 Methods

2.2.1 Subject details

We conducted the study using 3T BOLD fMRI on five subjects (5 females, age range 22-28, all right-handed) with normal or corrected-to-normal visual acuity. Each subject performed the experiment four times, one session per day. We excluded the first

two sessions from the first subject for non-conformity with the rest of the measurements, since they were measured with the online motion correction of the scanner software. We conducted the experiments with the approval of the local ethical committee and as per the ethical standards established by the 1964 declaration of Helsinki. We obtained informed consent from all the subjects.

2.2.2 Experimental setup

Subjects performed the experiments in complete darkness. We ensured no light penetrated the scanner room by covering windows, scanner displays, and the opening of the scanner bore with black opaque sheets. Subjects rested the palm of their left hand on a palm-rest (Figure 2.1 B) with four slits shaped according to the four fingers used for the experiment (excluding the thumb). The palm-rest in turn rested on a stand placed across the waist of the subjects (Figure 2.1 A). Pneumatic stimulators (Figure 2.1 C) were placed in a notch on the uppermost part of the slits in the palm-rest making contact with the respective fingertips. Changes in air pressure brought about by a compressor regulated the diaphragms of the pneumatic stimulators, causing tactile stimulation on fingertips. Fibre optic cables carried light from green and red LEDs into holes drilled above each of the four finger slits on the palm rest (Figure 2.1 A, B). 8 fibre optic cable endings reached the fingertips: 2 per fingertip, 1 of each colour, hence, making up four targets. Each target would glow red or green depending on the trial type. The white LED formed the fixation point and was attached to the scanner bore. The targets were placed at a distance of 9°away from the fixation point, and at a varying distance of 4°, 3°and 2°between them (from the index finger to the little finger, respectively) owing to the angle subtended between the four fingers. Subjects looked at the fixation point directly, eliminating the need for a mirror. We placed cushions specially manufactured for fMRI research (NoMoCo Pillow, Inc., La Jolla, USA) into the head-coil of the scanner, immobilising the head of the subjects. We programmed a microcontroller - 'Mbed LPC1768' (Arm Limited.) to control target

LEDs, and air pressure regulating valves connected to pneumatic stimulators. In addition, the microcontroller was also programmed to collect button press timings, display experimental events on screen, and write all event timings to a file. We used two MR compatible cameras (MRC systems GmbH.) that operated at 30Hz: one to check fixation and the other to monitor reaching movements to targets. The cameras were in turn connected to a frame grabber (Matrox Imaging) which was controlled via MATLAB (version R2018a, The MathWorks Inc., Natick, MA, USA) for video recording. The first TTL pulse from the scanner triggered the microcontroller to execute the experimental paradigm and the frame grabber to start video capture in MATLAB.

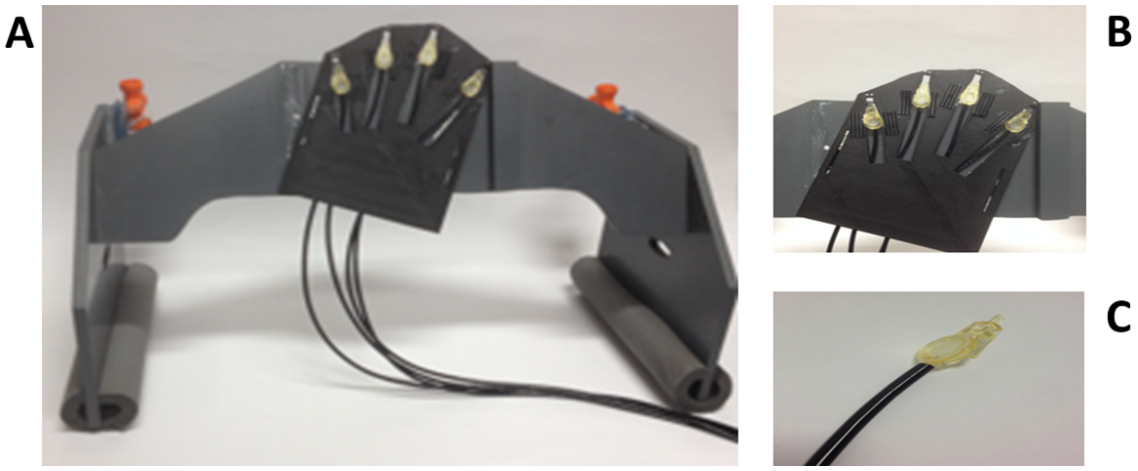

Figure 2.1: A - The stand onto which the palm rest was attached. B – palm rest with attached pneumatic stimulators and air tubes. C – a single pneumatic stimulator.

2.2.3 Experimental paradigm

Each experimental session consisted of four conditions – VM (visuo-motor); SM (somato-motor); VS (visuosensory); and SS (somatosensory); put together in a factorial design, resulting in a combination of two conditions in each of the four runs (Figure 2.2. The four runs thus formed comprised of the following conditions: run 1 - VM, SM; run 2 - VM, VS; run 3 – VS, SS and run 4 - SM, SS. The conditions

that required a reaching response: VM and SM were our conditions of interest while the conditions that required sensory discrimination: VS and SS, formed the controls.Green and red LEDs formed the targets in the visual conditions, and single or double tactile stimulation formed the targets in the 'somatic' conditions. Subjects were required to fixate on the central white LED above the targets throughout the experiment. The central fixation light turned on with the receipt of the first TTL pulse from the scanner marking the start of a run. All runs started with an initial fixation period of 12s. The two conditions forming a run alternated as blocks of four targets each, with each block adding up to 8.8 seconds (stimulus time of 0.2s and inter-stimulus interval of 2s). A 12s baseline period followed each block apart from the set of blocks where the sensory modality was the same i.e. the task to be performed in the impending block was not obvious. Such blocks were preceded by a cue (blink of the fixation light) within the 12s baseline period, 3 seconds before the start of the block. For example, somatic stimulation (SS) and somatic reaching (SM) blocks were preceded by one blink and two blinks of the cue respectively. Both the blocks repeated 14 times each, adding up to around 10 minutes of scanning time for a run. Each of the four targets in a block appeared in a pseudo-randomised manner with most of the tactile stimulation being single stimulation, and visual targets being green in colour depending on the respective block. One in eight targets was an oddball: either red in colour or a double tactile stimulation depending on the condition block they belonged to. In the sensory conditions, subjects were required to respond to the oddball (red target or double tactile stimulation) with a button press. This resulted in 28 button presses per session, totalling 112 button press responses per subject with all four sessions combined. In the reaching conditions, subjects had to make a reaching movement towards a target with their right hand irrespective of whether it was green or red in colour, or whether it was a single or double tactile stimulation i.e. irrespective of whether it was a regular target or an oddball. Only the forearm was used to make reaching movements while the rest of the arm fixed to the scanner

bed. This was done to reduce movements of the head while executing reaching movements. The total number of block repetitions per subject with all the four sessions combined were 448 (112 block repetitions from each of the four conditions VM, SM, VS and SS) with the exception of the first subject with 224 repetitions (since two sessions were excluded). To register the time taken to make the movement, subjects continuously pressed a button placed on their chest, releasing it only to make reaching movements in response to peripheral targets and returning to it soon after. In the sensory discrimination conditions, responses were recorded when subjects pressed a second button with the index finger of their right hand.

	Visual	**Somatic**
Reaching (motor)	Visuo-motor (VM)	Somato-motor (SM)
Sensory (stimulation)	Visuosensory (VS)	Somatosensory (SS)

Figure 2.2: *The four conditions of the experiment arranged in a 2x2 factorial design.* The four runs in the experiment were derived from a combination of the two tasks – reaching and sensory discrimination, and the two modalities – visual and somatic.

2.2.4 fMRI data acquisition

We acquired the images on a Siemens Prisma 3 Tesla MRI scanner with a 32-channel head coil. 300 T2* weighted functional images (echo-planar imaging (EPI) sequence) were acquired per run with a slice thickness of 2mm, TR=2s, TE=35ms, flip angle of 80°and FOV - 192 x 192 mm (96 x 96 matrix). Each functional image consisted of 23 slices in a transversal orientation covering structures of our interest: the SC and the primary visual cortex (V1). We also acquired high resolution T1 weighted structural images once per subject (MP-RAGE sequence, slice thickness of 0.8 mm, TR=2.4s, TE=2.22ms, flip angle of 8°and FOV – 240 x 256 mm (300 x 320 matrix).

A whole-brain EPI image was acquired in each of the four sessions of a subject with the same parameters as above except for the number of slices (72) and TR (6.1s). The whole-brain EPI images were acquired to ensure good co-registration between the functional and whole-brain images (details in the pre-processing section below).

2.2.5 Analysis

Saccade data analysis

A deep neural network framework called DeepLabCut (Mathis et al., 2018) was used to extract eye traces from video recordings of the eye. A threshold of 2°(visual angle) was applied for extracting saccades from these eye traces using Python (version 3.7.10, Python Software Foundation, `https://www.python.org`). Synchronisation errors in the frame grabber made some videos unreliable for analysis (details of number of videos per subject in the results section). Among the videos that were available, some frames were missing randomly which meant that a temporal analysis of these videos was not possible. Hence, we analysed the total number of saccades per run.

Pre-processing

We used SPM12 (Wellcome Trust Centre for Neuroimaging, London, UK) implemented in MATLAB (version R2018a, The MathWorks Inc., Natick, MA, USA) to pre-process the images and later perform a GLM analysis. The first five images at the start of all runs were deleted to allow signals to reach a steady state. This was followed by a re-alignment procedure (as defined in SPM) on the rest of the images. We then co-registered the mean functional image (resulting from re-alignment) with the whole-brain EPI image followed by a co-registration of the whole-brain EPI image with the anatomical image (T1). This was performed for each of the four sessions in a subject, separately, to achieve good registration between the functional images (partial volumes) and the anatomical images. We confirmed the co-registration by

matching the functional images with the anatomical scans in each session. We then normalised the anatomical and functional images to the MNI152 (Montreal Neurological Institute) template. We inspected the co-registration in each subject and manually adjusted the outcome of the automatic co-registration procedure resulting in alignment of all the functional images from the four sessions to one anatomical image (from the first session), in each subject. This was followed by smoothing of all functional images with a FWHM (Full Width Half Maximum) Gaussian kernel of 3mm.

GLM analysis

We used SPM12 for a first-level analysis pooling all the data from the four sessions in each subject. We modified the HRF (Haemodynamic Response Function) parameters to use an onset-to-peak time of 4s which is considered apt for the SC (Wall et al., 2009). A mask of the CSF space adjoining the SC was created for all subjects using MRICron (NITRC, University of South Carolina, Columbia, SC, USA). A mean time course across all functional images per subject was obtained from the mask using Marsbar (`http://marsbar.sourceforge.net`). This mean time course, along-with motion parameters derived from the re-alignment procedure in the pre-processing stage, were used as regressors of no-interest . We used the button press condition and cues as additional regressors of interest. We used movement onset times as onsets in the GLM analysis for the reaching conditions. In the sensory discrimination conditions, button press onsets were used for oddball stimuli, while onsets for non-oddball stimuli and cues were derived by an addition of mean reaction times from the reaching conditions to the onset times of stimulus presentation. This ensured coherence in onsets between conditions. The duration of each of the events was set to 0. The results were analysed centred at our VOI (voxel-of-interest) -6, -28, -6 in MNI (Montreal Neurological Institute) co-ordinates, at a significance threshold of $p < 0.001$, uncorrected.

Time course analysis

Part 1: Heatmap

To analyse the raw data acquired from the experiment in our primary VOI (-6, -28, -6) and the voxels surrounding it in the deep layers of the SC, we created a 3x3x3 grid (forming a cube of 27 voxels) centred around the primary voxel. Next, we extracted the raw time course for each voxel with a high-pass filter of 128 hz. We de-meaned the time courses and used the same regressors of no-interest as in the GLM analysis (motion parameters + mean time course of the CSF mask). We interpolated the time course to 0.1 seconds from the 2s TR (Repetition time) and then resampled the data back to 2s starting from stimulus or movement onsets, as applicable, in each of the four conditions. We selected a time window where we expected the largest signal from the reaching task (4s to 8s), informed by the HRF in the SC. We computed the mean intensity value in the selected time window from every block repetition, resulting in 112 data points per condition per voxel in the grid (used in the permutation test detailed below). We then computed a mean intensity value from the 112 data points per condition from a voxel, and plotted such values for all conditions from all voxels in the grid, as a heatmap (Figure 2.6).

Part 2: Permutation based maximum t-statistic test

The permutation based maximum t-statistic test (referred to from now on as PBMT-S test; adapted from Blair and Karniski, 1993 with n=2000, alpha level – 0.05; the test inherently controls for multiple comparisons) was performed between three sets of conditions: the VM (visuo - motor) condition and its corresponding control condition VS (visuosensory) forming one test pair, the SM (somato - motor) and SS (somatosensory) forming the second, the motor conditions VM and SM forming the third test pair. The procedure began with a permutation of the data points (112 per condition per voxel, see Part 1 for details) between the test pair conditions for each of

the 27 voxels. This was followed by a two-sample t-test between the data points from the two conditions from each voxel. The largest T value from among the 27 voxels was chosen to be a part of a distribution. The distribution of the largest T values after 2000 permutations was used to compute the critical T value at a threshold of $p < 0.05$. T values obtained from testing the condition pairs in a t-test before undergoing permutations were compared against the critical T values. Testing for higher signals in motor conditions relative to sensory ones, voxels with a T value greater than or equal to the critical T value (right tailed) were considered to be significant findings. The VM – SM test pair was the only condition pair where a two-tailed test was performed.

2.3 Results

2.3.1 Behavioural data

Subjects performed reaching movements to targets within the inter-trial interval (ITI) of 2 seconds. The mean reaction time of subjects performing reaching movements towards visual targets was 0.38 seconds with an SD of 0.03 seconds, and that to somatic targets was 0.43 seconds with a SD of 0.06 seconds. The mean reaching duration across subjects was 1.6 seconds with a SD of 0.16 seconds. The reaction times of subjects for button presses towards oddballs among visual targets was 0.52 seconds with a SD of 0.07 seconds and that to somatic targets was 0.68 seconds with a SD of 0.06 seconds. Videos of the hand were monitored online to ensure that subjects complied with the requirements of the task. Due to issues with the frame grabber that we used (details in the methods section), out of 8 runs in subject 1 and 16 runs in the other 4 subjects; 3, 7, 16, 16 and 4 videos respectively were available for saccade analysis (from 46 runs out of a total of 72). The frequency of saccades across all runs was found to be 4.5 per run (runs consisted of 28 blocks with 4 trials each) with the exception of one subject (subject 3) with 11.25. For a relative

understanding of saccades in motor and sensory conditions, only runs with both motor and both sensory conditions were compared. Average number of saccades in runs which consisted of only sensory conditions was 1.875, and in those that consisted of only motor conditions was 0.625, with the exception of subject 3 with 16.25 and 16 saccades respectively. Overall, the results above indicated that there were very few saccades per run, compared to the number of blocks per run among the videos that were available for analysis. Also, the number of saccades per run in the sensory conditions were higher than in the motor conditions. Hence, higher activation in the SC corresponding to motor conditions when compared to sensory conditions could not be attributed to saccades.

2.3.2 GLM results

To validate our measurements, we conducted a pilot study of two sessions with our experimental paradigm that we did not include in the rest of the analysis since they were the only two sessions measured with the motion correction setting in the scanner. Both these sessions consisted of partial volumes that included the Superior Colliculus (SC); one of them was measured vertically and included the motor cortex while the other was measured with scans in a transverse orientation and included the visual cortex. A GLM analysis of these sessions with the conditions combining all reaching movements, and visual stimulation showed activations ($p < 0.05$, FWE corrected) in the contralateral side of the reaching arm in the primary motor cortex and in the primary visual cortex corresponding to visual stimulation (Figure 2.3).

We focused GLM analysis in the SC around our VOI (voxel-of-interest) -6, -28, -6 in MNI (Montreal Neurological Institute) co-ordinates. We chose this region of interest since it was the peak signal location in a GLM group analysis of the SC from an earlier study in the lab on visually guided reaching movements (Himmelbach et al., 2013). The VOI is located in the deep left SC, where a motor signal corresponding to the contralateral reaching arm (right arm in our case) could be expected. Activation

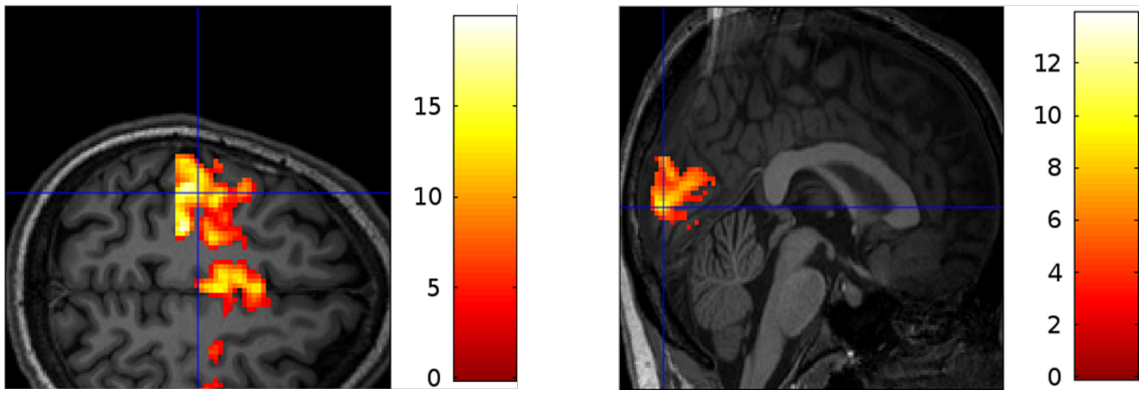

Figure 2.3: *Reliability test for the experiment.*
Activation clusters marked by crosshairs in M1 (fig 2.3. A) and V1 (fig 2.3. B); areas of the cortex responding to reaching movements and visual stimulation respectively in the pilot runs of subject 1.

clusters ($p < 0.001$, uncorrected) were seen in the SC in the motor conditions - VM and SM when contrasted against the baseline (Figure 2.4 A, C) in all 5 subjects. We found no significant activations for the contrasts in the sensory conditions VS and SS against the baseline. Activations were also consistently seen in all subjects when the motor conditions (VM, SM) were contrasted against the corresponding control conditions (VS, SS); Figure 2.4 B, D). Much larger clusters of signal increases are seen in the left SC (contralateral side of the reaching arm) as compared to the right SC across conditions, across subjects. Subjects 1, 2, 4 and 5 show no activation clusters in the right SC in the SM>SS condition (Figure 2.4 D).

To compare signal contributions from the different conditions at our VOI on the contralateral side of the reaching arm - left SC (-6, -28, -6) and its corresponding location in the right SC (6, -28, -6), we plotted contrast estimates (measure of effect size) at both the locations (Figure 2.5). The signal contributions from the VM and SM conditions are seen to be much higher than the VS and SS conditions across subjects. Similarity between signal contributions from the VM and SM conditions can also be observed in the plots. Although there is a large amount of variation in the

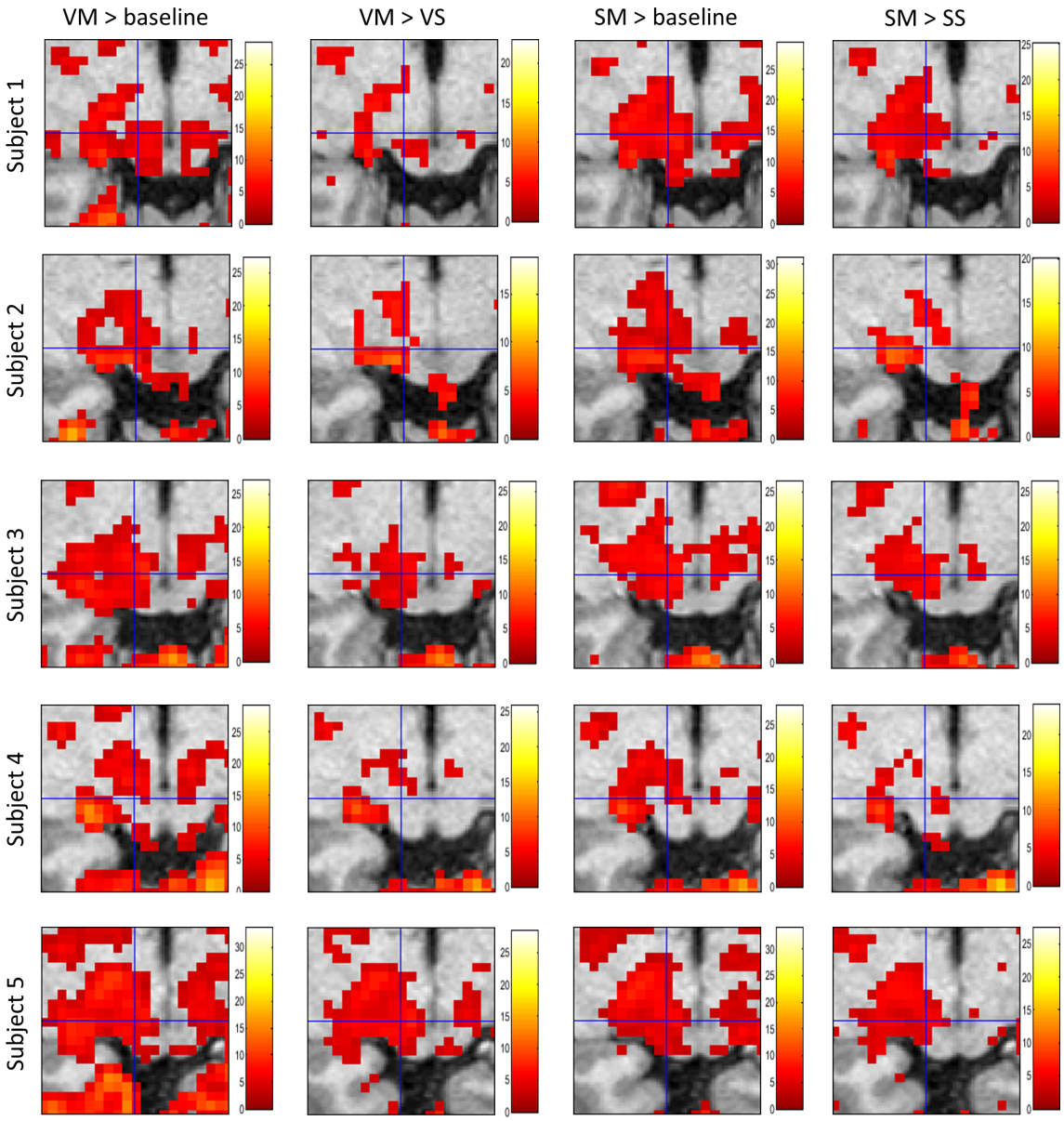

Figure 2.4: *VM and SM show a robust signal when compared to baseline and control conditions.*

The figures show a transverse section of the SC (neurological convention) centred at -6, -28, -6, indicated by the crosshair. Columns show significant signal increases ($p < 0.001$, uncorrected) for the contrasts - VM>baseline (A), VM>VS (B), SM>baseline (C) and SM>SS (D), with each row corresponding to a subject. The colourbar next to each figure denotes the range of T values.

signal amplitude, signal contribution from the button press condition is positive in 4 subjects at the VOI. The signal contributions from button presses at the VOI location ipsilateral to the reaching/button press arm does not show a consistent finding. The signal contribution from cues is fairly consistent in both the VOI and its corresponding location in the right SC.

2.3.3 Time course results

Heatmap

The time course analysis was designed to allow us a deeper understanding of the signal compared to the standard GLM approach while also helping to explore the left SC in more detail, spatially. The mean time courses from the 3×3×3 grid of 27 voxels for each condition in all 5 subjects would have been a substantial number to report. To circumvent this problem, we constructed a heatmap (Figure 2.6) of mean values derived from the time window where the maximum signal could have been expected in the mean time course for each condition (see methods for details). Black lines in the figure separate voxels while white lines separate experimental conditions. The conditions in the heatmap are arranged such that the motor conditions are on the left (upper and lower left squares) and the corresponding control conditions are on the right (upper and lower right squares) in each voxel (Figure 2.6.). A clear pattern of alternating bands of light and dark colours are seen across all subjects indicating that the mean values from the motor conditions (on the left) are higher than the sensory conditions (on the right).

PBMT-S test results

To test the result from the time course analysis empirically, we used a permutation test based on the maximum t-statistic (PBMT-S test). Figure 2.7 shows the results of the test with the map following the same structure as in Figure 2.6. Thick lines

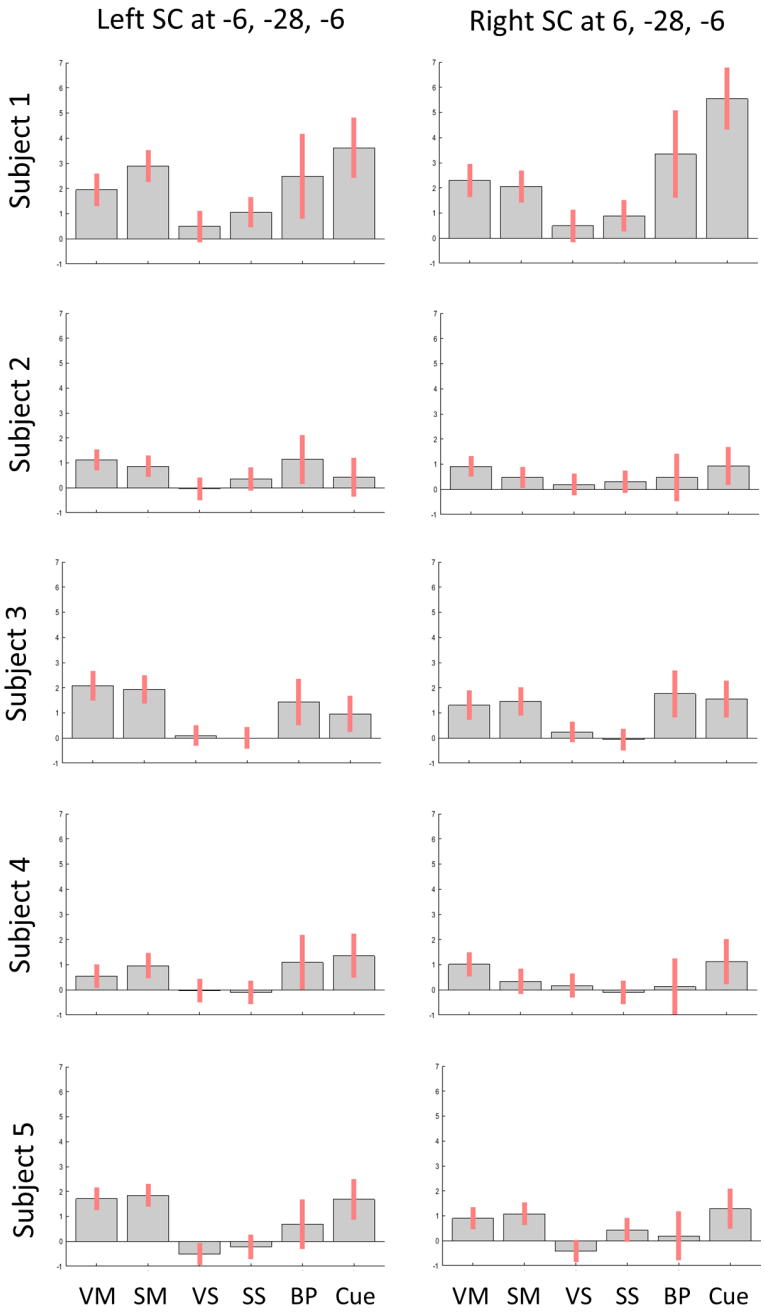

Figure 2.5: *Contrast estimates from the conditions of the experiment at –6, -28, -6 indicate higher signal contributions from the motor conditions.*

Contrast estimates for the four main conditions VM, SM, VS, SS along with estimates for the button presses (bp) are shown from left to right. The red bars indicate 90% confidence intervals (CI).

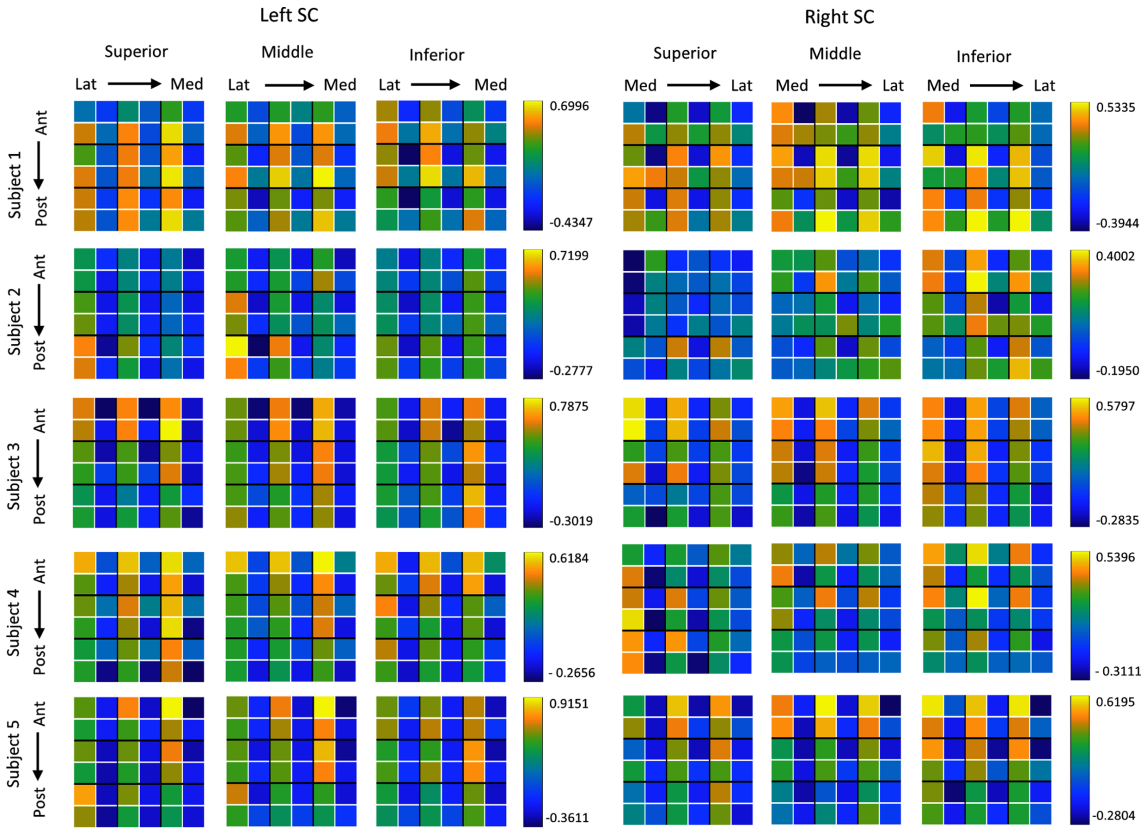

Figure 2.6: *Summary of time courses represented by a heatmap showing higher mean values from motor conditions.*

The three planes of voxels belonging to the 3×3×3 voxel cube centred at -6, -28, -6, were arranged in superior to inferior order. Each of the voxels in a plane were then arranged in anterior to posterior and medial to lateral order. Dark lines demarcate voxels while white lines separate conditions. Out of the four coloured squares in each voxel, going from left to right, top to bottom, the conditions are VM, VS, SM and SS respectively. The colourbar shows the range of mean intensity values.

separate voxels and thin lines separate experimental conditions. The upper half of each representative voxel denotes the condition pair VM-VS, while the lower half denotes the condition pair SM-SS. The condition pairs with a significant finding ($p < 0.05$) in the permutation test have been marked with a star: orange for the VM-VS pair and green for the SM-SS pair. The VM condition shows a significant finding against the VS condition for the central voxel -6, -28, -6 (Left SC) in 4 of the 5 subjects and in an adjacent voxel in the 5^{th} subject, replicating an earlier finding in the lab (Himmelbach et al., 2013). The SM condition shows a response at the central voxel in 3 of 5 subjects, and in adjacent voxels in the other 2 subjects, indicating that somatically guided reaching also elicits a consistent response in the SC. The response towards both VM and SM conditions is more consistent at the VOI compared to its corresponding location in the right SC, across subjects. The results of the third test; a two tailed test between the VM and SM condition pair did not show any differences between the two conditions (see discussion).

Time course plots

The plots in Figure 2.8 show examples of mean time courses across conditions that were used for the analysis detailed above. The x-axis spans the time duration of a block (8.8 seconds) preceded by 6 seconds, and succeeded by the duration of the baseline period – 12 seconds. We chose a time window of 6 seconds before the start of the block to observe the state of the signal before the block began. Figure 2.8 A shows the time courses across subjects from the VOI, -6,-28,-6 in MNI co-ordinates followed by the voxels in the 27 voxel grid with the most significant result in a right tailed t-test between the reaching (VM, SM) and control conditions (VS, SS) per condition. This is followed by the voxels with the least significant result. The time courses that belong to the motor conditions from the VOI and the voxels with the most significant result (Figure 2.8 A, B) show a consistently higher signal temporally aligned with the duration of the block. The signal is seen plateauing in the middle of

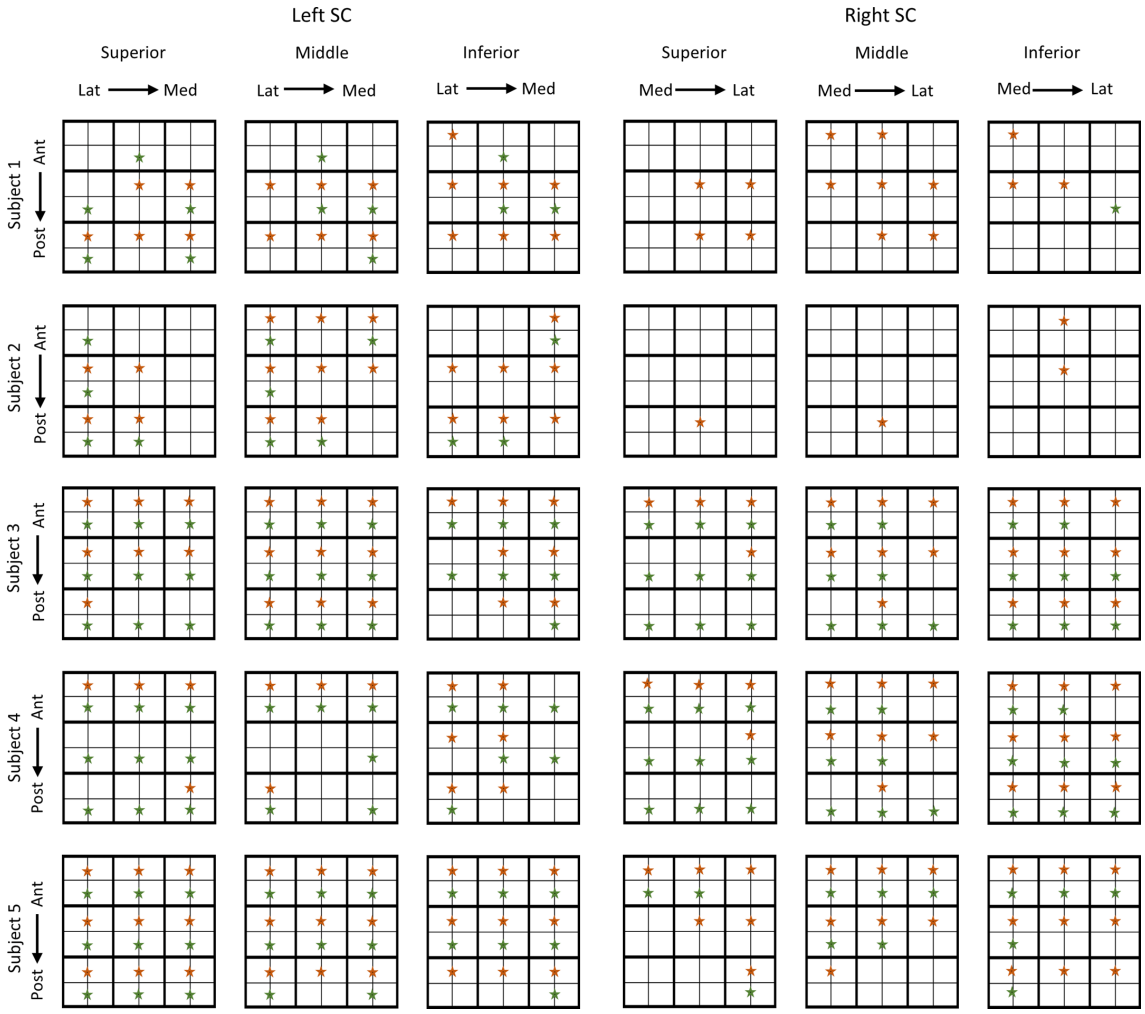

Figure 2.7: *Results of the PBMT-S (permutation based maximum t-statistic) test between the motor and sensory conditions, showing significant voxels from the VM and SM conditions.*

The layout of the map is similar to (Figure 2.6). Thick lines separate voxels while thin lines separate conditions. The significant findings involving the test pair VM-VS are coloured orange while those involving the test pair SM-SS are coloured green. The PBMT-S test, thresholded at $p < 0.05$ inherently controls for multiple comparisons.

the block and begins to dip towards the end of the block. The time courses from the least significant voxels of the grid on the other hand do not show any pattern, apart from a slight positive change corresponding to the visuomotor condition at the start of the block in 4 of the 5 subjects. The time courses of the sensory conditions do not show noteworthy changes throughout the block. The time courses of the visuo-motor and somato-motor conditions follow a similar pattern and do not exhibit large signal differences between them.

2.4 Discussion

Relation to previous studies

Although previous studies have looked at processing of tactile signals in the SC with respect to saccades (Tardif and Clarke, 2002), they have not gone as far as to study if it in some way relates to reaching movements. The only study that related tactile information to reaching is the one by Nagy et al. (2006) which suggests that the SC may be involved in interaction with objects. In this study, neuronal activity was seen in the SC when the hand of a monkey came in contact with an object, with the activity modulated by increased force. The question of whether processing of somatosensory signals in the SC helps in the execution of reaching movements had not yet been probed. All the other studies pertaining to the SC that used somatosensory stimulation have examined it in the context of execution of saccades or orienting movements of the head. Ours is the first study that looks at somatosensory processing in the SC in the context of reaching movements.

There is not much literature on fMRI in the SC. A few studies earlier (for eg. Linzenbold et al., 2011; Wall et al., 2009) have established that BOLD fMRI in the brainstem is reliable. For the current study we borrowed the same protocols and pre-processing procedures as the two previous studies in the lab on reaching in the human SC (Him-

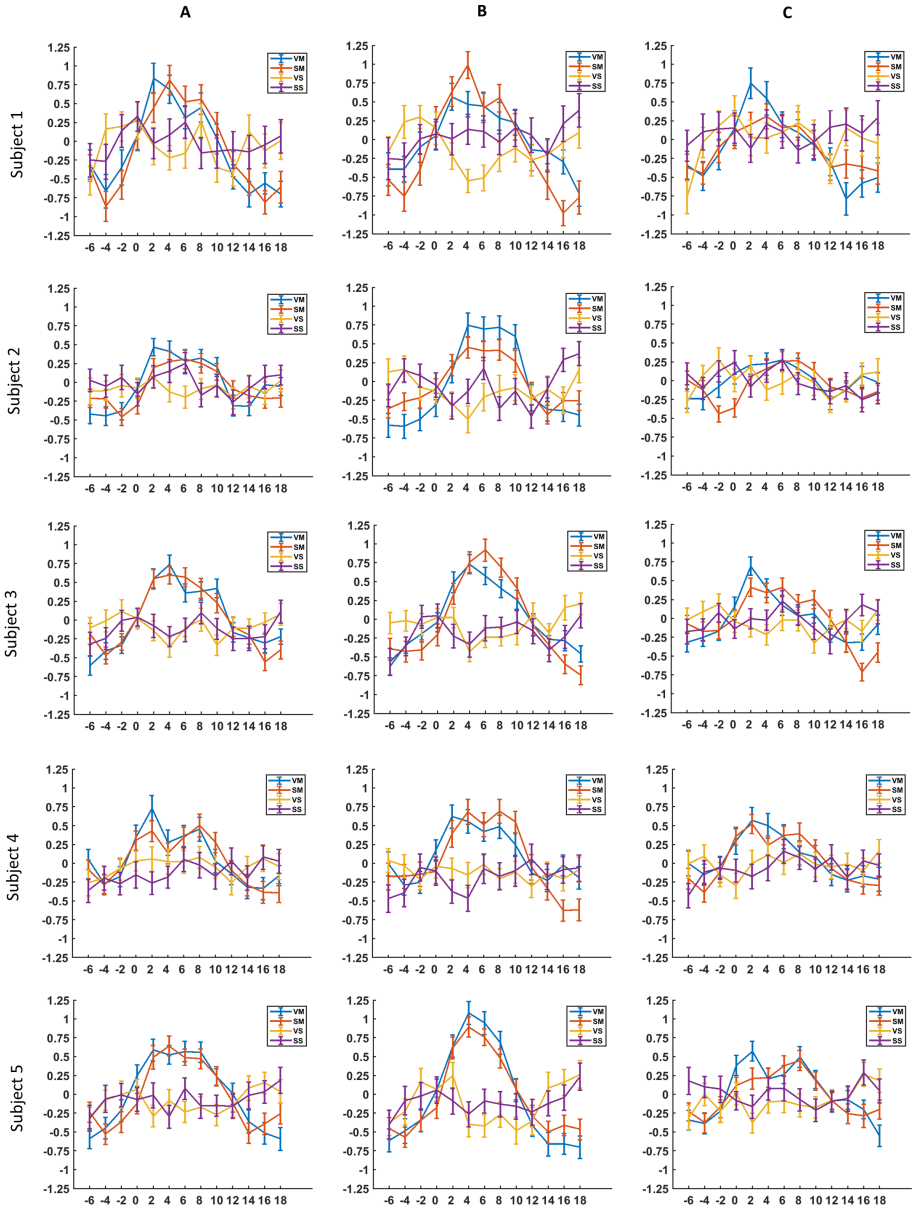

Figure 2.8: *Figure showing averaged time courses from the four conditions at the VOI, most significant, and least significant voxel, from the 27 voxel grid in the SC.*

A – VOI (voxel-of-interest), -6, -28, -6; B, C – voxels with the least p-value (most significant result) and highest p-value (least significant result) from the 27 voxel grid in the SC, respectively. The four conditions from the experiment (VM,SM,VS and SS) are labelled in the legend in the upper right corner. The error bars show standard error (SE).

melbach et al., 2013; Linzenbold and Himmelbach, 2012). The only exception was the co-registration procedure for functional and anatomical scans across different sessions of a subject. In the current study, we first co-registered the mean functional image from each session to its whole-brain T2* image. Next, we co-registered the T2* image from each session with the same anatomical image copied into each session separately. Finally, we normalised the four anatomical images to the MNI template, applied the deformation fields to all the functional images, and checked the registration of functional images with the anatomical image from the first session for inconsistencies. If inconsistencies were found, manual re-orientation was performed on the functional image, followed by application of transformation fields to all the functional images in the respective session. This helped us achieve good co-registration between the structural images and the partial functional volumes that were acquired on different days, as part of each session.

Relevance of this study

With this study, we advanced the understanding of sensory integration towards reaching movements in the SC. The peak voxel that we used for the current experiment was derived from a GLM group analysis from an earlier study in the lab. Since voxel location would not be precise to a single voxel in a single subject GLM analysis, we used a grid of voxels surrounding our voxel-of-interest by one voxel in all directions. In the visually guided reaching conditions the results showed a significant finding in 4 out of 5 subjects for the central voxel and in a neighbouring voxel in the 5^{th} subject, whereas in the somatically guided condition significant findings were seen in 3 subjects at the central location and in neighbouring voxels in the other 2. Although visually guided movements were expected to elicit a response, we are the first to show that somatically guided movements could do the same as well. The response to somatically guided reaching in the SC might be of importance when the somatic stimulation falls outside the purview of vision at the particular moment. This could

be imagined, for example, when a mosquito is felt on the skin and a motor reaction is elicited to swat it, before foveation is initiated.

We contrasted two different analysis methods in this study – GLM analysis and PBMT-S test with time course data. While GLM analysis is suitable for analysing a large number of voxels (cortical regions for example), it is not well suited to analyse individual voxels, especially, when the region-of-interest is very small. One of the main reasons for this is the multiple comparisons problem. Using FWE correction is very conservative for a small number of voxels as in our case (27 voxels). Hence, we used a PBMT-S test (see the methods section for details). This test takes the multiple comparisons problem into consideration and is less conservative than FWE (family-wise-error) correction. The PBMT-S test helps calculate critical T values which can then be used to test significance for conditions contrasted against each other using t-tests. The major difference between the data used in these tests is – the GLM built into SPM takes into account the entire block for the analysis, whereas for the PBMT-S test we used the mean value within a time window where we expected the maximum signal in each block. Using the PBMT-S test allowed us to explore individual voxels around our VOI, and compare them across conditions, something that would not have been possible using FWE correction.

The lack of statistical differences in signals between the motor conditions (VM and SM) seems to indicate that the signal in the SC could be due to reaching, irrespective of the modality guiding it. This result is similar to the study by Groh and Sparks (1996) where they found that almost all the cells in the SC that responded to saccades for visual targets also did so for saccades to somatic targets. A study by (Song and McPeek, 2015) showed that inactivation of the macaque SC impaired target selection in reaching movements. It could be that the SC has a common sensory target selection framework irrespective of modality. Although further studies are needed to establish the nature of the reaching signal that would elicit a response, with this experiment we prove that visual information is not necessary for the representation of reaching

movements in the SC.

Although our results indicate that saccades are not correlated with reaching movements, an argument stating that microsaccdes executed during reaching movements could have caused the activation in the SC, is plausible. An earlier study in macaques by Reyes-Puerta et al. (2010) indicated that 'reach' neurons in the SC show increased activity in reaching trials where trials with microsaccades were excluded. This means that although there is a possibility that a part of the signal could be owed to microsaccades correlated with reaching movements, it is unlikely that the signal is completely due to them.

Limitations and shortcomings

The experiment teases apart activity in the SC towards reaching movements corresponding to visual and somatic targets from that which could have been expected from sensory stimulation alone. Although it is established that a representation for visual or somatic stimulation on their own exists in the SC, we did not see it in our experiment. This could be due to the large distance (9°) between the centre of the four visual targets and the fixation LED. Chen et al. (2019) have shown that responses to visual stimuli in the SC are tightly linked with foveation. Hence, there could have been an under-representation of these peripheral targets. The somatic stimulation was probably too weak and lasted for a very short time for the corresponding activity to be sensitive enough for detection with fMRI in the SC.

The responses to reaching in the SC are not clearly lateralised. This might have to do with the reaching movement directed towards the contralateral arm in our experiment. This is similar to the gaze-independent neurons in the SC responding more strongly to contralateral arm position (Lünenburger et al., 2001).

Future outlook

The evidence presented in the current study points to the SC being more than just an oculomotor or visuomotor structure. It seems to integrate sensory input from a range of modalities towards building its motor responses. This could mean that the SC also plays a role in the generation of movement guided by audition. Studying this would complete the story of the SC being a multi-sensory accumulator of responses towards generation of motor output.

The SC has so far been postulated to be a rudimentary processing centre, with more complex processing being attributed to cortical areas. It would be interesting to examine if the SC exhibits learning with respect to sensory stimulation that it processes, which otherwise is a prerogative of the cortex. Perhaps, it exhibits learning at an elementary level, just enough for it to be able to produce an immediate reactive response that does not require complex processing. What also remains to be seen is if the SC processes and computes all its responses in a retinotopic frame of reference especially when modalities other than vision are used to elicit a motor response.

The current experiment required that subjects press a button in response to oddball stimuli during the sensory trials (VS and SS; control conditions) so that they perform the task attentively. During the GLM analysis, we used these button press timings as a regressor to separate signals associated with it from the signal contributed by passive sensing. Plotting contrast estimates at our VOI -6, -28, -6 revealed a consistent positive signal contribution from the button press trials, even though these trials were eight times fewer in number than the rest of the trials (Figure 2.5). We explored this intriguing finding further in the following experiments.

Conclusion

We detected signal increases in the SC for somatically guided reaching movements in all five subjects. We also reproduced results from earlier work in the lab implicating

the SC in visually guided reaching movements. These results show that the SC integrates somatic information towards realization of reaching movements, without the need for visual inputs. Taken together, these results suggest a role for the SC beyond the visual realm that is has been conventionally confined to, while also opening new avenues for exploration in the integration of sensory information towards reaching movements in subcortical systems.

Chapter 3

Role of the SC in simple and complex finger tapping sequences

3.1 Introduction

The contribution of cortical areas in upper-limb movement generation and execution is well studied, but the role of sub-cortical areas in these networks is hardly known. With the SC being a fast detection and early response system towards stimuli in the environment that need a response (Soares et al., 2017), presumption of its role in upper-limb movements is plausible. With two earlier experiments in the lab on the correlates of reaching in the human SC (Himmelbach et al., 2013; Linzenbold and Himmelbach, 2012), and with the first study in this thesis (Chapter 2), it has been shown that the human SC plays a role in reaching movements. A question that could be asked at this point is if the SC's role in limb movements is restricted to reaching or is it more generic? Does it take part in more simpler movements as well?

Firstly, for the SC to be recognized as a part of the motor network, it is imperative to investigate if it also responds to simple movement tasks used to map motor areas in the network. Secondly, the responses in the SC towards infrequent single taps of the finger corresponding to visual stimuli in the first experiment called for an investigation of finger tapping in the SC with a more thorough paradigm designed primarily to elucidate such a response. Lastly, earlier studies (for example, Borra et al., 2014) have indicated a connection between the SC and the premotor cortex; whose role in hand and finger movements has been well established. Hence it is plausible

that a co-activation could be found between the SC and the dorsal pre-motor cortex (PMd), a structure known to play a role in the execution of motor sequences.
The two parts of the current study, were designed to investigate if the SC responds to simple and complex finger tapping tasks that have been used to generate motor maps of the brain. If the SC plays a role in finger tapping sequences it would have to be considered as one of the key centres of the brain necessary for movement control.

Part I

For the first part of the study we used a dataset generated by the Human Connectome Project (HCP). The HCP task fMRI dataset consists of a large number of subjects, tested on a battery of tasks, as a part of their endeavour to map the myriad functions of the brain. For this study we used the motor task dataset. Here, they used a task modified from a study by Buckner et al., 2014 consisting of right and left-toe movements, right and left hand finger movements, and movements of the tongue. We only used finger tapping movements from 130 subjects for our analysis. We started with an a-priori hypothesis of finding activation in the SC at the voxel with the highest T value from the finger tapping task of the first experiment (Chapter 2). The averaged voxel across the 5 highest T values from the 5 subjects in the first experiment turned out to be -6, -28, -6 in MNI (Montreal Neurological Institute) co-ordinates located in the deep left SC. This location which happened to be the same as the one used for the reaching experiment (Chapter 2) formed our VOI (voxel-of-interest) for the rest of the analysis. A second-level GLM analysis of the HCP data showed activation clusters in M1 ($p < 0.05$, FWE i.e. family-wise-error corrected) when the finger tapping tasks were tested against the baseline, but no activations were seen in the SC. We also modelled the cue presented before each block which showed a consistently significant response on both sides in the SC.

Part II

The null result from the analysis of the HCP dataset necessitated that the SC be tested more thoroughly, including with a finger tapping task of increased complexity since this would involve higher-order processing. The HCP dataset also had a few other shortcomings that had to be addressed with a new paradigm and experimental controls (see discussions for details). For this study, we designed a paradigm with simple and complex finger tapping tasks (adapted from Kuhtz-Buschbeck et al., 2003) guided by visual and auditory pacing. The complex finger tapping task was included in the paradigm to investigate if the interactions between the SC and premotor cortex could potentially elicit a response for sequential tasks. Pacing stimuli were used to increase compatibility and uniformity of movements as advocated by Witt et al. (2008). The use of auditory and visual stimuli would have also potentially differentiated activation clusters in the SC, depending on the sensory modality that was used to guide these movements. GLM analysis results showed robust activation clusters in M1 and PMd. GLM analysis centred at the VOI -6, -28, -6 showed a response in the SC for the cue condition but not for the tapping conditions. Time course analysis in M1 and PMd showed a substantial rise, plateau, and dip temporally aligned with the finger tapping blocks. However, in the SC there was no difference in signal between the block period and thereafter. Hence, we conclude that the SC does not play a role in the execution of sequential finger tapping movements

3.2 Methods: Part 1

3.2.1 Subject details

We conducted the study on 130 subjects from the HCP database that had a complete dataset for the motor task (73 females and 57 males, age range 22 -36 years, 10 left-handed and 120 right-handed) with normal or corrected-to-normal visual acuity. All

experimental procedures were approved by Washington University (for more details, refer to the HCP database; link below).

3.2.2 Experimental setup and paradigm

The motor task consisted of 13 blocks per run. 10 of them were movement blocks, with 3 interspersed fixation blocks. Each movement block lasted 12s and consisted of 10 movements. A movement block could consist of tapping the fingers of the left hand or the right hand, or squeezing of the left or right toe, or a movement of the tongue depending on a 3 second cue that was shown just before the start of the block. The 10 movement blocks were split into 2 tongue movements blocks, 4 hand movement blocks (2 right and 2 left) and 4 foot movement blocks (2 right and 2 left). The 3 fixation blocks in a run lasted 15s in duration. 2 runs comprising of the 13 blocks were measured from each subject. (The HCP also provides a database of a range of tests including alertness, cognitive and psychological functions of the subjects. For further details refer to `https://wiki.humanconnectome.org/display/PublicData/HCP-YA+Data+Dictionary-+Updated+for+the+1200+Subject+Release`)

3.2.3 fMRI data acquisition

Data acquisition was performed at Washington University using a modified 3T Siemens Skyra MRI scanner. A 32-channel head coil was used for the whole-brain acquisition of functional measurements (Gradient echo - EPI) with a TR = 720 ms, TE = 33.1 ms, flip angle = 52°, FOV = 208, 72 slices, with a voxel resolution of 2.0 mm isotropic, and a multi-band acceleration factor of 8. The two runs in each task were measured with opposing phase-encoding directions of right to left and left to right respectively. Physiological parameters were available in the HCP dataset but were not considered for our analysis. The structural images were acquired with a 3D MPRAGE sequence TR = 2400s, TE = 2.22ms, flip angle = 8°, FOV = 224 x 224 mm (320 x 320 matrix) and a voxel resolution of 0.7 mm

isotropic. For further details on imaging protocols of the HCP, please refer to `https://www.humanconnectome.org/hcp-protocols-ya-3t-imaging`

3.2.4 Data analysis

Peak co-ordinate for finger tapping

In the reaching experiment (Chapter 2), the SC elicited a response towards finger tapping (recorded as button presses) corresponding to oddball stimuli that were shown in the control conditions. We wanted to find a voxel in the SC with the highest response for finger tapping. Since the boundaries of the SC are not clearly demarcated, we extracted a set of voxels spanning one voxel on all sides of the VOI and its corresponding location in the right SC. This led to a 3x3x3 grid of 27 voxels on both sides in the SC, with the voxel we began from at the centre of the grid. We then examined the two grids of voxels to find the voxel with the highest t-value in the finger tapping condition of the reaching experiment (Chapter 2; labeled as 'bp') and then averaged these voxel co-ordinates across subjects. The resultant voxel was found to be -6, -28, -6 (in MNI co-ordinates; left SC) and would be a voxel with the highest probability for finding a response corresponding to the finger tapping condition. Hence, the voxel which also happened to be the VOI in the reaching experiment was used as the VOI for the current study and the next (Chapter 4). In addition, we also examined results at the corresponding location of the VOI in the right SC: 6, -28, -6.

Pre-processing

We used the 'minimally pre-processed dataset' that was available with the HCP consortium. This data had already undergone pre-processing procedures like realignment, co-registration and normalisation except for smoothing (for details refer to Glasser et al., 2013). We smoothed the data with a full-width half-maximum (FWHM) Gaussian kernel of 3.0 mm.

GLM analysis

The first-level model in the HCP data consisted of block onsets for the cue, left hand finger movements, right hand finger movements, left toe movements, right toe movements and tongue movements. The regressors were built with a block duration of 12s. The HCP data consisted of 12 re-alignment parameters out of which the first 6; corresponding to 3 directions and 3 rotations of movement, were used as regressors of no-interest. 6 additional parameters which were the temporal derivatives of the initial 6 parameters were available but were not used for the analysis, for congruence with the analysis in the reaching experiment (Chapter 2). Contrasts were then built with all the conditions in the experiment compared against the baseline. The second-level model was built with the contrasts of interest – cue, left hand and right hand finger movements. We used a modified HRF function with a lower onset-to-peak time of 4s that would suit GLM analysis in the SC (Wall et al., 2009). All results were examined at the VOI -6, -28, -6 at a threshold of $p < 0.001$.

Time course analysis

The time course analysis toolbox rfxplot (Gläscher, 2009); run on MATLAB, was used to generate time courses. The mean time courses for the voxel from three conditions: cue, right hand, and tongue were computed after interpolation to 1s from a TR (repitition time) of 0.720 s. These time courses were plotted in a time interval of 6 seconds before the onset of the blocks/cue to 12 seconds after onset (duration of the block).

3.3 Methods: Part 2

3.3.1 Subject details

We conducted the study using 3T BOLD fMRI with four right-handed healthy volunteers (2 females, 2 males, age range – 25 to 32 years) with normal or corrected-to-normal visual acuity. Each subject performed the experiment four times, one session per day. The experiments were conducted with the approval of the local ethical committee and as per the ethical standards established by the 1964 declaration of Helsinki. Informed consent was obtained from all participants.

3.3.2 Experimental setup and paradigm

Subjects held a button box in their right hand consisting of four buttons and wore headphones before they lay their heads in the head-coil of the scanner. We placed cushions made specially for fMRI experiments (NoMoCo Pillow, Inc., La Jolla, USA) in the head-coil of the scanner to immobilise the head of the subjects. Two MR-compatible cameras (MRC systems GmbH, Germany) operating at 30 Hz; one to monitor finger movements and the other to monitor eye movements, were attached to a stand (same as the reaching experiment; Chapter 2) that was placed across the waist of the subject. Fibre optic cables carrying light from three LEDs; a white fixation/pacing LED, a green cue LED and a red cue LED were attached to the uppermost central part of the stand. Subjects saw the optic fibre endings through a mirror attached to the head-coil. Auditory pacing stimuli were delivered through headphones. The entire experimental paradigm including stimulus delivery and control of timing was established by programming a 'MBED LPC 1768' microcontroller (Arm Limited). All the analyses were carried out using MATLAB (version R2018a, The MathWorks Inc., Natick, MA, USA). In addition, MATLAB also acquired images from the two cameras which were connected to a frame grabber (Matrox Imaging) attached to a

computer.

We trained subjects to pace finger tapping in accordance with visual or auditory stimuli, just before the experiment began, until they were successfully able to match two blocks of stimuli with finger tapping in a row. Subjects were able to accomplish this in a maximum of 10 minutes. Finger tapping could have been of two kinds – simple or complex finger tapping. Simple finger tapping involved pressing of one of the four buttons paced by cues while complex finger tapping involved repetitions of the four buttons; 2 times first button (index finger), 4 times second button (middle finger), 1 time third button (ring finger), 3 times fourth button (little finger) followed by finger tapping in the reverse order starting from the little finger (task adapted from Kuhtz-Buschbeck et al., 2003). The simple and complex finger tapping sequence blocks were informed by a cue of 1s duration. A green LED cued the simple finger tapping block and a red LED cued the complex finger tapping block. For the simple finger tapping task, the green LED also cued the finger (any of the four) to be used in the impending block with the number of times it blinked i.e. one blink for the first finger (index finger), two blinks for the second finger (middle finger) and so on. Block pacing stimuli were of two kinds - visual and auditory, and were presented at 2Hz with either a blinking white LED or a 'beep' delivered through headphones, respectively. The scanner room was completely darkened by covering windows and scanner displays with black opaque film. Subjects were required to fixate on the central fixation light throughout the experimental run time of around 10 minutes per run. The two modalities – visual and auditory; along with the two types of responses – simple and complex finger tapping; were put together in a 2×2 factorial design (Table 3.1). This resulted in 4 conditions: visual simple (VS), visual complex (VC), auditory simple (AS) and auditory complex (AC), two of them being part of each run, with one common factor. The four runs thus formed: AS-VS, AC-VC, AS -AC and VS-VC, were ordered in a Latin square arrangement to control for sequence effects. The two conditions in each run alternated as 20s blocks of 40 trials followed by a

fixation baseline of 15.5s. This resulted in 320 trials per condition and 2560 trials per condition, over all four sessions.

	Visual	**Auditory**
Simple (finger tapping)	Visual-simple (VS)	Auditory-simple (AS)
Complex (finger tapping)	Visual-complex (VC)	Auditory-complex (AC)

Table 3.1: *Experimental conditions arranged in a 2x2 factorial design.*
The two tasks - simple and complex finger tapping, and the two modalities – visual and auditory, made up the four runs of the experiment.

3.3.3 fMRI data acquisition

We performed the measurements using a 3T Siemens Prisma scanner with a 64-channel head-coil. 258 functional images (T2* weighted) were acquired as part of each run – interleaved BOLD imaging of 28 slices in a coronal orientation covering the pre-motor areas and the brainstem, bilaterally. The images were acquired at a resolution of 2 mm isotropic with a TR = 2360 ms, TE = 35.0 ms, flip angle = 90°, FOV = 180 mm x 180 mm (90 x 90 matrix) and a phase encoding direction of foot to head. At the end of each imaging session a whole-brain EPI image was acquired to aid in co-registration with the functional partial volumes. A structural image (T1 weighted) was acquired per subject using an MP-RAGE sequence with a resolution of 0.8mm isotropic and TR = 2400 ms, TE = 2.22 ms, flip angle: 8°, FOV = 240 mm x 256 mm (300 x 320 matrix).

3.3.4 Data analysis

Saccade data

Eye videos were converted into eye traces with the help of a deep neural network framework called DeepLabCut (Mathis et al., 2018). Saccade data with a threshold of 2°(visual angle) were extracted from these eye traces using Python (version 3.7.10, Python Software Foundation, `https://www.python.org`). Synchronisation errors in the video frame grabber meant that a lot of videos were unreliable for analysis. Even among those videos that were written to disk, missing frames did not allow for a temporal analysis of saccades in the video. Hence, we have reported the total number of saccades per subject per run.

Pre-processing

Pre-processing and the following GLM analysis was carried out using Statistical Parametric Mapping (SPM12, Wellcome Trust Centre for Neuroimaging, London, UK), which was implemented in MATLAB (version R2018a, The MathWorks Inc., Natick, MA, USA). During an inspection of the images converted into the Nifti format we observed that some runs had distorted images. Such runs with image artifacts, along with those where button press timings were not reliable due to technical errors, were discarded from further analysis. A list of excluded runs is shown in Table 3.2. Thus, the number of runs that underwent further analysis were all 16 runs from the first subject, 12 runs from the second, 12 runs from the third, and 15 runs from the last subject (55 runs in total). We deleted the first five images from all runs to allow scanner signals to reach a steady state. The rest of the images underwent a re-alignment procedure as defined in SPM, correcting for motion. The co-registration procedure was modified from the procedure used in the reaching experiment (Chapter 2). First, the mean EPI scans from each of the sessions in a subject were co-registered with the whole-brain EPI scan of the respective session. Next, the whole-brain EPI scans from

all sessions of a subject were co-registered with the whole-brain EPI image from the first session of the subject. Lastly, the whole-brain EPI scan from the first session was co-registered with the structural image, followed by an inspection for conformity between the mean functional scans across sessions with the respective structural image. Mis-aligned images were first manually oriented with the structural images before undergoing normalisation with a MNI152 (Montreal Neurological Institute) template. This resulted in good co-registration between the functional images, structural images and the template. The images were then smoothed with a full-width half-maximum (FWHM) Gaussian kernel of 3mm.

Subject	Session	Run	Exclusion criterion
2	1	1	Artifacts
	1	2	Artifacts
	1	3	Artifacts
	1	4	Artifacts
3	1	1	Missing button presses
	2	2	Artifacts
	2	4	Artifacts
	4	4	Missing button presses
4	3	4	Last 16 images were excluded due to artifacts
	4	4	Missing button presses

Table 3.2: Runs excluded from analysis due to artifacts in images or missing button press recordings.

GLM analysis

A first-level analysis was performed using SPM12 with a dataset that included all sessions from each subject. Motion parameters (the first six) from the re-alignment

step of the pre-processing stage were used as regressors of no-interest. We also used a modified HRF function for the analysis to suit the SC (onset-to-peak time of 4s; Wall et al., 2009). The first level model was designed with block onsets from each condition: Visual simple (VS), Visual complex (VC), Auditory simple (AS) and Auditory complex (AC) along with block durations, as regressors of interest. Contrasts were built to examine results ($p < 0.001$, uncorrected) for each of the conditions against the baseline, followed by simple tasks against the corresponding complex condition. An Omnibus F-contrast was also built to examine activity in the SC ($p < 0.001$, uncorrected) from all conditions together. All the results were examined at the VOI (voxel-of-interest) -6, -28, -6 and compared with those at the corresponding location in the right SC, 6, -28, -6.

Time course analysis

To examine time courses in the area surrounding our VOI -6, -28, -6 we built a grid consisting of one voxel on all sides of the VOI. This gave rise to a 3x3x3 grid of 27 voxels with the VOI at its centre. Raw time courses spanning all sessions from a subject were extracted from each of these voxels. The raw time courses were then de-meaned across sessions, regressed with motion parameters and high-pass filtered at 128 Hz. The time courses were interpolated to 0.1 s (data had a TR of 2.36 s) and later re-sampled to 2 s intervals aligned to the start of each experimental block. The time courses were then separated by conditions using their respective block onsets. A mean time course with standard error was computed for each condition, and plotted together with the other conditions from the voxel in a time interval of 6 seconds before block onset to 34 seconds after block onset (block duration + fixation baseline). The same procedure was applied in plotting time courses of voxels from M1 and PMd.

3.4 Results : Part 1

We first present the results of a second-level GLM analysis of right and left hand finger tapping conditions from 130 subjects ($p < 0.05$, FWE corrected). The simple and complex tapping conditions were pooled together for the analysis (Figure 3.1). Finger tapping conditions are expected to show robust activation clusters in the primary motor cortex (M1) (see Witt et al., 2008 for a meta-analysis). The crosshair in Figure 3.1 A has been centred on the global maximum -38, -22, 50 in the left M1 corresponding to right hand finger tapping. Note that there is no activation in the analogous location in the ipsilateral hemisphere (right M1; Figure 3.1 2B). The crosshair in Figure 3.1 B has been centred on the global maximum 42, -16, 50 in the right M1 corresponds to left hand finger tapping. Also note that there are no activation clusters in the analogous location on the ipsilateral side (left M1; Figure 3.1 2B). The global maxima in both the left hand and right hand finger tapping conditions pointing to activation clusters in the right and left M1 respectively, showed that the dataset produced predicted results and hence could be proceeded with for an analysis directed at the SC.

We examined second-level GLM analysis results for the three conditions of interest: cue, left hand finger tapping and right hand finger tapping at our VOI -6, -28, -6 (see methods for details) and at the corresponding location in the right SC: 6, -28, -6 with a significance threshold of $p < 0.001$, uncorrected. We chose these three conditions out of a total of six conditions available in the dataset (see methods) since these were the only conditions for which we expected a response in the SC. We expected a signal in the SC for cue presentation since it is a profound visual stimulus. We observed a very strong response for the cues but found no response whatsoever for the right- and left hand finger tapping movements (all conditions compared against the baseline) in either the left or right SC (Figure 3.2). These results indicate that the SC shows

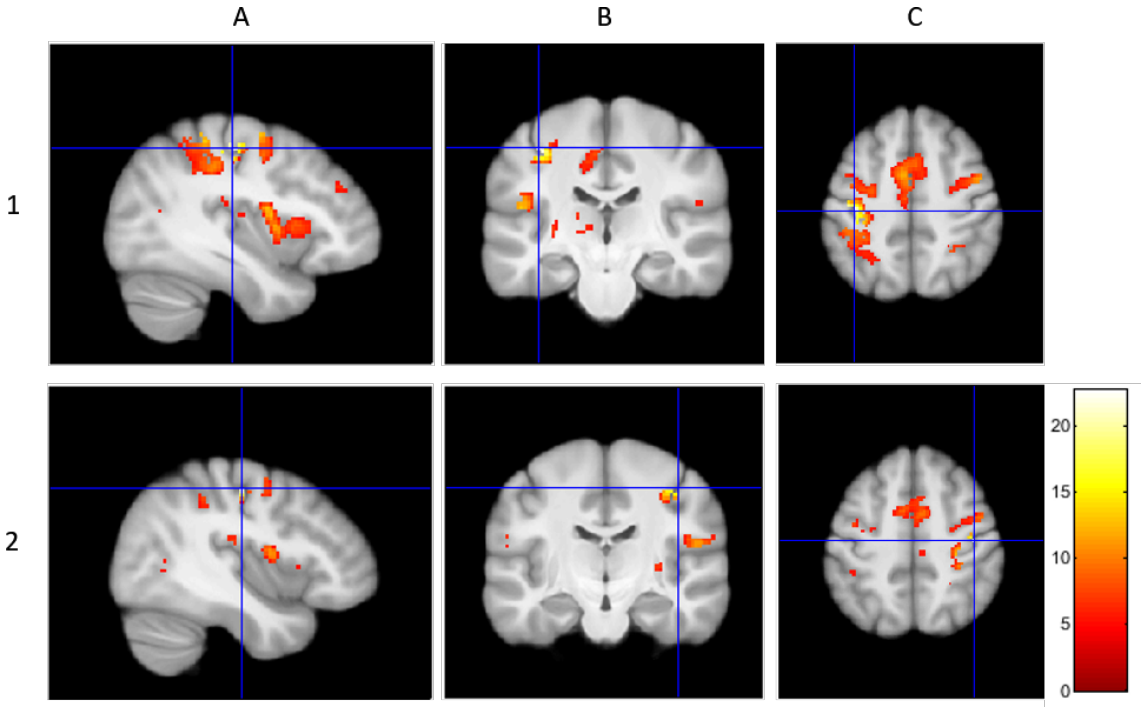

Figure 3.1: *Reliability test.*

Second-level GLM analysis results centred on left (panel 1) and right M1 (panel 2) corresponding to right and left hand finger tapping respectively. The co-ordinates that the crosshairs have been centred on; -38, -22, 50 in panel 1 and 42, -16, 50 in panel 2 are the global maxima for right and left hand finger tapping respectively ($p < 0.05$, FWE corrected). The three columns show images in sagittal, coronal and transverse orientations (A, B and C). The colourbar shows the range of T values.

activation in response to visual stimuli (cues) but not to finger tapping conditions.

Next, we plotted contrast estimates (shows effect size) at -6, -28, -6 and its corresponding location in the right SC: 6, -28, -6 between the three conditions: cue, right hand and left hand finger tapping (Figure 3.3). This allowed us to examine the difference in signal contributions from the three conditions. The results showed a large signal contribution from the cues compared to right and left hand finger tapping. The signal contribution from the cues is slightly higher at the VOI (left SC) compared to the right. The signal contribution from right and left hand finger tapping conditions is insignificant at both the locations. These results reiterate the findings from the second-level GLM analysis shown earlier.

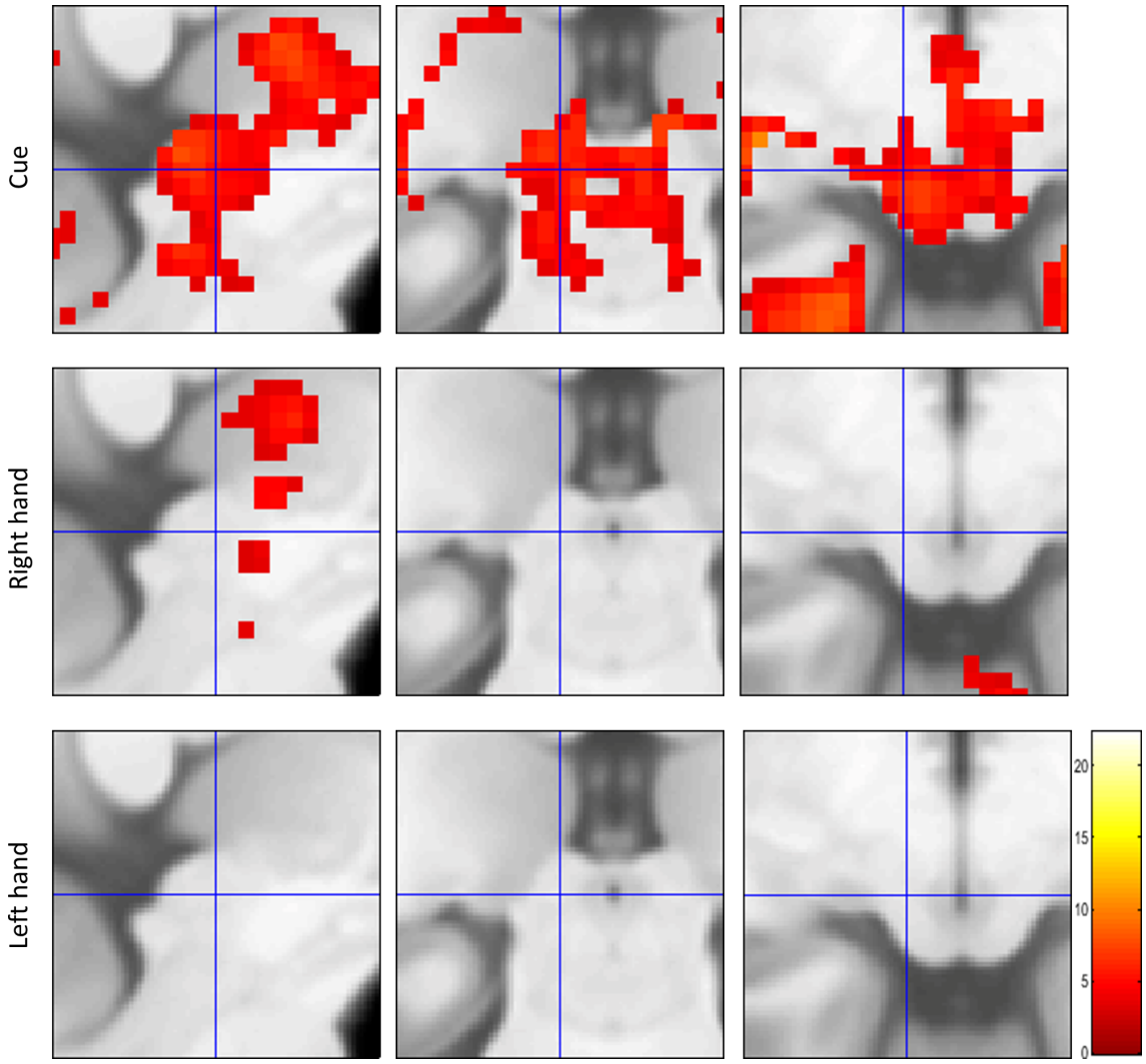

Figure 3.2: *SC responds to cues but not to finger tapping.*

Second-level GLM analysis from the cue, left hand and right hand finger tapping conditions compared against the baseline ($p < 0.001$, unc); centred on the VOI -6, -28, -6. No activation clusters are present in both left and right SC. The colourbar shows the range of T values.

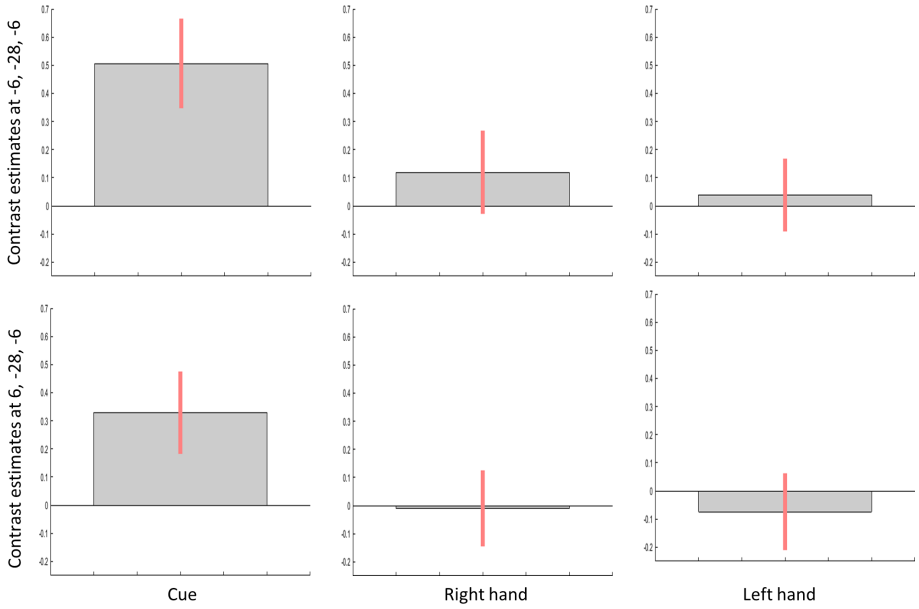

Figure 3.3: *Only cues show a strong signal contribution at the VOI.*
Signal contributions from the three conditions – cue, right and left hand finger tapping at the VOI -6, -28, -6 and its corresponding location in the right SC: 6, -28, -6. Error bars indicate 90% confidence intervals (CI).

3.5 Results: Part 2

3.5.1 Behavioural data

We monitored fixation, obeyance to cues and finger tapping (recorded as button presses) while the experiments were being conducted. We also verified this offline and found that subjects pressed the requisite number of buttons adhering to the sequence, for every block. Out of a total of 55 runs from the 4 subjects, eye videos from 44 runs were available for analysis i.e. 12, 10, 12 and 10 videos respectively, from the 4 subjects. A mean of 1.6 saccades were made per run (28 blocks; 4 trials per block) across subjects with the exception of subject 4 with a mean of 15.6 saccades per run.

3.5.2 GLM results

To ensure that the experimental paradigm elicited a response in well-established motor areas we first examined results from the hand knob in M1 (primary motor cortex) and PMd (dorsal pre-motor cortex). The co-ordinates corresponding to the hand knob in M1 (Figure 3.4) were localised by visual inspection to be the centre of the omega-shaped structure on the pre-central gyrus. The PMd co-ordinates were derived by plotting the local maximum closest to the peak co-ordinates in PMd, obtained from 118 subjects published in the meta-analysis by Mayka et al., 2006. The PMd co-ordinates thus obtained were verified to lie within the boundaries of the PMd as described in Mayka et al., 2006. Figure 3.4 shows the co-ordinates (one each for M1 and PMd) for each subject on which all the four conditions have been centred with a threshold of $p < 0.05$, FWE corrected. The results show a robust response corresponding to all four task conditions in both the M1 and PMd. This ensured that the tasks conditions were well-suited to examine responses towards finger tapping in the SC.

Next, we examined results in the right SC at our VOI -6, -28, -6 derived from the reaching experiment (see methods section of Part I for details) and in the corresponding location in the right SC: 6, -28, -6. We first ensured that we saw a response in the SC corresponding to the visual stimulation from the cue, as seen in the HCP data (Part I of this chapter). Figure 3.5 shows the results of a first-level analysis using a T contrast against the baseline for the cue condition in all the four subjects ($p < 0.001$, uncorrected). Subject 2 and 4 show a strong response to cues in the SC. Subject 1 shows a weaker response while subject 3 shows the weakest response.

Having found activation in the SC for cues, we examined results at the same VOI in all the four finger tapping conditions (AS, VS, AC and VC) using a T contrast against the baseline ($p < 0.001$, uncorrected). We did not see any response in the SC crossing the threshold. We then used an F-contrast adding all the finger tapping

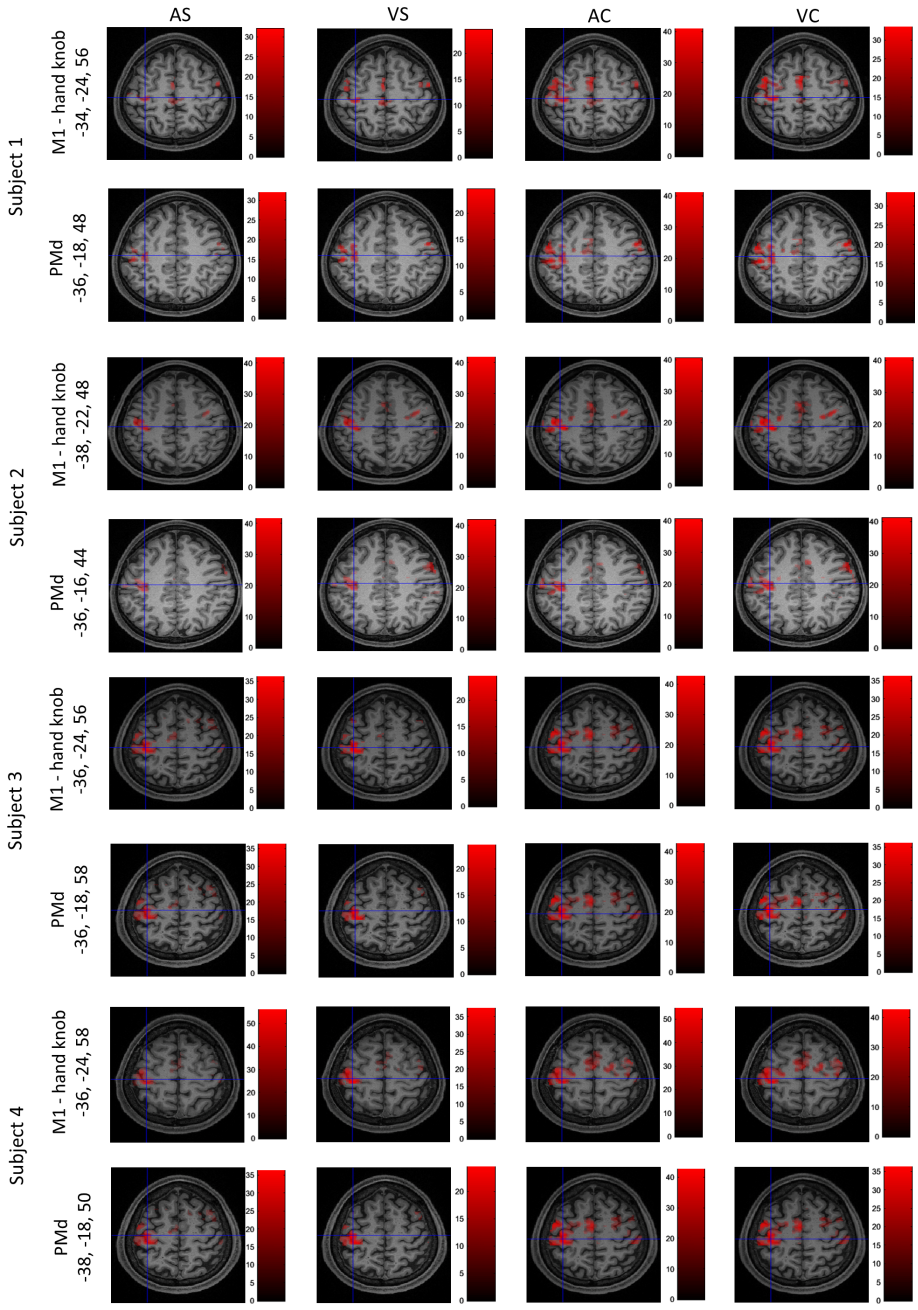

Figure 3.4: *Reliability of the paradigm.*

Activation maps with crosshairs centred on the hand knob area of M1 and the local maximum in the PMd across all 4 subjects. T-contrasts for the four conditions:auditory simple (AS), auditory complex (AC), visual simple (VS) and visual complex (VC) thresholded at $p < 0.05$, FWE corrected. Colourbars show the range of T values.

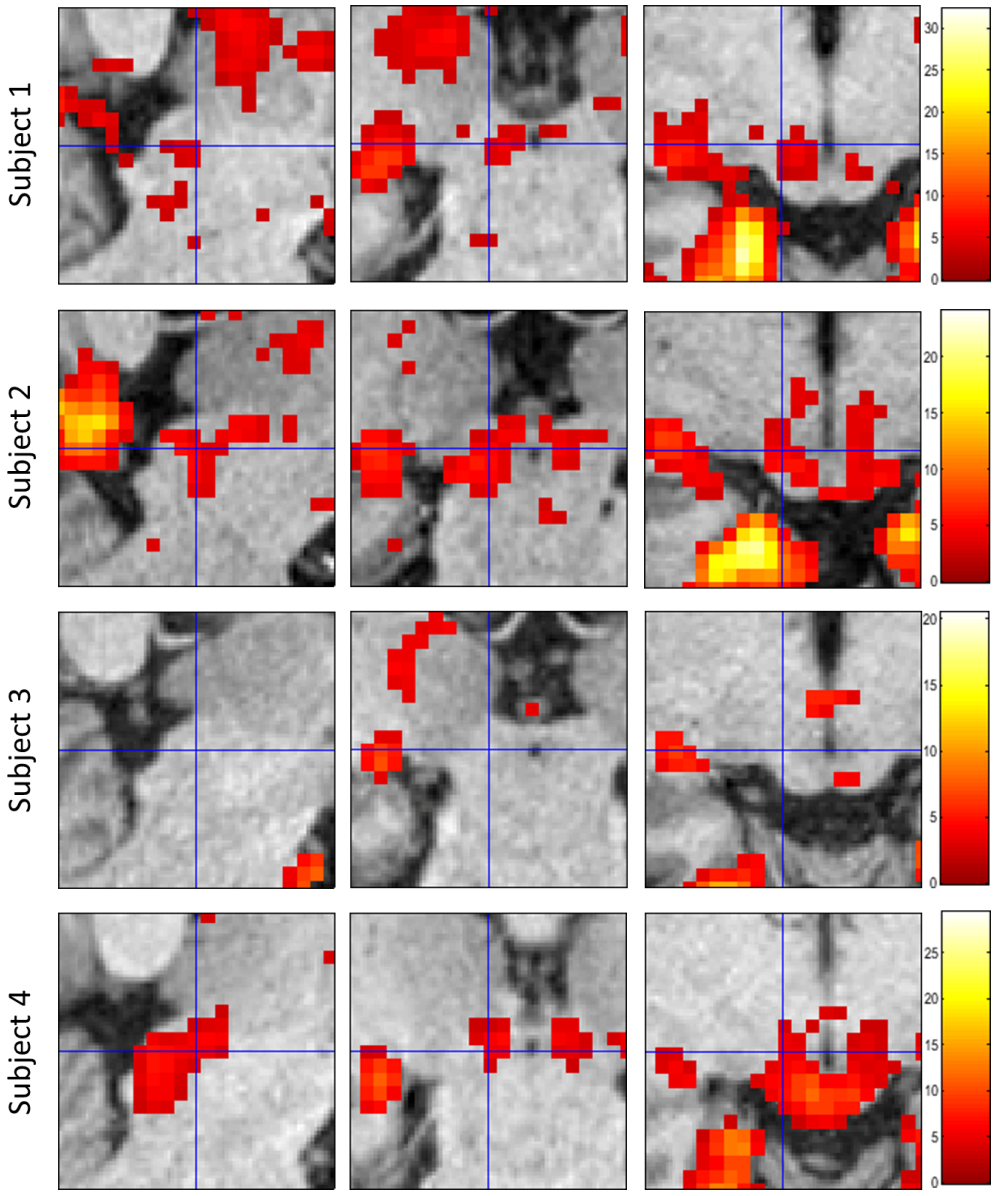

Figure 3.5: *Cues elicit a response in the SC.*

The three panels show the results of a first-level GLM analysis corresponding to cue>baseline in the sagittal, coronal and transverse sections of the SC centred on the voxel-of-interest -6, -28, -6 at a threshold of $p < 0.001$, unc. Colourbars show the range of T values.

conditions together to look for any activation in the SC corresponding to finger tapping (Figure 3.6) using the same threshold of $p < 0.001$, uncorrected. Here again, all four subjects did not show any response whatsoever.

Plotting the contrast estimates (measure of effect size) at the VOI and at the corresponding location in the left SC in all four subjects shows strong signal contributions only from the cue condition Figure 3.7. All of the four finger tapping conditions do not contribute to the signal.

3.5.3 Time course plot

To compare time courses corresponding to the four conditions in the SC, M1 and PMd we plotted them together in Figure 3.8. The mean time courses in the SC are from our voxel-of-interest whereas those from M1 and PMd are the same as the voxels from the earlier figure (Figure 3.4). The X-axis (Figure 3.8) shows time in the range of -6 seconds before onset (0 seconds) to 34 seconds after onset. A time window of 34 seconds was used since the block duration was 20 seconds followed by a baseline period of 15 seconds. The Y-axis shows the mean intensity values from the voxel. The slight rise in signal at the start of the block in the SC could be contributed to by the cues since these were shown 1 s before the start of the block. The highest peak among the time courses is seen in the PMd, followed by M1. The time courses in M1 rise with the onset of the block, reach a plateau, then gradually fall with the end of the block. A slightly higher peak is seen corresponding to complex tapping tasks compared to simple ones in 3 of 4 subjects. The time course in PMd also follows a similar trend as in M1 but with a more clear distinction between simple and complex tapping tasks. Complex finger tapping tasks, as expected, reach a much higher intensity in PMd than simple tapping tasks. In contrast to time courses in M1 and PMd, there seems to be no distinction in signal between the block and baseline time periods in the time course of the VOI and its corresponding location in the right SC.

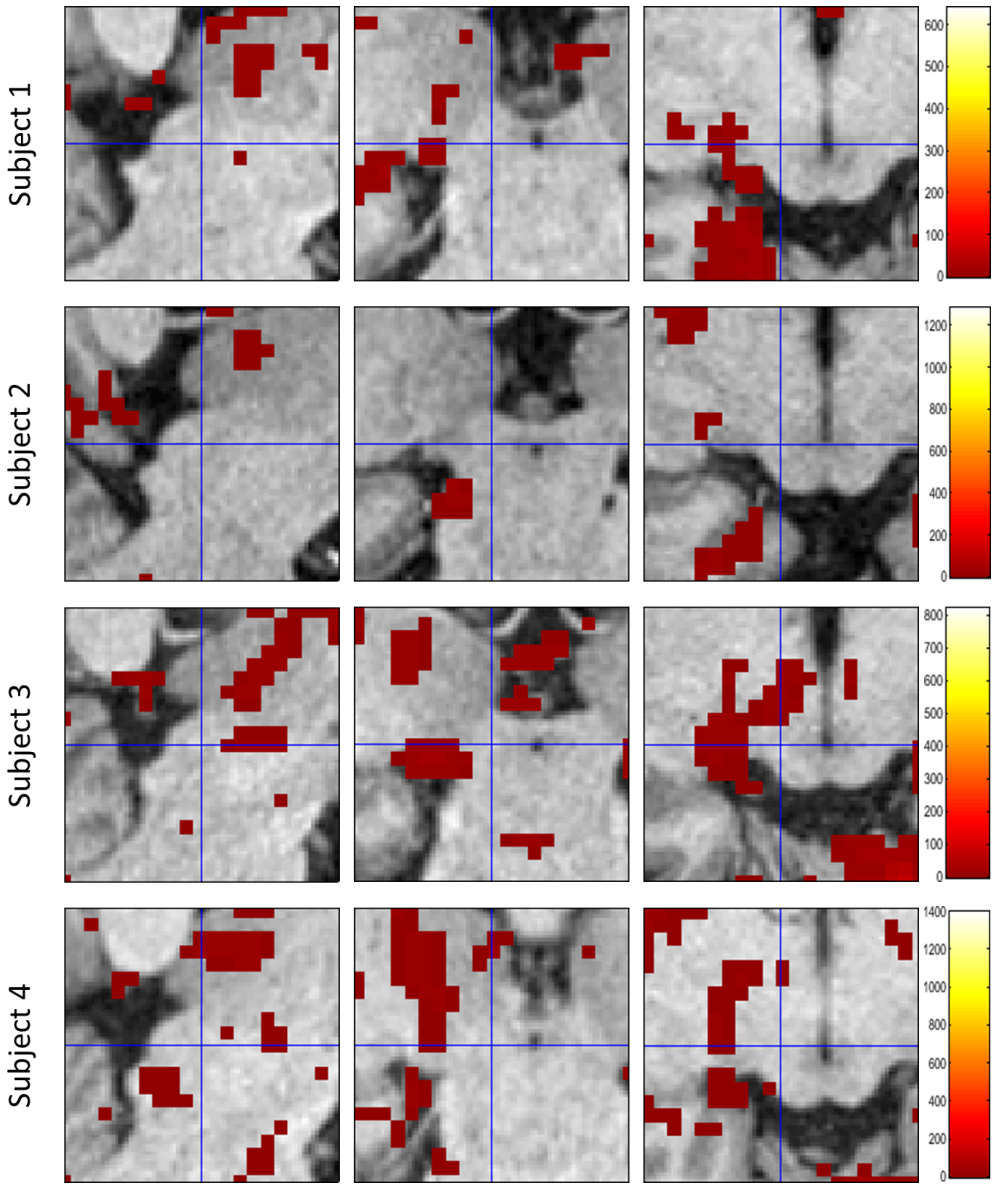

Figure 3.6: *Finger tapping conditions show no activation clusters in the SC.* Results of an F-contrast ($p < 0.001$, uncorrected) with all four tapping conditions added together, centred on the voxel-of-interest: -6, -28, -6. No activation clusters are seen in both left and right SC.

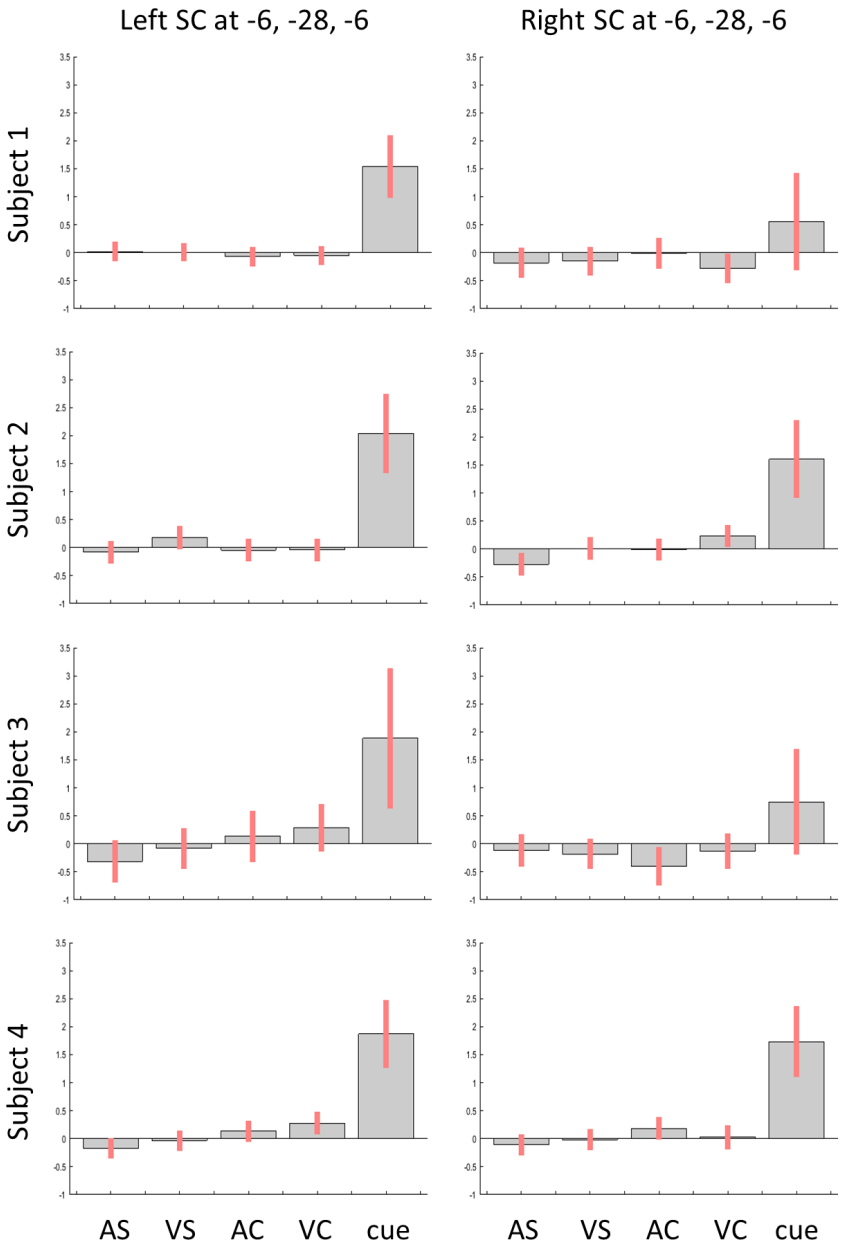

Figure 3.7: *Strong signal contribution only from cues in the SC.*
Contrast estimates as a representation of signal contribution from the four tapping conditions: auditory simple (AS), visual simple (VS, auditory complex (AC), visual complex (VC) and the cue at -6, -28, -6 and 6, -28, -6. The error bars indicate 90% confidence intervals (CI).

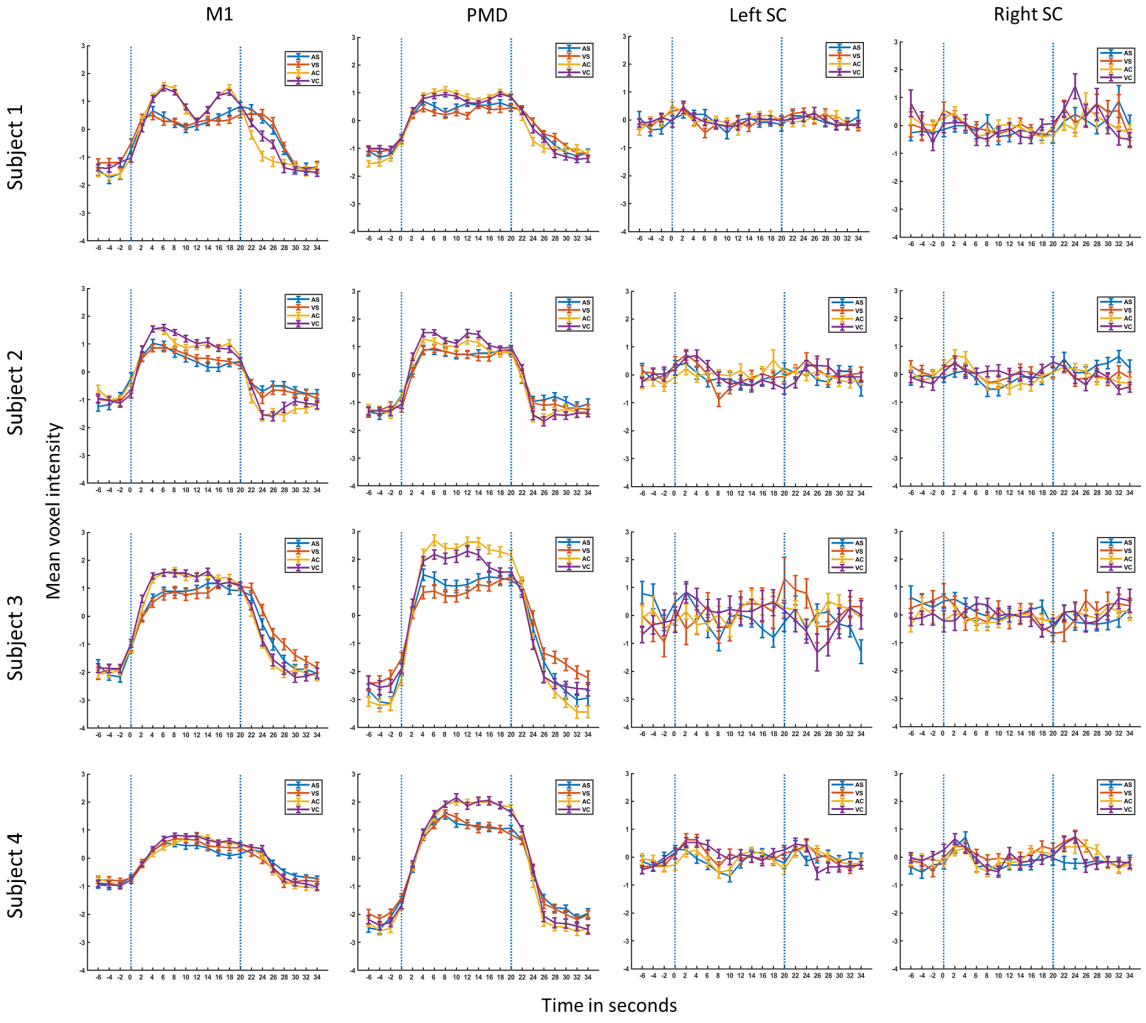

Figure 3.8: *Mean time courses show a signal aligned with the block in M1 and PMd but not in the SC.*

Mean time courses from the four finger tapping conditions corresponding to voxels in M1, PMd (the same voxels as in Figure 3.4), the VOI (-6, -28, -6) and its corresponding location in the right SC (6, -28, -6). The four conditions are coloured as follows: Blue – Auditory simple (AS), Red – Visual Simple (VS), Yellow – Auditory Complex (AC) and Purple – Visual Complex (VC); also seen in the legend in the upper right corner. The X-axis shows time from -6 s of block onset to 15 s from the end of the block. The two vertical blue dotted lines indicate the start and end of the block – 0 and 20 s respectively. The error bars indicate standard error (SE).

3.6 Discussion

Relation to previous studies

Although Boehnke et al. (2011) had shown that repetitive stimuli cause a decrease in magnitude of the response in the visual neurons of the SC, they had not tested motor responses to these stimuli. The premotor cortex has been implicated in the integration of sensory information towards realisation of movements (Witt et al., 2008). The dorsal premotor cortex (PMd), especially, is known to modulate sequential movements (Hoshi and Tanji, 2007). Studies by (Fries, 1985) and (Borra et al., 2014) have shown a connection between the premotor cortex and the SC with retrograde and anterograde tracing, respectively. Borra et al., 2014 also suggested a possible role for the projections from the premotor cortex to SC in motor control. The prospect of interactions between the SC and an area (PMd) that is involved in the execution of sequential movements, prompted us to investigate if the SC also plays a role in such movements. Additionally, the intention of testing the motor qualities of the SC, and the signal contributions at the deep SC location -6, -28, -6 corresponding to infrequent finger taps in the reaching experiment (Chapter 2), supplied impetus for the current study.

Relevance of this study

With the SC playing a role in reaching movements towards visual targets (Werner, 1993; Himmelbach et al., 2013; Linzenbold and Himmelbach, 2012) presuming a role for it in other simpler movements is not implausible. Finger tapping tasks have been used in numerous neuroimaging studies to elucidate brain areas that form a part of the motor architecture (see Witt et al., 2008 for a meta-analysis of 38 such studies). The current study though is the first to explore whether the human SC is involved in finger tapping movements, more so, those of varying complexities. Activation clusters

in M1 and PMd from the first-level analysis showed that the paradigms were adequate to elicit responses in motor areas corresponding to finger tapping. The time course analysis confirms this finding with a substantial change in signal amplitude temporally aligned with the block in M1, and in addition, with a clear delineation between simple and complex finger tapping tasks in PMd. A change in signal amplitude temporally aligned with the block was not observed in any of the voxels in the grid surrounding the VOI and that in the right SC. Activation clusters for the cue condition from the second-level analysis of the HCP dataset and first-level analysis of our experiment indicate that the paradigms and sequences were suited for a signal detection at the SC. With the HCP analysis, we showed that the SC does not play a role in the execution of simple, single finger tapping movements. With the second study, we replicated findings from the analysis of the HCP dataset. In addition, we found that the SC does not play a role in the execution of a more complex but overlearned sequential finger tapping sequence involving four fingers, that were paced by visual and auditory stimuli.

Limitations and shortcomings

There were a few limitations with the HCP dataset that encouraged us to conduct the second study, namely: a) No pacing stimuli were used to control the frequency of finger tapping which is common in such studies. Most of the older studies have used metronomes to pace visual or auditory stimuli to guide finger tapping movements (Catalan et al.,1998; Colebatch et al., 1991; Sadato et al., 1996a), while the more recent ones have used blinking lights (Indovina et al., 2001; Jäncke et al., 2000b). b) No controls were used to monitor finger tapping such as video camera recordings or collection of individual finger tap timings. c) The paradigm used was not conducive for a more sensitive time course analysis. The major limitation being that all blocks were not followed by fixation, instead fixation periods occurred twice randomly in-between blocks.

In the first and second study, measurements were made in a 3T MRI scanner. This is the most commonly used scanner and hence the results are reliable. With definitive results from a 3T scanner a study using ultra high field would gain from better localization, increased resolution, and shorter stimulation time for deep brain structures (Loureiro et al., 2017).

The time course plot did not show time courses corresponding to the cue condition since it always occurred 1 second before each block. Hence, plotting its time course would have resulted in an averaged signal of finger tapping tasks through the block. An event-related design with long gaps in-between cues and expected responses could help examine time courses for cues comprehensively.

Future outlook

Activation clusters in the SC corresponding to cues suggests that the SC could be a centre that is involved in the preparation of movements. A study that could disentangle preparation of movements from execution could answer such a question. It could also be that the cue acts as a pop-out stimulus that drives activity in SC neurons. Studies using such pop-out stimuli would help in better understanding of this response in the SC.

The results of the first experiment clearly show a response in the SC for finger tapping, but the current comprehensive study does not. The difference between finger tapping in the first experiment and the current study is that in the first study, finger tapping (recorded as button presses) was discrete and infrequent. Also, they were produced in response to stimuli that were distinct from the rest. It could be that the SC does not play a role in repetitive finger tapping movements and responds only when discrete movements are necessary. It could also be that the response in the SC is driven by the distinct stimulus that guides it rather than by finger tapping itself. Future studies are necessary to tease these differences apart.

Conclusion

We found no activations in the SC corresponding to simple finger tapping from 130 subjects of the HCP dataset. We replicated these findings from our dataset of multiple sessions in 4 subjects. In addition, analysis of our own dataset also showed that the SC does not play a role in the execution of complex finger tapping sequences. These results suggest that the SC is distinct in its contributions to movement in comparison with cortical centres that take part in movement execution. Even though the SC is known to be connected to the premotor cortex, it does not play a role in the execution of finger tapping movements. Overall, the findings from this study help broaden the understanding of the contributions of the SC towards sensorimotor networks that guide movements.

Chapter 4

Representation of novel stimuli in the SC

4.1 Introduction

The neurons from the retina branch to form two pathways, one that reaches the LGN (Lateral Geniculate Nucleus) and the other that reaches the SC (Kaas and Huerta, 1988). The pathway that runs to the SC also connects with the pulvinar and together forms a sub-cortical visual system (Kaas and Huerta, 1988). Although the sub-cortical visual system connects with cortical systems, it is also known to function independently (Basso and May, 2017). The SC has long been known to be a structure that plays a role in gaze orienting (see book chapter on the SC by White and Munoz, 2012). More recently, it has been implicated in several other functions such as visual processing, target selection, decision-making, and orientation movements towards targets (see Basso and May, 2017 for a review).

The SC is one of the earliest structures to receive sensory information and is the first and fastest responder to sensory stimuli of interest in the surroundings; these could also be stimuli that are harmful in nature and need an immediate evasive response (Soares et al., 2017). Because of this function it is imperative that the SC detects novel stimuli among otherwise repetitive ones and indeed neurons in the SC have been shown to do so (Boehnke et al., 2011).

Indovina and Sanes, (2001) compared attention to a stimulus followed by finger tapping, with finger tapping only, and found an activation cluster in the SC. But, they did not compare attention followed by movement with attention alone. In Chapter

3 we examined if the SC plays a role in sequential finger tapping movements of increasing complexity and did not find any response. On the other hand, in the first experiment (Chapter 2) we found a consistent positive signal contribution from finger tapping in response to oddballs at our VOI (voxel-of-interest). We postulated that since the activity is not due to finger tapping alone, it might be a result of responding to a novel stimulus. Hence, with the current study we investigated if the human SC plays a role only when a novel stimulus is seen or if the novel stimulus needs to be responded to by movement, such as the tap of a finger. To study this, we asked subjects to fixate on a point and respond to visual or somatic oddball stimuli, among regular stimuli in a block, by pressing a button or counting the oddballs. Responses in the SC to button presses and counting conditions, were seen in some subjects and not in others. This hints at the SC taking part in the detection of novel stimuli. We envisage that for a more clear conclusion, further investigation in terms of an event-related design and farther placement of targets from the fixation would help immensely.

4.2 Methods

Subject details

We conducted the study with 3T BOLD fMRI on four participants (3 females, 1 male, age range 24-27 years, 1 left-handed, 3 right-handed) with normal or corrected-to-normal visual acuity. Each experimental session consisted of four runs, the subjects were required to perform the experiment four times, one session per day. We performed the experiment in accordance with the ethical standards established by the 1964 declaration of Helsinki and approved by the local ethical committee. We also obtained informed consent from all the subjects.

Experimental setup

The experimental setup was similar to that in the reaching experiment (Chapter 2). Targets were of two kinds – visual and somatic. The visual targets were 4 red LEDs and 4 green LEDs, with 1 green and 1 red LED forming a pair. The target LEDs were attached to a plexi-glass stand in a straight line horizontally 2 cm apart from each other. A fixation LED was fixed to the plexi-glass stand 2 cm vertically above the centre of the row of horizontal target LEDs. Any references to the targets that provided somatosensory/tactile information will henceforth be prefixed with 'somatic'. Somatic targets were attached to 4 fingers (index, middle, ring and little fingers) of the left hand which rested on the scanner bed (refer to methods section of Chapter 2 for details). A button box was used to transmit finger tapping responses to MATLAB (version R2018a, The MathWorks Inc., Natick, MA, USA) through a microcontroller (Mbed LPC 1768, Arm Holdings). An eye tracker (EyeLink 1000, SR Research Limited) that performed online saccade detection was used to record eye movements. The edf files obtained from the eye tracker were converted into MATLAB files by using the Edf2Mat toolbox (©2013, Adrian Etter, University of Zurich). The plexi-glass with the visual targets was placed behind the head of the subjects while they lay inside the scanner in such a way that they were able to look at the targets through a mirror attached to the head-coil. The experiment was executed using MATLAB with Psychtoolbox and EyeLink extensions (Brainard, 1997; Cornelissen et al., 2002; Kleiner M, Brainard D, 2007; Pelli, 1997) which then communicated with the microcontroller to control LEDs and somatic stimulators.

Experimental paradigm

The design of the experiment was kept as similar to the first study (Chapter 2) as possible so that similar responses to button press conditions could be elicited in the SC. We assigned four conditions, namely - visual button press (VBP), somatic button press (SBP), visual counting (VCO) and somatic counting (SCO) to form four runs,

two conditions per run, as part of a factorial design (Table 4.1). Four sessions were measured from each subject, one session per day. Each session consisted of the four runs: VBP, SBP; VCO, SCO; VBP, VCO and SBP, SCO ordered in a Latin square arrangement, so that the sequence of runs did not repeat among sessions in a subject. This was done to control for sequence effects. The task demanded that the subject respond to oddballs among distractors either by pressing a button or counting them depending on the condition. In the runs with the same modality (for example, VBP and VCO) individual blocks were preceded by a cue that informed subjects whether the response required in the upcoming run would be button presses or counting. The fixation light blinked once to indicate the finger tapping condition and twice to indicate counting. These cues appeared 2 seconds before the start of the block. In the visual conditions, we required subjects to respond to red LEDs among green ones and in somatic conditions to double stimuli among single stimuli. The finger tapping conditions were our conditions of interest while those that required counting served as controls. Oddballs appeared with a frequency of either 1 in 7 or 1 in 8 consecutive targets randomly. In each of the four runs that made up a session, two conditions alternated with each other, with four trials of a condition forming one block followed by four trials of the next block separated by a 25 second baseline. We chose a longer baseline period than the first experiment to obtain a clear, extended period towards the end of the baseline devoid of any signal corresponding to the last target in the block. This would help in robust time course analysis. There were 14 blocks per condition in a run, making up 29 finger tapping and 29 counting oddball trials per session and adding up to 116 finger tapping and 116 counting oddball trials per subject from the four sessions.

fMRI data acquisition

We performed our measurements on a Siemens Prisma 3 Tesla MRI scanner with a 64-channel head-coil. We acquired 540 T2* weighted functional images per run,

	Visual	Somatic
Button press (motor)	Visual button press (VBP)	Somatic button press (SBP)
Counting (sensory)	Visual counting (VCO)	Somatic counting (SCO)

Table 4.1: The four conditions in the experiment – VBP, SBP, VCO and SCO arranged in a 2x2 factorial design. The four runs in the experiment were derived from a combination of the two tasks – button press and counting, and the two modalities – visual and somatic.

with a slice thickness of 2 mm, TR=2 s, TE=35 ms, flip angle = 80°and an FOV of 192 x 192 mm (96 x 96 matrix). The images were partial volumes consisting of 23 transversely oriented slices covering the SC, thalamus and the primary visual cortex (V1). High resolution T1 weighted structural images were acquired once per subject with an MP-RAGE sequence, slice thickness - 0.8 mm, TR=2.4 s, TE=2.22 ms, flip angle of 8°and FOV - 300 x 320 mm (240 x 256 matrix). We also acquired a T2* weighted whole-brain image for each of the four sessions in a subject, to ensure good co-registration between the partial EPI volumes and the structural images (details below).

Pre-processing

SPM12 (Statistical Parametric Mapping, version 12, Wellcome Trust Centre for Neuroimaging, London, UK) implemented in MATLAB (version R2018a, The MathWorks Inc., Natick, MA, USA) was used for pre-processing and GLM (General Linear Model) analysis of the data. The first five images at the start of all runs were deleted to allow scanner signals to reach a steady state. Pre-processing on the rest of the images was performed in 4 stages, namely: re-alignment, co-registration, normalisation and

smoothing. Images were first re-aligned to correct for motion followed by a three-step co-registration process. The whole-brain EPI image from each session of a subject was first co-registered with the mean functional image of the session (derived from the re-alignment procedure). The whole-brain EPI image was then co-registered with the T1 image (structural image) of each subject. This process still led to a few discrepancies between the structural and functional images. Hence, the mean functional images were normalised with the structural images from each session followed by the application of the resulting transformation field to all the other functional images. In the next pre-processing step, the structural images from each subject were normalised with the MNI (Montreal Neurological Institute) template with the resulting transformation field applied to all the functional images. This was followed by the last pre-processing step - smoothing, with a FWHM (full-width half-maximum) kernel of 3 mm.

Analysis

GLM (General Linear Model)

A first-level (single-subject) analysis was performed on the pre-processed data. Stimulus onsets were divided into oddballs and normal stimuli and grouped by the task condition to which they belonged. The mean reaction time of the motor trials VBP (visual button press) and SBP (somatic button press) from each run were added to the onset time of regular stimuli, so that all stimulus onset times were in congruence. These onsets were then built into a first-level model with 0 s durations. Mean time courses of CSF (Cerebro-spinal fluid) and re-alignment parameters (resulting from the pre-processing step) from each of the runs were used as regressors of no-interest. CSF mean time courses were obtained by first creating a per subject mask of the CSF using MRICron (NITRC, University of South Carolina, Columbia, SC, USA) and later extracting the corresponding mean averaged time course with the Marsbar toolbox (`http://marsbar.sourceforge.net`). The HRF function used to model re-

sponses as part of the first-level analysis was modified to use an onset-to-peak time of 4 s (suitable for the SC) instead of the usual 6 s (Wall et al., 2009). Contrasts were generated for each of the four main conditions: Visual button press (VBP), Somatic button press (SBP), Visual counting (VCO), Somatic counting (SCO), and the cue condition against the baseline. The four main conditions were also compared to regular sensory stimulation (non-oddball stimuli) labelled as visual stimulation (VST) and somatic stimulation (SST). Results were examined at a threshold of $p < 0.05$ at the VOI (voxel-of-interest). The anatomy toolbox in SPM was used to delineate primary visual cortex (V1) and secondary somatosensory cortex (SII) shown in Figure 4.1 of the results section. Results were focussed on our VOI -6, -28, -6 in MNI (Montreal Neurological Institute) co-ordinates and its corresponding location in the right SC with a significance threshold of $p < 0.001$, uncorrected.

Permutation based maximum t-statistic test (PBMT-S)

The procedure of raw time course extraction from a voxel grid around the VOI was the same as in the first study (see methods section of Chapter 2 for details). All trial blocks were separated into those that contained oddball trials and those that did not contain them. The blocks that contained oddball trials were then separated according to the four main conditions that they belonged to: VBP, VCO, SBP and SCO. The blocks that did not contain oddball stimuli were divided into two parts: one with non-oddball visual stimulation (VST) and the other with non-oddball somatic stimulation (SST). Hence the condition pairs tested were: VBP>VST, VCO>VST, SBP>SST and SCO>SST. Two time windows were decided upon; one for the oddball stimuli (2 s after the onset of the oddball stimulus + reaction time, to 6 s after onset + reaction time) and the other for non-oddball blocks (4 s after the onset of the block to 8s after onset; corresponding to an expectation of the peak response in the block). This was followed by the computation of a mean value of the time course within the selected time window, for each repetition of a condition. Similar to the time course

analysis reported earlier (see methods section of Chapter 2), we computed maximum T-values across all the voxels in the grid, from 2000 permutations between mean time course values from the condition pairs, creating a t-distribution. Two sample t-tests were performed on the mean time course values from the condition pairs. These t-values were compared with the critical T values generated from the t-distribution created earlier at a threshold of $p < 0.05$, to determine significance. The PBMT-S test controls for multiple comparisons inherently.

4.3 Results

4.3.1 Behavioural results

The mean reaction times across all subjects for visual button presses was 0.54 s, SD 0.12 s and 0.84 s, SD 0.12 s for somatic button presses. Apart from two saccades (thresholded at 2°of visual angle) associated with two oddball trials in subject 3, no other saccades were found associated with oddballs in any of the subjects.

4.3.2 GLM results

To ensure that the paradigm elicited a response in cortical areas, we first examined the primary visual cortex (V1) and secondary somatosensory cortex (S2) (the only cortical somatosensory covered by our partial volume) for voxels responding to visual and somatosensory oddball stimuli respectively (Figure 4.1). Activation clusters were seen in somatosensory and visual areas in all subjects at a threshold of $p < 0.05$, FWE corrected. Images from an example subject are shown with the crosshair centred on V1 in Figure 4.1 A. The crosshair is centred on the Secondary Somatosensory cortex (S2) of the same subject in Figure 4.1 B. These results ensured that the oddball stimuli elicited specific and expected responses in cortical areas.

We focused our results on the VOI -6, -28, -6 in MNI co-ordinates which was the

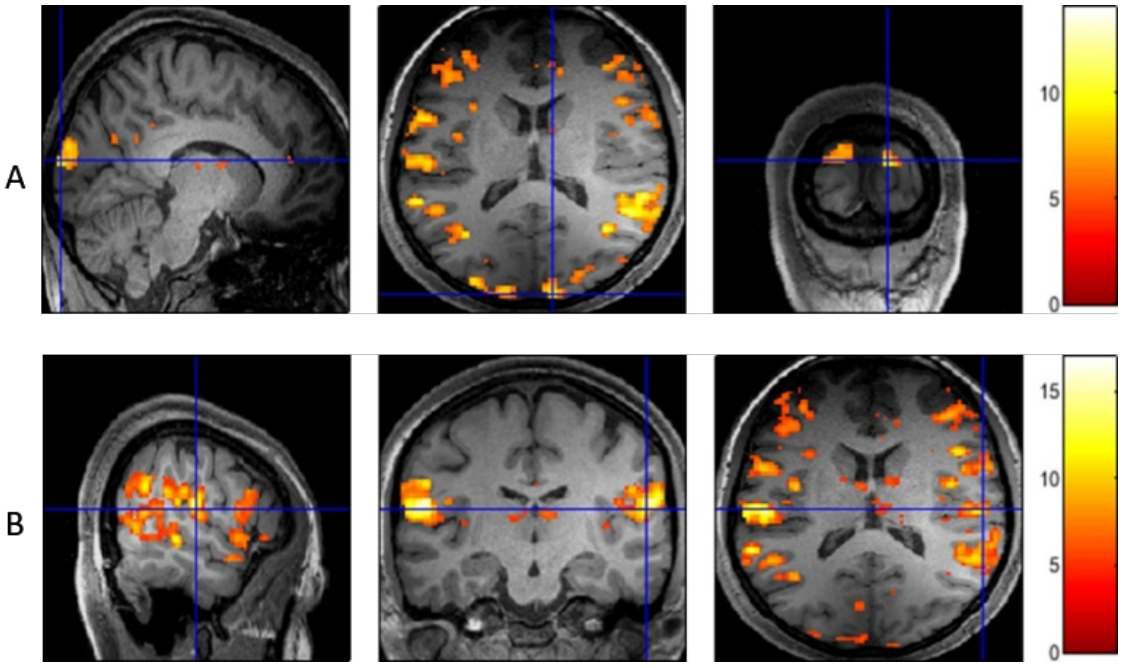

Figure 4.1: *Testing the paradigm.*

A. Structural fMRI image of a subject showing activations in response to all visual oddball stimuli in the paradigm with the crosshair centred on the primary visual cortex (V1). B. Images from the same subject showing activations in response to all somatosensory oddball stimuli. The crosshair is centred on the secondary somatosensory area (SII). Both the images were generated with T-contrasts thresholded at $p < 0.05$, FWE corrected.

peak location for oddball button presses derived from the first experiment and was also used in the second experiment (see methods section of Chapter 2 for details). In addition, we also examined results at the corresponding location of the VOI in the right SC: 6, -28, -6.

First, we report signal contributions (through contrast estimates; also a measure of effect size) at the VOI and the corresponding location in the right SC with all oddball trials combined together (visual and somatic button presses; visual and somatic counting: VBP + SBP + VCO + SCO). As seen in Figure 4.2, oddballs elicit a pos-

itive signal contribution in the SC that is much larger than non-oddball stimulation and cues in two subjects at the VOI, and all four subjects in the corresponding location on the right. The difference in signal contribution is more relevant given that the number of oddball trials are far lower than non-oddball stimuli (non-oddball stimuli occur 7-8 times more in number depending on the frequency of oddball trials per run). We then separated the oddball conditions into button presses and counting, labelled as 'BP' and 'CO' respectively, and plotted their signal contributions along-with non-odball stimulation (visual -VST; somatic - SST) and cues (Figure 4.3). 'BP' consisted of visual and somatic oddball button press trials (VBP + SBP) and 'CO' consisted of visual and somatic oddball counting trials (VCO + SCO). The signal contribution from BP at the VOI is positive in 3 subjects, out of which it is not significant in 2 of them and shows no response in the fourth subject, whereas at the corresponding location in the right SC, it is positive in all 4 subjects and not significant in 1 of them. Signal contribution from CO at the VOI is positive in 3 subjects, out of which it is not significant in 1 of them and shows a negative contribution in the fourth subject, whereas at the corresponding location in the right SC it is positive in 3 subjects and does not show any response in the fourth subject. On the other hand, non-oddball visual and somatic stimulation (VST and SST) show very low/zero/negative signal contributions across subjects at both the VOI and its corresponding location in the right SC. The cues show a positive signal contribution in 2 subjects at the VOI, and across all subjects at the location corresponding to the VOI in the right SC. To examine differences in signal when the oddball button press and counting conditions are separated by modality i.e. visual and somatic stimuli, we conducted a GLM analysis with VBP, VCO, SBP and SCO as separate conditions from here on.

Visual oddball stimuli

Figure 4.4 shows both visual oddball conditions (VBP - visual oddball button press; VCO - visual oddball counting) contrasted against the baseline at a threshold of

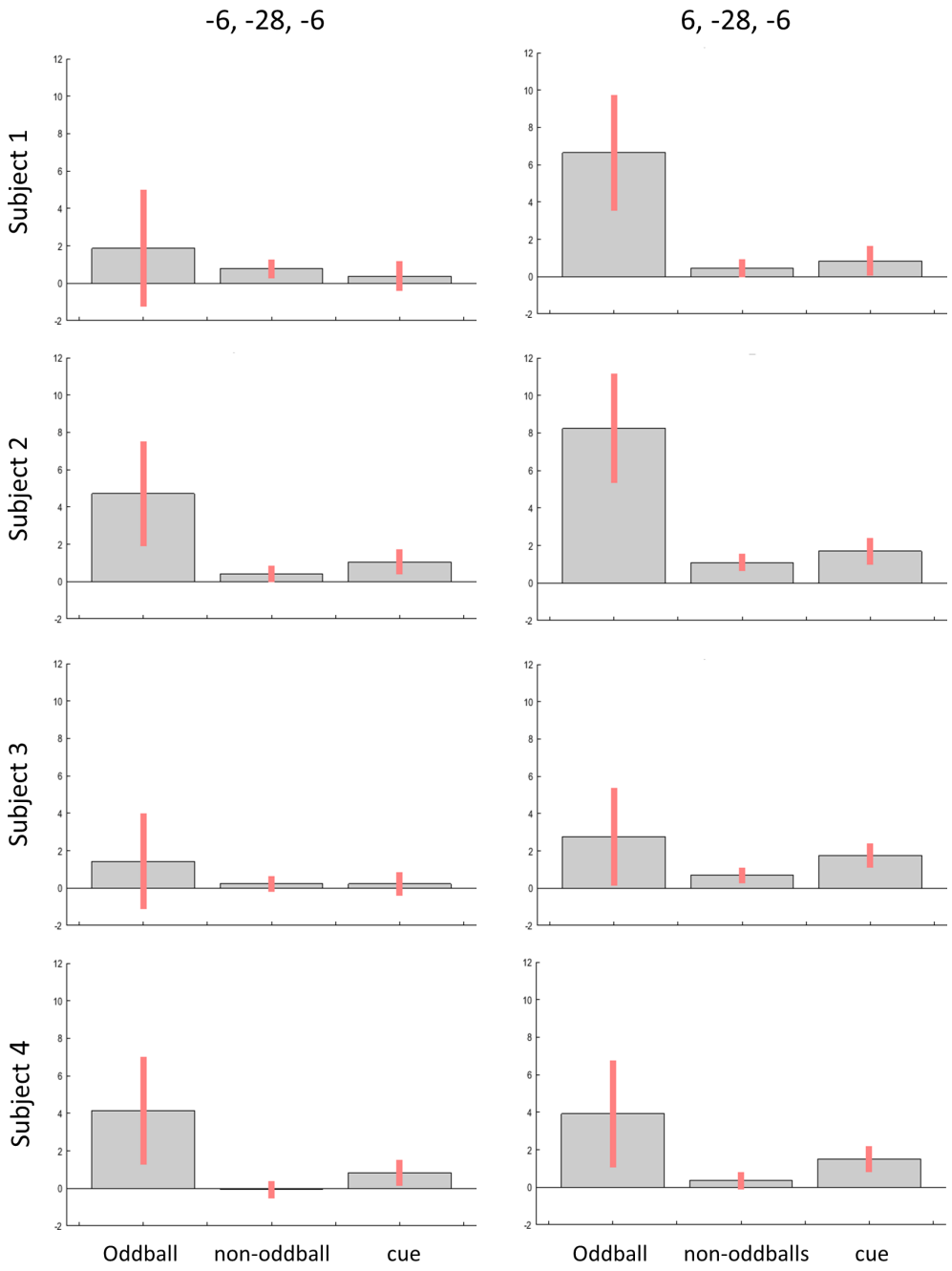

Figure 4.2: *Signal contributions from oddball stimuli are consistently higher than non-oddball stimuli across subjects.*

Contrast estimates from oddball stimuli, non-oddball stimuli, and cues are plotted from left to right. The red bars indicate 90% confidence intervals (CI).

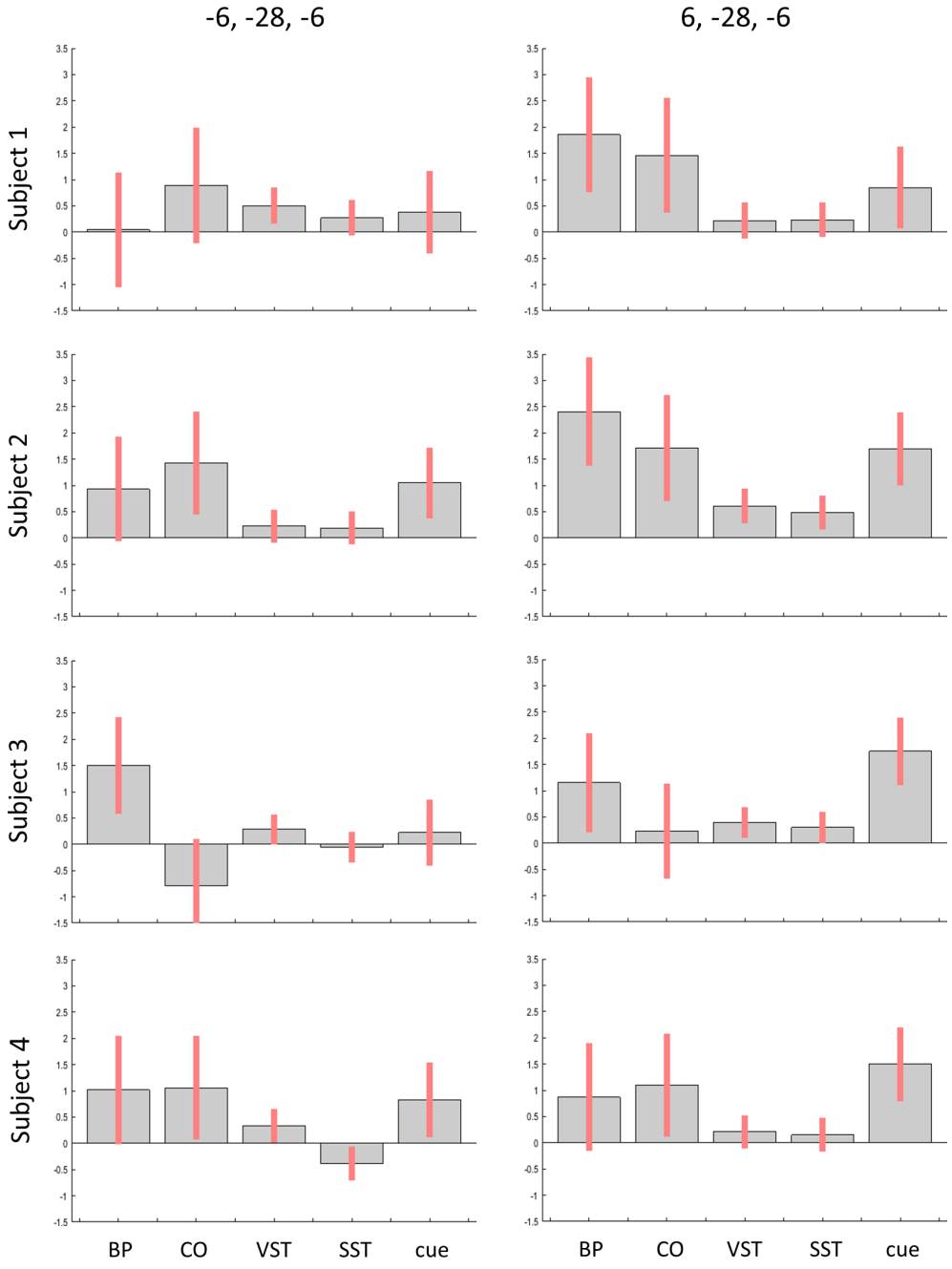

Figure 4.3: *Signal contributions from oddball button presses (BP) and oddball counting (CO) are higher than non-oddball stimulation.*

Contrast estimates from all oddball button presses (BP), oddball counting (CO), non-oddball visual stimulation (VST), non-oddball somatic stimulation (SST) and cues are plotted from left to right. The red bars indicate 90% confidence intervals (CI).

$p < 0.001$, uncorrected. The crosshairs are centred on our VOI. No activation clusters are seen at the VOI in both VBP> baseline and VCO> baseline comparisons across all subjects. There is some response elicited in voxels surrounding the VOI and its corresponding location in the right SC with respect to both conditions, but it is not consistent across subjects. These results indicate that the response in the SC to visual oddball stimuli is not robust with GLM analysis.

Somatic oddball stimuli

Similar to the visual conditions we also looked for somatic-oddball button press (SBP) and counting (SCO) led activations at the VOI in a comparison against the baseline ($p < 0.001$, uncorrected). No activation is seen at the VOI in response to both the SBP>baseline and SCO>baseline comparisons (Figure 4.5). Similar to the visual conditions, some voxels surrounding the VOI are seen responding to somatic oddball stimulation but these responses are not consistent across subjects. This indicates that the results from the GLM analysis are weak for somatic oddball conditions as well.

Contrast estimates

We then plotted contrast estimates at the VOI (-6, -28, -6) and the corresponding location in the right SC (6, -28, -6) (Figure 4.6). The figure shows the individual signal contributions from all the conditions that were a part of the experiment at the two locations. The non-oddball conditions show a consistently weak signal contribution across all subjects at both the locations. There is a clear distinction between signal contributions from oddball conditions (VBP, VCO, SBP and SCO) and non-oddball conditions (VST and SST) across subjects at our location of interest, on both sides of the SC. The response to the cue is consistent at the location in the right SC but not in the left SC. SBP and SCO are the only two conditions with strong signal contributions in 2 subjects out of 4 at the VOI. VBP and VCO show positive signal contributions with low variability in one of the 4 subjects on both sides of the SC.

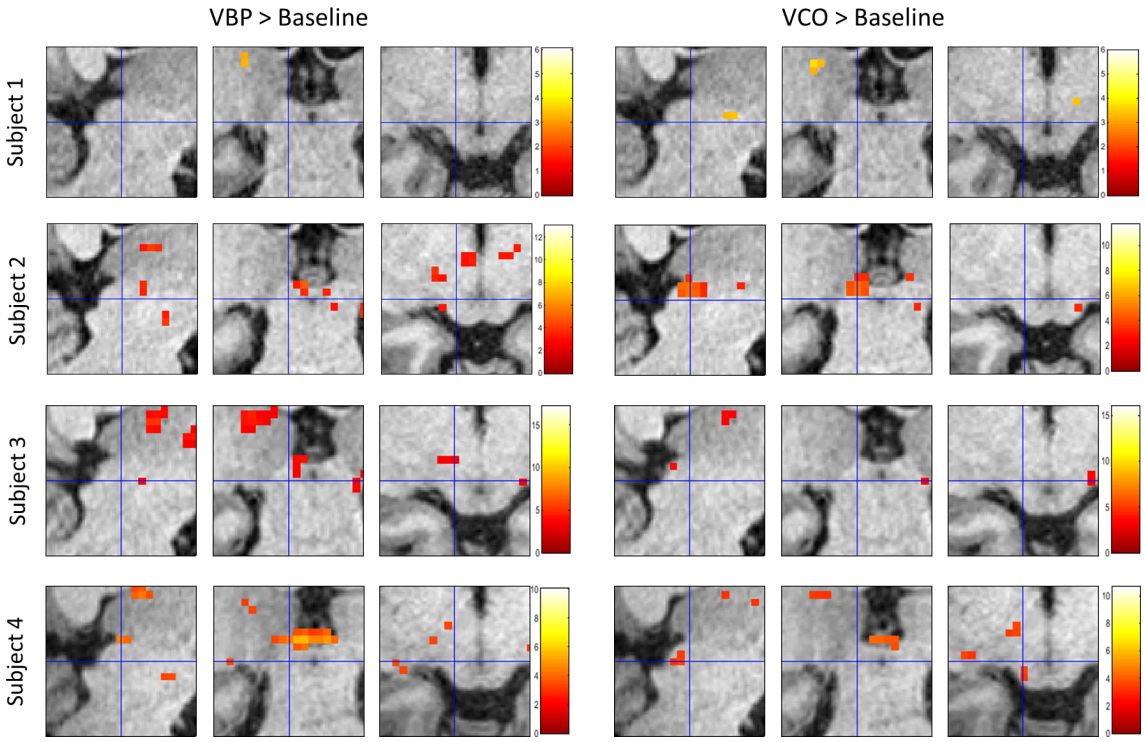

Figure 4.4: *Visual oddball stimuli followed by button presses and counting do not elicit a response at the VOI.*

The panel on the left shows the results of button presses in response to visual oddball stimuli contrasted against the baseline (VBP>baseline). The panel on the right shows the results of the same stimuli being responded to by counting, contrasted against the baseline (VCO>baseline). The activation maps have been built with T-contrasts with crosshairs centred on the VOI (-6, -28, -6) at a threshold of $p < 0.001$, uncorrected.

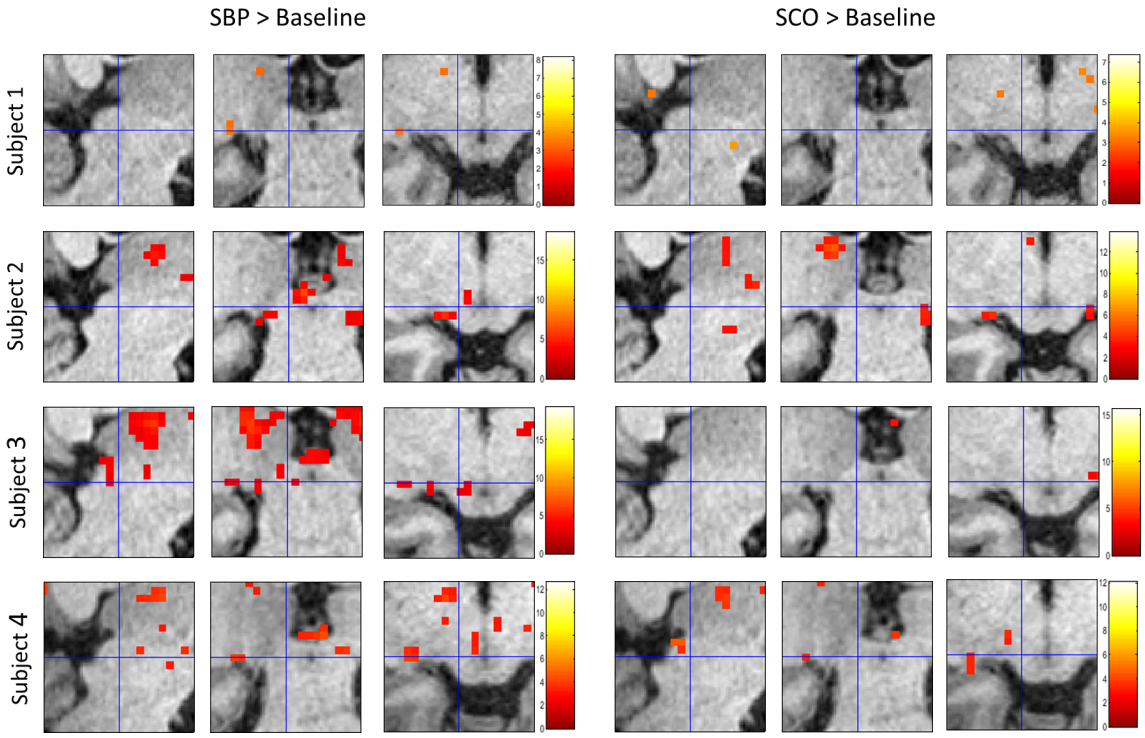

Figure 4.5: *Somatic oddball stimuli followed by button presses and counting do not elicit a response at the VOI.*

The panel on the left shows the activation map of T-contrasts in the SC with button presses in response to somatic oddball stimuli contrasted against the baseline (SBP>baseline). Similarly, the panel on the right shows the activation map for somatic oddball stimuli responded to by counting, contrasted against the baseline (SCO>baseline). The colourbar shows the range of t-values in the respective images. The crosshair is centred at the VOI (-6, -28, -6). The images are thresholded at $p < 0.001$, uncorrected.

These findings indicate that there is some response in the SC towards all the oddball conditions tested but fall short of allowing for a definitive conclusion.

PBMT-S test results

As a final step, we used a PBMT-S (permutation based maximum t-statistic) test that takes into account multiple comparisons and is also more sensitive and reliable than the GLM analysis. We first compared all oddball and non-oddball conditions against the baseline. The results, as expected, showed consistent activity in voxels across subjects in both the oddball and non-oddball condition comparisons against the baseline, at both the VOI and its corresponding location in the right SC. To differentiate between non-oddball and oddball conditions we conducted another PBMT-S test of oddball conditions against the respective non-oddball conditions (VBP>VST, VCO>VST, SBP>SST, SCO>SST). Figure 4.7 shows the results of this test. The 27 boxes separated by thick lines in a subject represent the 27 voxels of the 3×3×3 grid. The central voxel in the middle plane is our VOI, all the other voxels in the two other planes are one voxel adjacent to the VOI. In a slight departure from the PBMT-S figure in Chapter 2, here, the thin lines indicate the four oddball condition comparisons against the respective non-oddball conditions. Each of these comparisons if significant at a threshold of $p < 0.05$ in the PBMT-S test have been marked with a star in the respective voxel, and assigned a colour in order to differentiate between them namely - red for VBP>VST, green for SBP>SST, brown for VCO>VST and blue for SCO>SST. Very sparse activity is seen in the SC corresponding to each of the four oddball to non-oddball comparisons (Figure 4.7). The results indicate that there is some activity in the SC corresponding to each of the four oddball conditions, but the activity is not consistent enough for definitive conclusions.

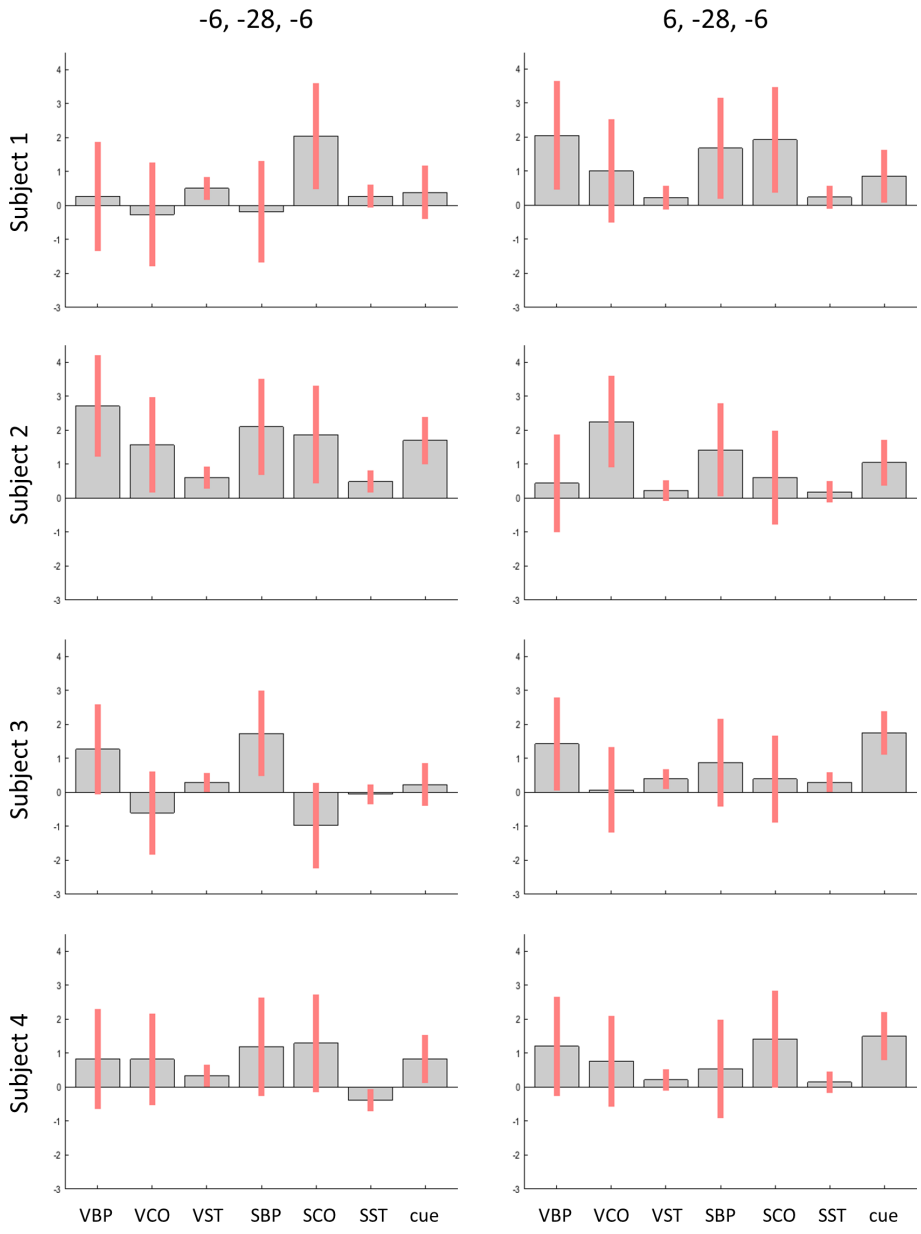

Figure 4.6: *Contrast estimates at the VOI show a positive signal contribution from oddball conditions in some subjects and not in others.*

The figure shows contrast estimates at the VOI (-6, -28, -6) and its corresponding location in the right SC. The signal contributions from the four oddball conditions – VBP, SBP, VCO and SCO, non-oddball conditions – VST and SST, and the cue have been represented. The bars in red indicate 90% confidence intervals (CI).

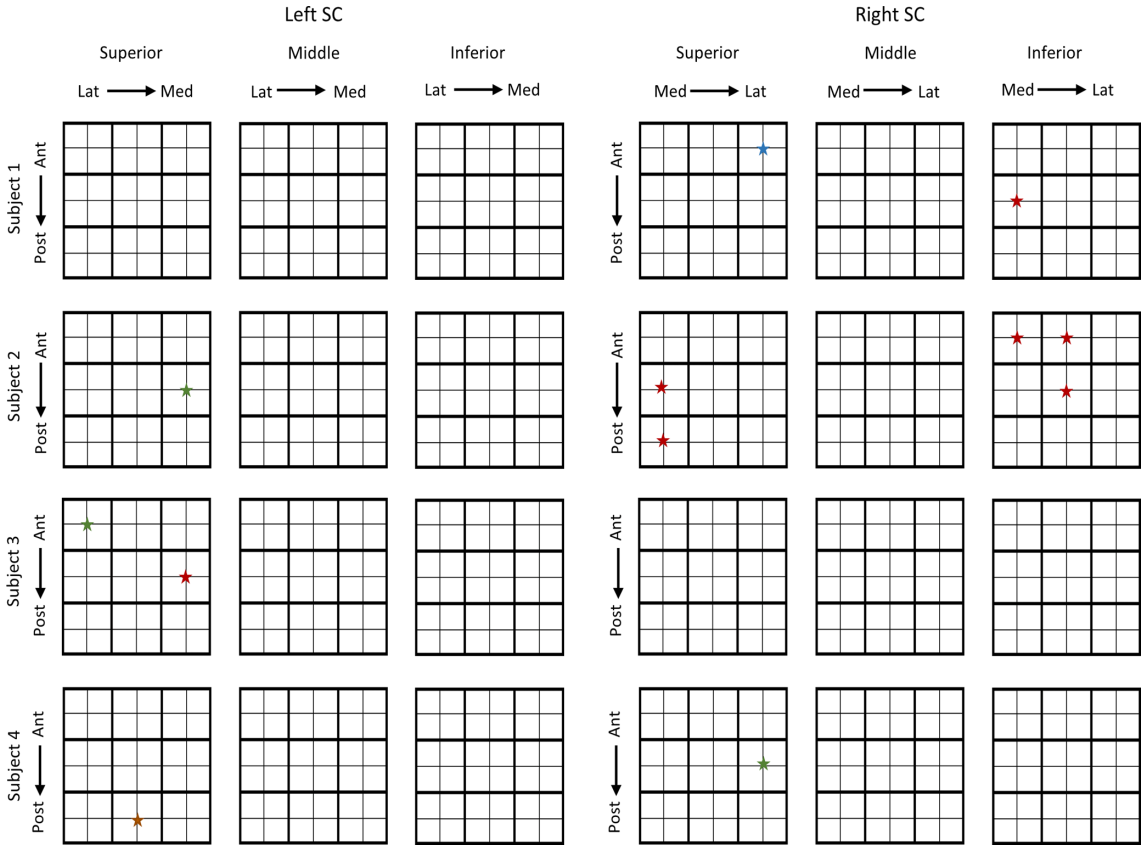

Figure 4.7: *Oddball to non-oddball stimulus comparisons in a PBMT-S test do not show a consistent result across subjects.*

The figure shows the results of a PBMT-S test ($p < 0.05$) controlling for multiple comparisons. The three planes of voxels that belong to the 3×3×3 voxel cube centred at the VOI (-6, -28, -6) and its corresponding location in the right SC (6, -28, -6) respectively, arranged in superior to inferior order. Each of the voxels in a plane were then arranged in anterior to posterior and medial to lateral order. Thick lines demarcate voxels, while thin lines separate comparisons of oddball conditions against the corresponding non-oddball conditions. Voxels significant in the VBP>VST comparison are marked with a red star, SBP>SST with a green star, VCO>VST with a blue star and SCO>SST with a brown star. The stars have been marked at the centre of each voxel for ease of differentiation.

4.4 Discussion

4.4.1 Relation to previous studies

Mikulić and Hoffmann (2016), showed neuronal activity in SC neurons during arm movement perturbations in macaques and concluded that this was a result of an unexpected sensation. Ignashchenkova et al. (2004), showed that visuo-motor neurons in the SC are known to be active even during covert shifts of attention. Studies in macaque SC have examined the effects of repetitive stimuli (Goldberg and Wurtz, 1972; Mayo and Sommer, 2008) and compared them to neuronal activity induced by novel stimuli (Boehnke et al., 2011). These studies have found that repetitive stimuli cause a depletion of neuronal activity in the SC while novel stimuli caused an increase in neuronal activity. All the studies mentioned so far examined saliency in terms of attention, or in terms of a motor behaviour not induced internally. As per our knowledge only one study so far compared 'movement only' tasks to 'attend and move' in a whole-brain analysis using fMRI and showed a response in the human SC (Indovina and Sanes, 2001). The results of this study though do not allow a clear characterization of the signal found at the SC since the study did not include an 'attend and move' vs 'attend' comparison.

4.4.2 Relevance of this study

With the earlier experiment on finger tapping (Chapter 3) we have shown that the SC does not play a role in simple or complex finger tapping sequences. But, in the reaching experiment (Chapter 2) we observed strong signal contributions from button presses in spite of the corresponding stimuli being very low in number. This led us to hypothesize that the response in the SC could have been caused by novel stimuli that inform button presses. With the current experiment we explored this response further by looking for activity in the SC due to novel stimuli, in terms of

oddballs that could be responded to by button presses or counting. This would help examine if the SC reacts to oddball stimuli among non-oddball stimuli, moreover, if the response to oddballs is specific to button presses only. We designed the paradigm to be similar to the reaching experiment (Chapter 2) using visual and somatic stimuli, so that we could expand on its results showing responses in the SC towards oddball button presses. Although the results of the current study are not conclusive, they show that the SC does respond to oddball stimuli. A paradigm that is more sensitive to differences between oddball and non-oddball stimulation such as an event-related design that separates these stimuli, which in this study are part of the same block, might improve delineation between them. In the second experiment (Chapter 3) we showed that sequential finger tapping tasks (recorded through pressing of buttons) did not elicit a response in the SC in spite of varying complexities. In light of the oddball button press results from the reaching experiment (Chapter 2), and the few positive findings across oddball trials in the current study, there is some indication that the SC might be responding to novel stimuli alone (encoding value), irrespective of whether they are followed by button presses or counting. Further experimentation is necessary for a definitive conclusion.

In our study, the cue is a visual stimulus that is shown briefly to inform the subject of the task in the upcoming block only in conditions where the modalities are the same, but the response required is not. For example, when a VBP block alternates with a VCO block the cue informs subjects that they should press a button as a response to oddballs in the VBP block whereas they should count the oddballs in the VCO block. It is important to note that the contrast estimates (indicating effect size) from the cue at the VOI and its corresponding location in the right SC, show a strong contribution in some subjects. We postulate that the cue elicits a response in the SC since it carries value (information about the impending block).

4.4.3 Limitations and shortcomings

The study was designed to be as similar as possible to the first experiment (Chapter 2) since we saw signal contributions for button presses in that experiment and wanted to replicate the design as much as possible, albeit with more repetitions and other conditions to test. Our study found some activity in response to all oddball conditions: visual button press (VBP), visual counting (VCO), somatic button press (SBP) and somatic counting (SCO) but it was not stable across subjects. Each oddball stimulus in the experiment was one among the four stimuli in a block. This allowed for superimposition of the activity from non-oddball stimuli with that of oddball stimuli. An event-related design would probably help in improved detection of oddball-specific signals and allow for a more reliable time course analysis. Another point to note is that signal contributions were stronger when oddball button press and counting responses were combined but became much weaker and variable after bifurcation into the four conditions. It is also important to note that the number of oddball stimuli in the current experiment were very few compared to non-oddball stimuli, which were 7-8 times greater in number. Event-related designs with more repetitions of all oddball conditions might help improve differentiation not only between oddball and non-oddball stimulation, but also between different oddball conditions.

In the current experiment the targets were much closer to the fixation (3°) than in the first experiment (9°). This could have been another reason for the difficultly in teasing apart signals pertaining to oddballs from non-oddball stimulation. If the targets were placed far away from the fixation point, just enough for detection, that would possibly make the signal for oddballs more prominent in the SC. In addition, the difficulty of the task would demand greater attention from subjects which could potentially have led to stronger signals.

4.4.4 Future outlook

The SC is a structure that plays a role in several processes, from orientating towards an object to acting on it like target selection, decision-making, and shifting of attention. In a study like ours the SC needs to process visual information, perceive differences between stimuli to establish uniqueness and then play a role in the execution of a movement in response. With a vast range of functions that the SC seems to be involved in, what remains to be seen is what parts of the SC contribute to each of these functions. Do the same neurons take part in all these processes or is there a division of functions? One such question could be addressed with electrophysiological recordings from visuo-motor neurons with a paradigm that differentiates between visual stimuli by the responses that follow, such as with button presses or shifts of attention alone. Following up on this, would visuo-motor neurons also play a role in decision making in addition to processing visual and motor information?

It would also be interesting to study how both sides of the SC interact in this decision-making process. If stimuli are presented in both the right and left hemi-fields at the same time, and a decision has to be made taking into account both sets of information (such as with an oddball on one side), which hemisphere of the SC would show increased neuronal activity? The hemisphere ipsilateral/contralateral to the novel/regular stimulus? Or would the activity be similar in both the hemispheres?

While our study presents results using visual and somatic novel stimulation, it also paves the way for studying other sensory modalities that might give rise to similar activity in the SC. Since it is already known that auditory information is processed in the SC, it would be the ideal modality to begin with.

4.4.5 Conclusion

The SC used to be known as a rudimentary structure that controlled eye movements. In the last few decades this notion has gradually changed. We now know that the SC

is a structure that takes part in several functions from visual processing to decision making. With our study we aimed to add to this knowledge by investigating if the human SC not only takes part in detection of novel stimuli, but also in the execution of a response to it in terms of finger tapping or shifting of attention alone. We produced weak results hinting at a role of the SC in detection of novel stimuli. While these results were not strong enough for specific assertions, they have provided impetus for similar studies with more sensitive paradigms that would help answer these questions more formidably.

Chapter 5

Conclusion and final remarks

Although there have been numerous studies on the Superior Colliculus (SC), most of them have been conducted on rodents, cats and non-human primates (see Cang et al. 2018, for a review). Comparatively, a small number of studies have been conducted on humans (Furlan et al., 2015). The differences in the SC of humans and other mammals indicate that a straightforward extrapolation of functions is questionable (May, 2006). Also, most of these studies have focused on the SC being a visually oriented structure, hence other sensory modalities have not been tested extensively. Although there have been numerous studies on the motor functions of the SC, most of them have studied the structure through saccades. Little is known about the role of the SC in classical movement paradigms like finger tapping. While the SC is known to take part in reactions to stimuli of salience in the environment, it is not known if these reactions ought to be motor responses, or if it would also participate if the reaction is in terms of a covert response like counting. Overall, the studies detailed in this thesis would help us characterise the motor functions of the SC not just by helping us gain a deeper understanding of the kind of motor tasks that it plays a role in, but also of how these movements are modulated by various sensory stimuli; be it by means of guiding sequential movements, or acting as a novel stimulus informing discrete ones. This, in turn, would help us establish the role that the SC plays in the complex sensory-motor architecture of the brain.

With the first study (Chapter 2), we examined whether, apart from vision, the SC integrates other sensory information such as somatosensation in the execution of reaching movements. Since it was the first time a study like this was being carried out,

we first replicated earlier findings on visually-guided reaching at the peak location derived from these fMRI studies. We could then examine the SC for activations corresponding to somatic reaching. Five subjects performed visually and somatically guided reaching with targets in the periphery while fixating. The control conditions were formed by the same targets with an occasional button press in response to oddballs. Our GLM results showed that the SC participates in somatically guided reaching as seen at our VOI (voxel-of-interest). With the intentions of extending the investigation of the SC beyond the VOI as well as constructing more sensitive and reliable analyses, we examined time courses with a PBMT-S (permutation based maximum t-statistic) test that intrinsically controls for multiple comparisons. This analysis allowed us to examine the spread of the responses not only at the VOI but also one voxel adjacent to it on all sides. The PBMT-S test results confirmed findings from the GLM that somatically guided reaching elicits a response in all of the five subjects that we tested at the VOI, or one voxel adjacent to it. This study shows that the SC is not just a visually driven structure but also integrates somatic information towards reaching movements.

With our second study (Chapter 3), we advanced the results from the first experiment, and checked whether the SC also plays a role in finger tapping movements. Finger tapping movements have been used to map cortical movement centres. We postulated that if the SC has strong motor characteristics, we would see activations in response to finger tapping movements as well. We first analysed a dataset of 130 subjects from the motor task of the Human Connectome Project (HCP) database, and examined if we see a response at our VOI (derived from the button press responses in the reaching study). A second-level GLM analysis (group analysis) did not find a response in all of the SC. We then performed an experiment with sequences tailored for measurements in the SC. We used simple and complex movement sequences paced by visual and auditory cues for this experiment. Even in this experiment, we did not see any response in the SC with a first-level GLM analysis in any of the four subjects. A

GLM and time course analysis of the response in the primary motor cortex (M1) and dorsal premotor cortex (PMd) showed a robust response temporally aligned with the task, but did not show any signal above noise in the SC. This result conclusively shows that repetitive, simple or complex sequential finger tapping tasks do not elicit a response in the SC. The results also do not explain the strong signal contribution at the VOI from finger tapping in response to oddballs, in the first experiment.

With our third study (Chapter 4) we examined whether the activation corresponding to oddball button presses from the first experiment (Chapter 2) was because of the execution of a motor response to a novel stimulus, or if the activation could also be seen with counting (and hence attending to) an oddball stimulus alone. In this study, four participants pressed buttons in response to visual and somatic oddball stimulation, or counted them, depending on the respective stimulus blocks. We saw that there was some response in the SC surrounding our location of interest in a first-level GLM analysis. The SC also showed variable activity at the VOI, its corresponding location in the right SC, or their adjacent locations, when oddball responses were compared with non-oddball stimulation using a PBMT-S test. Although contrast estimates of combined oddball stimuli did show some consistency (GLM analysis), bifurcating these oddball responses further into four conditions that represented each of the two modalities (visual and somatic) and the two tasks (button presses and counting) showed a positive finding in some subjects but not in others (PBMT-S test). These results along with oddball button press responses seen in the first experiment (Chapter 2), hint that the SC might be involved in responding to novel stimuli but a more sensitive paradigm might be necessary to establish confidence, and to be able to clearly differentiate if the effect is dependent on a motor response, or could be seen with allocation of attention alone.

Overall, with these four studies we showed that the human SC integrates multisensory information towards reaching movements, but does not take part in simpler nonetheless repetitive movements like finger tapping. It might play a role in finger

tapping movements, if they are executed as a response to novel sensory stimulation, but this needs further investigation for an assertive conclusion. We hope that these studies help not only in advancing knowledge on the motor functions of the SC, but also throw light on its less studied multi-sensory integration capabilities towards the generation of motor responses.

In the future, it would be essential to investigate responses in the SC towards reaching movements guided by auditory stimuli. Comparison of these results with studies where reaching is unaided by sensory stimulation would help gain a better understanding of sensory-motor integration in the SC. The SC, with its capabilities of multi-sensory integration towards modulation of motor responses, would be a very interesting candidate to investigate learning. With the myriad other cortical features found among neurons in the SC, finding evidence for learning would not be implausible. The frequent strong response to cues in our studies indicates that the SC plays a role in stimuli that impart value. Future studies could be aimed at deciphering if these responses increase in a graded manner with increase in the value encoded by the stimuli. Methods such as multi-variate fMRI analysis would allow for a finer study of responses in the SC while opto-genetic tools would help execute a range of manipulations in the neurons of the tiny structure. With these and other recent advances in techniques measuring neuronal activity, the future of functional studies in the SC is very bright.

References

Basso, M.A., and May, P.J. (2017). Circuits for Action and Cognition: A View from the Superior Colliculus. Annu. Rev. Vis. Sci. 3, annurev-vision-102016-061234.

Basso, M.A., and Wurtz, R.H. (1997). Modulation of neuronal activity by target uncertainty. Nature 389, 66–69.

Basso, M.A., and Wurtz, R.H. (1998). Modulation of Neuronal Activity in Superior Colliculus by Changes in Target Probability. J. Neurosci. 18, 7519–7534.

Bell, A.H., Fecteau, J.H., and Munoz, D.P. (2004). Using Auditory and Visual Stimuli to Investigate the Behavioral and Neuronal Consequences of Reflexive Covert Orienting. J. Neurophysiol. 91, 2172–2184.

Bogadhi, A.R., Bollimunta, A., Leopold, D.A., and Krauzlis, R.J. (2018). Brain regions modulated during covert visual attention in the macaque. Sci. Rep. 8, 15237.

Blair, R.C., and Karniski, W. (1993). An alternative method for significance testing of waveform difference potentials. Psychophysiology 30, 518–524.

Boehnke, S.E., Berg, D.J., Marino, R.A., Baldi, P.F., Itti, L., and Munoz, D.P. (2011). Visual adaptation and novelty responses in the superior colliculus. Eur. J. Neurosci. 34, 766–779.

Borra, E., Gerbella, M., Rozzi, S., Tonelli, S., and Luppino, G. (2014). Projections to the superior colliculus from inferior parietal, ventral premotor, and ventrolateral prefrontal areas involved in controlling goal-directed hand actions in the macaque. Cereb. Cortex 24, 1054–1065.

Brainard, D.H. (1997). The Psychophysics Toolbox. Spat. Vis. 10, 433–436.

Buckner, R.L., Krienen, F.M., Castellanos, A., Diaz, J.C., Koutsouleris, N., Riecher-rössler, A., Meisenzahl, E.M., Smieskova, R., Kambeitz-ilankovic, L., Saldern, S. Von, et al. (2014). The organization of the human cerebellum estimated by intrinsic functional connectivity The organization of the human cerebellum estimated by intrinsic functional connectivity. 02138, 2322–2345.

Cang, J., Savier, E., Barchini, J., and Liu, X. (2018). Visual Function, Organization, and Development of the Mouse Superior Colliculus. Annu. Rev. Vis. Sci. 4, 239–262.

Cavanaugh, J. (2004). Subcortical Modulation of Attention Counters Change Blindness. J. Neurosci. 24, 11236–11243.

Cavanaugh, J., Alvarez, B.D., and Wurtz, R.H. (2006). Enhanced Performance with Brain Stimulation: Attentional Shift or Visual Cue? J. Neurosci. 26, 11347–11358.

Chen, C.Y., Hoffmann, K.P., Distler, C., and Hafed, Z.M. (2019). The Foveal Visual Representation of the Primate Superior Colliculus. Curr. Biol. 29, 2109-2119.e7.

Cornelissen, F.W., Peters, E.M., and Palmer, J. (2002). The Eyelink Toolbox: Eye tracking with MATLAB and the Psychophysics Toolbox. Behav. Res. Methods, Instruments, Comput. 34, 613–617.

Courjon, J.H., Olivier, E., and Pélisson, D. (2004). Direct evidence for the contribution of the superior colliculus in the control of visually guided reaching movements in the cat. J. Physiol. 556, 675–681.

Cowie, R.J., and Robinson, D.L. (1994). Subcortical contributions to head movements in macaques. I. Contrasting effects of electrical stimulation of a medial pontomedullary region and the superior colliculus. J. Neurophysiol. 72, 2648–2664.

Crapse, T.B., Lau, H., and Basso, M.A. (2018). A Role for the Superior Colliculus in Decision Criteria. Neuron 97, 181-194.e6.

Fecteau, J.H., Bell, A.H., and Munoz, D.P. (2004). Neural Correlates of the Auto-

matic and Goal-Driven Biases in Orienting Spatial Attention. J. Neurophysiol. 92, 1728–1737.

Fecteau, J., and Munoz, D. (2006). Salience, relevance, and firing: a priority map for target selection. Trends Cogn. Sci. 10, 382–390.

Freedman, E.G. (2008). Coordination of the eyes and head during visual orienting. Exp. Brain Res. 190, 369–387.

Fries, W. (1985). Inputs from motor and premotor cortex to the Superior Colliculus of the macaque monkey. 18, 95–105.

Furlan, M., Smith, A.T., and Walker, R. (2015). Activity in the human superior colliculus relating to endogenous saccade preparation and execution. J. Neurophysiol. jn.00825.2014.

Gandhi, N.J., and Katnani, H.A. (2011). Motor Functions of the Superior Colliculus. Annu. Rev. Neurosci. 34, 205–231.

Glasser, M.F., Sotiropoulos, S.N., Wilson, J.A., Coalson, T.S., Fischl, B., Andersson, J.L., Xu, J., Jbabdi, S., Webster, M., Polimeni, J.R., et al. (2013). The minimal preprocessing pipelines for the Human Connectome Project. Neuroimage 80, 105–124.

Glimcher, P.W., and Sparks, D.L. (1992). Movement selection in advance of action in the superior colliculus. Nature 355, 542–545.

Goldberg, M.E., and Wurtz, R.H. (1972). Activity of superior colliculus in behaving monkey. I. Visual receptive fields of single neurons. J. Neurophysiol. 35, 542–559.

Gordon, E.M., Laumann, T.O., Gilmore, A.W., Newbold, D.J., Greene, D.J., Berg, J.J., Ortega, M., Hoyt-Drazen, C., Gratton, C., Sun, H., et al. (2017). Precision Functional Mapping of Individual Human Brains. Neuron 95, 791-807.e7.

Groh, J.M., and Sparks, D.L. (1996). Saccades to somatosensory targets. III. eye-position-dependent somatosensory activity in primate superior colliculus. J. Neuro-

physiol. 75, 439–453.

Hafed, Z.M., Lovejoy, L.P., and Krauzlis, R.J. (2013). Superior colliculus inactivation alters the relationship between covert visual attention and microsaccades. Eur. J. Neurosci. 37, 1169–1181.

Hafed, Z.M., and Clark, J.J. (2002). Microsaccades as an overt measure of covert attention shifts. Vision Res. 42, 2533–2545.

Herman, J.P., Katz, L.N., and Krauzlis, R.J. (2018). Midbrain activity can explain perceptual decisions during an attention task. Nat. Neurosci. 21, 1651–1655.

Herman, J.P., and Krauzlis, R.J. (2017). Color-Change Detection Activity in the Primate Superior Colliculus. Eneuro 4, .0046-17.2017.

Himmelbach, M., Linzenbold, W., and Ilg, U.J. (2013). Dissociation of reach-related and visual signals in the human superior colliculus. Neuroimage 82, 61–67.

Horwitz, G.D., Batista, A.P., and Newsome, W.T. (2004). Representation of an Abstract Perceptual Decision in Macaque Superior Colliculus. J. Neurophysiol. 91, 2281–2296.

Horwitz, G.D., and Newsome, W.T. (1999). Separate signals for target selection and movement specification in the superior colliculus. Science 284, 1158–1161.

Horwitz, G.D., and Newsome, W.T. (2001). Target Selection for Saccadic Eye Movements: Prelude Activity in the Superior Colliculus During a Direction-Discrimination Task. J. Neurophysiol. 86, 2543–2558.

Hoshi, E., and Tanji, J. (2007). Distinctions between dorsal and ventral premotor areas: anatomical connectivity and functional properties. Curr. Opin. Neurobiol. 17, 234–242.

Ignashchenkova, A., Dicke, P.W., Haarmeier, T., and Thier, P. (2004). Neuron-specific contribution of the superior colliculus to overt and covert shifts of attention.

Nat. Neurosci. 7, 56–64.

Indovina, I., and Sanes, J.N. (2001). Combined visual attention and finger movement effects on human brain representations. 265–279.

Kaas, J. H., and Huerta, M.F. (1988). "The subcortical visual system of primates." In Comparative Primate Biology, Vol.4, H. D. Steklis and J. Erwin, ed. (New York, NY: Alan R. Liss), pp. 327–391.

Kleiner M, Brainard D, P.D. (2007). "What's new in Psychtoolbox-3?" Percept. 36 ECVP Abstr. Suppl.

Kuhtz-Buschbeck, J.P., Mahnkopf, C., Holzknecht, C., Siebner, H., Ulmer, S., and Jansen, O. (2003). Effector-independent representations of simple and complex imagined finger movements: A combined fMRI and TMS study. Eur. J. Neurosci. 18, 3375–3387.

Laumann, T.O., Gordon, E.M., Adeyemo, B., Snyder, A.Z., Joo, S.J., Chen, M.Y., Gilmore, A.W., McDermott, K.B., Nelson, S.M., Dosenbach, N.U.F., et al. (2015). Functional System and Areal Organization of a Highly Sampled Individual Human Brain. Neuron 87, 657–670.

Linzenbold, W., and Himmelbach, M. (2012). Signals from the deep: reach-related activity in the human superior colliculus. J. Neurosci. 32, 13881–13888.

Linzenbold, W., Lindig, T., and Himmelbach, M. (2011). Functional neuroimaging of the oculomotor brainstem network in humans. Neuroimage 57, 1116–1123.

Lovejoy, L.P., and Krauzlis, R.J. (2010). Inactivation of primate superior colliculus impairs covert selection of signals for perceptual judgments. Nat. Neurosci. 13, 261–266.

Lünenburger, L., Kleiser, R., Stuphorn, V., Miller, L.E., and Hoffmann, K.P. (2001). A possible role of the superior colliculus in eye-hand coordination. Prog. Brain Res.

134, 109–125.

Mathis, A., Mamidanna, P., Cury, K.M., Abe, T., Murthy, V.N., Mathis, M.W., and Bethge, M. (2018). DeepLabCut: markerless pose estimation of user-defined body parts with deep learning. Nat. Neurosci. 21, 1281–1289.

May, P.J. (2006). The mammalian superior colliculus: laminar structure and connections. In Progress in Brain Research, pp. 321–378.

Mayka, M.A., Corcos, D.M., Leurgans, S.E., and Vaillancourt, D.E. (2006). Three-dimensional locations and boundaries of motor and premotor cortices as defined by functional brain imaging: A meta-analysis. Neuroimage 31, 1453–1474.

Mayo, J.P., and Sommer, M.A. (2008). Neuronal Adaptation Caused by Sequential Visual Stimulation in the Frontal Eye Field. J. Neurophysiol. 100, 1923–1935.

McPeek, R.M., and Keller, E.L. (2004). Deficits in saccade target selection after inactivation of superior colliculus. Nat. Neurosci. 7, 757–763.

Mikulić, A., and Hoffmann, K.P. (2016). Primate superior colliculus neurons activated by unexpected sensation. Exp. Brain Res. 234, 3465–3471.

Müller, J.R., Philiastides, M.G., and Newsome, W.T. (2005). Microstimulation of the superior colliculus focuses attention without moving the eyes. Proc. Natl. Acad. Sci. U. S. A. 102, 524–529.

Munoz, D.P., and Wurtz, R.H. (1995). Saccade-related activity in monkey superior colliculus. I. Characteristics of burst and buildup cells. J. Neurophysiol. 73, 2313–2333.

Nagy, A., Kruse, W., Rottmann, S., Dannenberg, S., and Hoffmann, K.P. (2006). Somatosensory-Motor Neuronal Activity in the Superior Colliculus of the Primate. Neuron 52, 525–534.

Ottes, F.P., Gisbergen, J.A.M. van, and Eggermont, J.J. (1986). Visuomotor Colliculus: Fields of the Superior a Quantitative Model. 26, 857–873.

Pavlou, A., and Casey, M. (2010). Simulating the effects of cortical feedback in the superior colliculus with topographic maps. In The 2010 International Joint Conference on Neural Networks (IJCNN), (IEEE), pp. 1–8.

Pelli, D.G. (1997). The VideoToolbox software for visual psychophysics: transforming numbers into movies. Spat. Vis. 10, 437–442.

Philipp, R., and Hoffmann, K.P. (2014). Arm movements induced by electrical microstimulation in the superior colliculus of the macaque monkey. J. Neurosci. 34, 3350–3363.

Ratcliff, R., Cherian, A., and Segraves, M. (2003). A Comparison of Macaque Behavior and Superior Colliculus Neuronal Activity to Predictions From Models of Two-Choice Decisions. J. Neurophysiol. 90, 1392–1407.

Ratcliff, R., Hasegawa, Y.T., Hasegawa, R.P., Smith, P.L., and Segraves, M.A. (2007). Dual Diffusion Model for Single-Cell Recording Data From the Superior Colliculus in a Brightness-Discrimination Task. J. Neurophysiol. 97, 1756–1774.

Reyes-Puerta, V., Philipp, R., Lindner, W., and Hoffmann, K.-P. (2010). Role of the rostral superior colliculus in gaze anchoring during reach movements. J. Neurophysiol. 103, 3153–3166.

Roche, A. (2011). A four-dimensional registration algorithm with application to joint correction of motion and slice timing in fMRI. IEEE Trans. Med. Imaging 30, 1546–1554.

Sladky, R., Friston, K.J., Tröstl, J., Cunnington, R., Moser, E., and Windischberger, C. (2011). Slice-timing effects and their correction in functional MRI. Neuroimage 58, 588–594.

Soares, S.C., Maior, R.S., Isbell, L.A., Tomaz, C., and Nishijo, H. (2017). Fast detector/first responder: Interactions between the superior colliculus-pulvinar pathway and stimuli relevant to primates. Front. Neurosci. 11, 1–19.

Song, J.-H., and McPeek, R.M. (2015). Neural correlates of target selection for reaching movements in superior colliculus. J. Neurophysiol. 113, 1414–1422.

Sparks, D.L. (1978). Functional properties of neurons in the monkey superior colliculus: Coupling of neuronal activity and saccade onset Brain Res. 156, 1–16.

Sparks, D.L., and Mays, L.E. (1980). Movement fields of saccade-related burst neurons in the monkey superior colliculus. Brain Res. 190, 39–50.

Sparks, D.L., and Mays, L.E. (1990). Signal Transformations Required for the Generation of Saccadic Eye Movements. Annu. Rev. Neurosci. 13, 309–336.

Sprague, J.M. (1966). Interaction of Cortex and Superior Colliculus in Mediation of Visually Guided Behavior in the Cat. Science (80-.). 153, 1544–1547.

Stuphorn, V., Bauswein, E., and Hoffmann, K.P. (2000). Neurons in the primate superior colliculus coding for arm movements in gaze-related coordinates. J. Neurophysiol. 83, 1283–1299.

Tardif, E., and Clarke, S. (2002). Commissural connections of human superior colliculus. Neuroscience 111, 363–372.

Wall, M.B., Walker, R., and Smith, A.T. (2009). Functional imaging of the human superior colliculus: An optimised approach. Neuroimage 47, 1620–1627.

Wallace, M.T., Wilkinson, L.K., and Stein, B.E. (1996). Representation and integration of multiple sensory inputs in primate superior colliculus. J. Neurophysiol. 76, 1246–1266.

Wang, L., McAlonan, K., Goldstein, S., Gerfen, C.R., and Krauzlis, R.J. (2020). A Causal Role for Mouse Superior Colliculus in Visual Perceptual Decision-Making. J.

Neurosci. 40, 3768–3782.

Werner, W. (1993). Neurons in the primate superior colliculus are active before and during arm movements to visual targets. Eur. J. Neurosci. 5, 335–340.

Werner, W., Hoffmann, K.-P., and Dannenberg, S. (1997a). Anatomical distribution of arm-movement-related neurons in the primate superior colliculus and underlying reticular formation in comparison with visual and saccadic cells. Exp. Brain Res. 115, 206–216.

Werner, W., Dannenberg, S., and Hoffmann, K.P. (1997b). Arm-movement-related neurons in the primate superior colliculus and underlying reticular formation: Comparison of neuronal activity with EMGs of muscles of the shoulder, arm and trunk during reaching. Exp. Brain Res. 115, 191–205.

White, B.J., and Munoz, D.P. (2012). The superior colliculus. Oxford Handb. Eye Movements 195–213.

Witt, S.T., Laird, A.R., and Meyerand, M.E. (2008). Functional neuroimaging correlates of finger-tapping task variations: An ALE meta-analysis. Neuroimage 42, 343–356.

Xu, T., Opitz, A., Craddock, R.C., Wright, M.J., Zuo, X.-N., and Milham, M.P. (2016). Assessing Variations in Areal Organization for the Intrinsic Brain: From Fingerprints to Reliability. Cereb. Cortex 26, 4192–4211.

Zhang, B., Kan, J.Y.Y., Yang, M., Wang, X., Tu, J., and Dorris, M.C. (2021). Transforming absolute value to categorical choice in primate superior colliculus during value-based decision making. Nat. Commun. 12, 3410.

Acknowledgments

This thesis does not just represent the culmination of the projects detailed in it, but also marks a milestone along the course of a dream that I have been nurturing since I was a child. I would like to thank everybody that encouraged this dream thus far and helped me tide through all the vagaries that came along with it, in chronological order. First and foremost, I would like to thank my parents; Ayee and Pappa have stood like boulders beside me through my journey. It all began with their recognition of my love for science as a kid. I can't be more grateful to them for nurturing my scientific temper by not just buying me '101 experiments in science' and encouraging me to build my first instrument – the hair-hygrometer, but also for instilling in me the tenets of curiosity and reasoning that to-date play a major role in our dinner table conversations. For bolstering me, when my endeavours were arduous not just for me but also for them, and for so much more, I will always be indebted to them. Love you both so much!

It is not always that you have someone in your life who stands by you through all the phases of your life without judging you. I thank my brother Siddharth for the companionship that goes beyond what words can explain and for inspiring me with his dedication to science.

I thank Kumte Amma for being a role model with her courage, strength and resilience. I thank Hubli Amma, for the way she brought me up with unceasing love and affection and for the values she instilled in me.

Without the fervour imparted by my teachers and the influence that they have had on my thinking, I wouldn't be where I am today. I am very thankful to - John Sir for identifying my liking for Biology from a young age and devoting greater attention to me; Sapre Sir for the time he spent on me in spite of being the principal of the school,

giving me special assignments and things to ponder upon such as “Why is human evolution termed ‘descent of man’ and not ascent of man?”; Narasimha Rao Sir and Sheila ma’am for piquing my interest in Physiology as an undergraduate student. I am filled with gratitude when I recollect how Sheila ma’am helped me get into a Neuroscience workshop meant for post-grads and PhD students conducted by IBRO with visiting scientists from the best Universities around the world. I am deeply grateful to KMC, Manipal for the catalytic environment, especially, Prakash Rao Sir for initiating me into quality research, allowing me to discover what it entails. I will never forget how he would entertain my incessant ‘how and why’ questioning, even when it sometimes annoyed him.

I thank the researchers that I have worked and/or interacted closely with: Prof. Aditya Murthy, Prof. Yifat Prut, Prof. Israel Nelken, Prof. Richard Hahnloser, Dr. Axel Brockmann and Dr. Pallab Basu for recognizing me and allowing me to work with them. I also thank Adi and Axel for continually egging me on and being such amazing well-wishers.

The work that I undertook for the thesis wouldn’t have been possible without my advisor and mentor Dr. Marc Himmelbach. I am grateful to him for believing in me and choosing me to work on a project that was far from what I had undertaken until then. His guidance, encouragement and insight moulded me through the years helping me work independently with a critical bent of mind. The personal touch that he gave to every meeting and discussion that we had, be it with the numerous monty python anecdotes or sharing personal experiences and jokes made the office a fun place to be. His approaches to experimental design and data analysis, and the ability to put in the amount of hard work that he does, day-in and day-out, are something that have left a lasting impression on me.

For all that they offered, I am thankful to the Hertie Institute for Clinical Brain Research, the University Hospital Tuebingen and the following people associated with

them: Prof. Hans-Otto-Karnath for the numerous discussions on neurophysiology, the myriad directions in which he would encourage me to think during group meetings, and for the support he offered in my academic undertaking outside the University; Prof. Ziad Hafed and Prof. Thomas Ethofer for helping make the projects better with their inputs, for the critical evaluation they offered during all the board meetings and for being open to discussions whenever I reached out to them; Dr. Michael Erb for all the help with fMRI data acquisition, for constantly being enthusiastic about running simulations or whatever it would take to ascertain why an analysis approach could be better than another, and for aiding me in digesting concepts in fMRI; Bernd Kardatzki, and the HIH IT team for all the IT assistance no matter how many times they were approached; Ina Baumeister, for making administrative tasks seem easy and for all the fun talk.

I would like to thank all my labmates and interns: Mareike, Caterina, Sarah, Amin, Eric, Nicole, Dominik and Francesko for the vibrant atmosphere they helped create at work. I would like to additionally thank Amin for the great time we had in spite of being the only two members in the office most of the times, Nicole for her contribution and dedication towards the project on sequential finger tapping and Francesko for helping with measurements for the project on novel stimuli.

I feel blessed to have had so many friends and well-wishers around me during all the years. Viraj, Kranti, Aruna and Zhivago - I thank you for being such amazing all-weather friends. Kshitij, Elisa, Mohammed, Alessandra, Thomas, Marina, Srinethe, Vinod, Joana and Vikas - I cherish the times we have spent together, be it sharing laughter or tears. Sudarshan and Ashish - the legendary contests of sport and banter kept me feeling young. I thank Harsh for always being ready to help, more so, for printing this thesis!

This work wouldn't have seen the light at the end of the tunnel if not for your unwavering support, percipience, love and care; I owe it to you for the many ways that you bring out the best in me. Thank you, Akshata!

To the ones I have mentioned above and the ones I have not, albeit unintentionally, a big collective thank you for lifting me up from my lows, sharing my highs and making me realise who I am otherwise.

Statement of contributions

Somatically guided reaching in the SC (Chapter 2)

Nikhil Prabhu: contribution to study design, hardware + software design and implementation, data acquisition, data analysis, generation of manuscript

Marc Himmelbach: study design, data acquisition, manuscript review

Role of the SC in simple and complex finger tapping sequences (Chapter 3)

Nikhil Prabhu: contribution to study design, hardware + software design and implementation, data acquisition, data analysis, generation of manuscript

Nicole Knodel: data acquisition, artifact removal from data, contribution to data acquisition software implementation and analysis

Marc Himmelbach: study design, data acquisition, manuscript review

Representation of novel stimuli in the SC (Chapter 4)

Nikhil Prabhu: study design, hardware + software design and implementation, data acquisition, data analysis, generation of manuscript

Marc Himmelbach: contribution to study design, contribution to data acquisition, manuscript review